

การเคลือบผิวของไข่มุกเลี้ยงน้ำจืดด้วยสารละลายไฟโบรอินจากเส้นไหม



นางสาวกนกวรรณ ขำไข่

ศูนย์วิทยทรัพยากร
จุฬาลงกรณ์มหาวิทยาลัย

วิทยานิพนธ์นี้เป็นส่วนหนึ่งของการศึกษาตามหลักสูตรปริญญาวิทยาศาสตรมหาบัณฑิต

สาขาวิชาปิโตรเคมีและวิทยาศาสตร์พอลิเมอร์

คณะวิทยาศาสตร์ จุฬาลงกรณ์มหาวิทยาลัย

ปีการศึกษา 2553

ลิขสิทธิ์ของจุฬาลงกรณ์มหาวิทยาลัย

SURFACE COATING OF FRESHWATER CULTURED PEARLS WITH SILK
FIBROIN SOLUTION

Miss Kanokwan Kumkhai



ศูนย์วิทยทรัพยากร
จุฬาลงกรณ์มหาวิทยาลัย

A Thesis Submitted in Partial Fulfillment of the Requirements
for the Degree of Master of Science Program in Petrochemistry and Polymer Science

Faculty of Science


Chulalongkorn University

Academic Year 2010

Copyright of Chulalongkorn University


Thesis Title SURFACE COATING OF FRESHWATER
CULTURED PEARLS WITH SILK FIBROIN
SOLUTION
By Miss Kanokwan Kumkhai
Field of Study Petrochemistry and Polymer Science
Thesis Advisor Associate Professor Sanong Ekgasit, Ph.D.
Thesis Co-Advisor Associate Professor Chuchaat Thammacharoen

Accepted by the Faculty of Science, Chulalongkorn University in Partial
Fulfillment of the Requirements for the Master's Degree


.....Dean of the Faculty of Science
(Professor Supot Hannongbua, Dr. rer. Nat.)


THESIS COMMITTEE


.....Chairman
(Associate Professor Sirirat Kokpol, Ph.D.)


.....Thesis Advisor
(Associate Professor Sanong Ekgasit, Ph.D.)


..... Thesis Co-Advisor
(Associate Professor Chuchaat Thammacharoen)


.....Examiner
(Associate Professor Voravee P. Hoven, Ph.D.)


.....External Examiner
(Assistant Professor Pimthong Thongnopkun, Ph.D.)

กนกวรรณ จำไข่: การเคลือบผิวของไข่มุกเลี้ยงน้ำจืดด้วยสารละลายไฟโบรอินจากเส้นไหม.
(SURFACE COATING OF FRESHWATER CULTURED PEARLS WITH SILK
FIBROIN SOLUTION) อ. ที่ปรึกษาวิทยานิพนธ์หลัก: รศ.ดร. สนอง เอกสิทธิ์, อ. ที่ปรึกษา
วิทยานิพนธ์ร่วม: รศ.ชูชาติ ธรรมเจริญ, 116 หน้า.

เตรียมสารละลายไฟโบรอินด้วยใช้สารละลายเบส (ลิเทียมโบรไมด์, โซเดียมไฮดรอกไซด์ และโพแทสเซียมไฮดรอกไซด์) โดยละลายเส้นไหมไฟโบรอินที่ได้จากเศษไหมและรังไหมตก-
เกรดจากอุตสาหกรรมชุมชนและอุตสาหกรรมสิ่งทอภายในประเทศ หลังจากทำการทดลองพบว่า
การเตรียมสารละลายไฟโบรอินที่คุ้มค่าคือการใช้สารละลายโซเดียมไฮดรอกไซด์ 0.35 M
ละลายเส้นไหม 2 กรัม (2 % โดยน้ำหนักต่อปริมาตร) และจะทำการปรับพีเอชของสารละลายให้
เป็นกลางเพื่อใช้สำหรับการเคลือบผิว โดยที่สารละลายโซเดียมไฮดรอกไซด์มีราคาถูกกว่า
สารละลายโพแทสเซียมไฮดรอกไซด์ และสารละลายลิเทียมโบรไมด์ถึง 7.5 เท่า และใช้ความ
เข้มข้นของสารละลายเบสที่น้อยกว่า ซึ่งช่วยลดต้นทุน สารเคมี ลดปริมาณของเสียจากการ
กระบวนการเตรียม และยังลดเวลาในกระบวนการเตรียมและลดเวลาในกระบวนการไดอิเล็กทริก
หลังจากนั้นจะทำการเคลือบผิวของไข่มุกเลี้ยงน้ำจืดคุณภาพต่ำด้วยสารละลายไฟโบรอินและ
เคลือบด้วยเมทานอล ใช้เทคนิคเอทีอาร์ เอฟที-ไออาร์และ รามานสเปกโทรสโกปีในการวิเคราะห์
(ทั้งสองเทคนิคเป็นเทคนิคที่ไม่ทำลายตัวอย่างในการวิเคราะห์ผลิตภัณฑ์ที่ได้) ผลการทดลองแสดง
การเกาะติดของซิลล์ไฟโบรอินที่ชัดเจนบนผิวของไข่มุกโดยสังเกตพีคที่ตำแหน่งของการสั่นยืด
ของพันธะเอ็นเอช เอไมด์วัน และดิงพีคที่ตำแหน่งของเอไมด์ทูและเอไมด์ทรี เมทานอลจะเข้าไปถึง
น้ำออกจากโมเลกุลของซิลล์ไฟโบรอินทำให้ซิลล์ไฟโบรอินเปลี่ยนโครงสร้างออสฐานเป็น
โครงสร้างแบบผลึกทำให้ซิลล์ไฟโบรอินไม่ละลายน้ำและยังเพิ่มประสิทธิภาพในการเกาะติดบนผิว
ของไข่มุกได้ดี นอกจากนี้ฟิล์มซิลล์ไฟโบรอินที่เคลือบบนผิวไข่มุกจะทำหน้าที่ปกป้องผิวของ
ไข่มุกจากความร้อน สารเคมี น้ำหอม เครื่องสำอาง และสนุ นอกจากนี้ยังเพิ่มความมันวาวของ
พื้นผิวไข่มุก

สาขาวิชา ปิโตรเคมีและวิทยาศาสตร์พอลิเมอร์
ปีการศึกษา... 2553

ลายมือชื่อนิติศ..... กนกวรรณ จำไข่
ลายมือชื่อ..... ที่ปรึกษาวิทยานิพนธ์หลัก..... *SN*

ลายมือชื่อ..... ที่ปรึกษาวิทยานิพนธ์ร่วม..... *C. Thammachai*

5072202723: MAJOR PETROCHEMISTRY AND POLYMER SCIENCE
 KEYWORDS: FRESHWATER CULTURED PEARLS / SILK FIBROIN SOLUTION /
 ATR FT-IR MICROSPECTROSCOPY / RAMAN MICROSPECTROSCOPY

KANOKWAN KUMKHAI: SURFACE COATING OF FRESHWATER
 CULTURED PEARLS WITH SILK FIBROIN SOLUTION. THESIS
 ADVISOR: ASSOC. PROF. SANONG EKGASIT, Ph.D., THESIS CO-
 ADVISOR: ASSOC. PROF. CHUCHAAT THAMMACHAROEN, 116 pp.

Silk fibroin solutions are prepared using alkaline solution (LiBr, NaOH and KOH) by dissolving silk fibers from waste fabric industry or local community silk industry. From the experiment, it was found that the optimal silk fibroin solution can be prepared from 2 g (2 % w/v) of silk fibroin fiber dissolved in 0.35 M NaOH and adjusted the pH of solution to neutral pH for the coating. The price of NaOH is 7.5 times cheaper than that of LiBr and KOH. The concentration of NaOH used was also lower. These helped reduced costs, chemicals and waste from the preparation, the time for the dissolving and the time of the dialysis method. After that, the silk fibroin solution was coated on the surface of low quality freshwater cultured pearl followed by methanol treatment, then the coated objects were analyzed by ATR FT-IR and Raman microspectroscopy (both techniques are non- destructive). The results elucidated the stick of silk fibroin on pearl surface by observing characteristic peaks of N-H stretching, Amide I and the shoulder peaks of Amide II and Amide III. Methanol extracts water from molecular silk fibroin which causes the changing of the amorphous structure to crystalline. The silk fibroin became water insoluble so that the effectiveness of silk fibroin adhesion on pearl surface could be unproved. Moreover, silk fibroin film on pearl surface protect surface of pearl from heat, solvent and detergents. So, silk fibroin increases the luster of pearl surface.

Field of Study: Petrochemistry and Polymer Science. Student's Signature *Chanokwan Kumkhai*

Academic Year: ... 2010 Advisor's Signature *Sanong Ekgasit*

Co-Advisor's Signature *C. Thammacharoen*

ACKNOWLEDGEMENTS

I would like to express my sincere gratitude to Associate Professor Dr. Sirirat Kokpol, Associate Professor Dr. Voravee P. Hoven, and Assistant Professor Dr. Pimthong Thongnopkun for suggestions and contributions as thesis committee.

Gratefully thanks to Associate Professor Dr. Sanong Ekgasit, my thesis advisor and Associate Professor Chuchaat Thammacharoen, my thesis co-advisor, for the invaluable guidance, comments, suggestions, encouragement, understanding as well as patiently practices my technical skill during the whole research.

The author would like to acknowledge Mr. Prateep Meesilpa (Director of The Queen Sirikit Institute of Sericulture, Office of the Permanent Secretary for Agriculture and Cooperatives, Ministry of Agriculture and Cooperatives for silk fiber supply) and National Center of Excellence for Petroleum, Petrochemicals, and Advanced materials (NCE-PPAM).

I would like to thank my colleagues and organization: the Sensor Research Unit, Department of Chemistry, Faculty of Science, Chulalongkorn University, and their friendships and spiritual supports throughout this research.

Whatever shortcomings in the thesis remain, they are the sole responsibility of the author.

Above all, I am profoundly grateful to my wonderful parents and the endearing family for their patient love, perpetual encouragement, and overwhelming support.

CONTENTS

	Page
ABSTRACT (IN THAI).....	iv
ABSTRACT (IN ENGLISH).....	v
ACKNOWLEDGEMENTS.....	vi
CONTENTS.....	vii
LIST OF FIGURES.....	x
LIST OF TABLES.....	xvii
LIST OF ABBREVIATIONS.....	xviii
CHAPTER I INTRODUCTION.....	1
1.1 Background.....	1
1.2 Literatures Review.....	3
1.3 The objectives of this research.....	4
1.4 The scopes of this research.....	4
CHAPTER II THEORETICAL BACKGROUND.....	5
2.1 Pearl.....	5
2.1.1 Properties of pearls.....	5
2.1.2 Type of pearls.....	11
2.1.3 Quality of pearls.....	12
2.1.4 Enhancement of low quality pearls.....	14
2.2 Silk fiber.....	15
2.2.1 Silk fibroin structure.....	16
2.2.2 Secondary structure of silk fibroin.....	17
2.2.3 Chemical composition of silk fibroin.....	18
2.2.4 Preparation of silk fibroin solution.....	19

	Page
2.3 ATR FT-IR microspectroscopy.....	20
2.3.1 Fundamental of infrared spectroscopy.....	21
2.3.2 Attenuated Total Reflection Fourier Transform Infrared (ATR FT-IR) Microspectroscopy.....	22
2.3.3 Principles of light reflection and refraction.....	22
2.3.4 Internal reflection element (IRE).....	23
2.3.5 ATR spectral intensity and depth profiling.....	24
2.3.6 Principle of light entering the Ge μ IRE.....	26
2.3.7 Homemade Slide-on Ge μ IRE Accessory.....	27
2.4 Raman microspectroscopy.....	30
2.4.1 Theory.....	30
2.4.2 Raman spectroscopy.....	30
2.4.3 Dispersive Raman spectroscopy.....	31
2.2.4 Raman Microscope.....	31
 CHAPTER III EXPERIMENTAL SECTION.....	 33
3.1 Materials.....	33
3.2 Experimental section.....	34
3.2.1 Preparation of <i>Bombyx mori</i> silk fibroin solution.....	34
3.2.2 Preparation of coated silk fibroin solution on pearl surfaces.....	35
3.2.3 Resistance to corrosion of pearl surface.....	36
3.3 Characterization of coated silk fibroin solution on pearl surface.....	37
3.3.1 ATR FT-IR microspectroscopy.....	37
3.3.2 Raman microspectroscopy.....	39
3.3.3 UV-Visible spectroscopy.....	41
 CHAPTER IV RESULTS AND DISCUSSION.....	 43
4.1 Chemical information by ATR FT-IR and Raman microspectroscopy..	43

	Page
4.2.1 Silk fibroin film.....	43
4.2.2 Freshwater cultured pearls.....	47
4.2.3 Freshwater culture pearls coated with silk fibroin solution on pearl surface.....	53
4.2 Effect of the cleaning pearl surface for the sticking of silk fibroin on pearl surface.....	58
4.3 Preparation of silk fibroin solution.....	61
4.3.1 Alkaline solution.....	61
4.3.2 Weight of silk fibroin fibers.....	64
4.1.3 pH of silk fibroin solution.....	72
4.4 Effect of the temperature for the sticking of silk fibroin on pearl surface.....	76
4.5 Effect of the time for the sticking of silk fibroin on pearl surface....	78
4.6 Effect of the alcohol treatment for the sticking of silk fibroin on pearl surface.....	81
4.7 Effect of the methanol treatment for the sticking of silk fibroin on pearl surface.....	83
4.8 Effect of the polishing for the sticking of silk fibroin on pearl surface...	88
4.9 Resistance to corrosion of pearl after coated with silk fibroin solution on surface.....	91
4.9.1 Heat.....	92
4.9.2 Detergent and solvent.....	96
4.10 The role of the luster of pearl after the coating with silk fibroin solution.....	106
CHAPTER V CONCLUSIONS.....	108
REFERENCES.....	109
VITAE.....	116

LIST OF FIGURES

Figure	Page
2.1 Structural assembly of pearl consisting of aragonite nanocrystal glued together by conchiolin protein (biopolymer).....	6
2.2 SEM images of fractured surface of nacre show important microstructural features responsible for mechanical response of nacre that large deformations in the organic phase.....	7
2.3 FT-IR spectra of CaCO ₃ : calcite, aragonite and vaterite.....	8
2.4 FT-IR spectra of naturally-coloured cultured pearl.....	9
2.5 Raman spectra of CaCO ₃ : calcite, aragonite and vaterite.....	10
2.6 Freshwater pearls and saltwater pearls.....	12
2.7 Level of lustrous pearls.....	12
2.8 The surface of pearl	13
2.9 The size of pearls	13
2.10 The color of pearls.....	14
2.11 The shape of pearls.....	14
2.12 Structure of the silk fiber.....	16
2.13 The four levels of protein structure.....	16
2.14 The antiparallel (a) and parallel β -pleated sheet structures (b). Then, the β -turn structure is classified to Type I (c) and Type II (d).....	18
2.15 The secondary structure: (a) the α -helix and (b) random coil structure	18
2.16 Modes of molecular vibration.....	21
2.17 Position of beam after incident beam impinges on the sample.....	21
2.18 The reflection and refraction of the plane wave at the dielectric interface.....	23
2.19 The illustration of IRE configurations used in ATR experimental setups: Single reflection hemispherical crystal (A), and Multiple reflections (B).....	24

Figure

2.20	The ray tracing within the infrared objective focusing radiation travelling within the Ge μ IRE.....	27
2.21	Slide-on housing and parts of the homemade ATR assessor with germanium μ IRE miniature.....	28
2.22	The detailed drawings of the homemade miniature ATR accessory with germanium μ IRE. The housing attached to the objective (A), slide-on set with the Ge μ IRE (B) and complete accessory (C).....	29
2.23	The energy level diagram for Raman spectra.....	30
3.1	Preparation of <i>Bombyx mori</i> silk fibroin solution were performed by using LiBr, NaOH and/or KOH to dissolve 2 g (2 % w/v), 3 g (3 % w/v), 4 g (3 % w/v) and 5 g (5 % w/v) of silk fibroin fibers. Then, the solution was dialyzed in DI water by dialysis and/or was adjusted to the neutral pH.....	35
3.2	The cleaning surface of pearl and coated with silk fibroin solution plus alcohol treatment.....	35
3.3	Process of silk fibroin coating on pearl surfaces.....	36
3.4	The method tested resistance to corrosion of pearl surface (freshwater cultured, coated silk fibroin pearl, alcohol treatment-coated silk fibroin pearl).....	37
3.5	ATR FT-IR microspectroscope: (A) Continuum TM infrared microscope attached to the Nicolet 6700 FT-IR spectrometer, (B) the holder of pearl and the slide-on Ge μ IRE is fixed on the position of slide-on housing on the infrared objective, and (C) Homemade slide-on Ge μ IRE.....	39
3.6	DXR Raman Microscope.....	41
3.6	UV-Visible spectrometer and Integrating Sphere.....	42
4.1	ATR FT-IR spectra of silk fibroin film (A) and silk fibroin film treated with methanol (B).....	44

Figure	Page
4.2 Raman spectra of silk fibroin film (A) and silk fibroin film treated with methanol (B).....	46
4.3 ATR FT-IR spectrum of freshwater cultured pearl.....	48
4.4 ATR FT-IR spectra of CaCO ₃ different morphology (Chakrabarty et al. 1999) (A) and CaCO ₃ of freshwater cultured pearl (B).....	49
4.5 Raman spectrum of freshwater cultured pearl.....	50
4.6 Raman spectra of CaCO ₃ (Kontoyannis et al., 2000) of calcite, aragonite and vaterite crystal form (A) and CaCO ₃ of freshwater cultured pearl (B).....	51
4.7 Optical image of freshwater cultured pearl surface.....	52
4.8 ATR FT-IR spectra of conchiolin protein of pearl (A) and silk fibroin film (B).....	53
4.9 ATR FT-IR spectra of freshwater cultured pearl (A), silk fibroin film (B) and pearl coated silk fibroin solution (C).....	54
4.10 ATR FT-IR spectra of conchiolin protein of pearl (A), freshwater cultured pearl coated silk fibroin solution on pearl surface (B).....	55
4.11 Raman spectra of freshwater cultured pearl (A), silk fibroin film (B) and pearl coated silk fibroin solution (C).....	56
4.12 Raman spectra of conchiolin protein of pearl (A), freshwater cultured pearl coated silk fibroin solution on pearl surface (B).....	57
4.13 Optical image of freshwater cultured pearl coated with silk fibroin solution.....	58
4.14 ATR FT-IR spectra of freshwater cultured pearl cleaned by DI water (A) coated with silk fibroin solution (B). Pearl cleaning surface by water and 10% H ₂ O ₂ (C) that coated with silk fibroin solution (D).....	59
4.15 Optical image of freshwater cultured pearl cleaned by DI water (A), and coated with silk fibroin solution (B). The pearls surface cleaned by DI water and 10% H ₂ O ₂ (C), that coated with silk fibroin solution (D)...	60

Figure	Page
4.16 Silk fibroin solution are prepared from 5 g of silk fibroin fibers dissolved in LiBr, NaOH, and KOH at the concentrations of 9.3 M, 1.0 M, and 1.1 M, respectively.....	62
4.17 ATR FT-IR spectra of freshwater cultured pearl (A). Pearl coated with silk fibroin solution prepared from 5 g of silk fibroin fibers dissolved in 9.3 M LiBr (B), 1.0 M NaOH (C), and 1.1 M KOH (D).....	63
4.18 Silk fibroin solution prepared from 2 g (2 % w/v), 3 g (3 % w/v), 4 g (4 % w/v) and 5 g (5 % w/v) of silk fibroin fibers are dissolved in NaOH solution at the concentrations of 0.35 M, 0.55 M, 0.80 M, 1.00 M (A) and KOH solution at the concentrations of 0.40 M, 0.60 M, 0.85 M, 1.10 M (B), respectively.....	65
4.19 ATR FT-IR spectra of freshwater cultured pearl coated with silk fibroin solution prepared from 2 g (2 % w/v), 3 g (3 % w/v), 4 g (4 % w/v) and 5 g (5 % w/v) of silk fibroin fibers are dissolved in NaOH solution at the concentrations of 0.35 M (A), 0.55 M (B), 0.80 M (C) and 1.00 M (D), respectively.....	66
4.20 ATR FT-IR spectra of freshwater cultured pearl coated with silk fibroin solution prepared from 2 g (2 % w/v), 3 g (3 % w/v), 4 g (4 % w/v) and 5 g (5 % w/v) of silk fibroin fibers are dissolved in KOH solution at the concentrations of 0.40 M (A), 0.60 M (B), 0.85 M (C) and 1.10 M (D), respectively.....	67
4.21 Optical images of freshwater cultured pearl coated with silk fibroin solution prepared from 2 g (2 % w/v), 3 g (3 % w/v), 4 g (4 % w/v) and 5 g (5 % w/v) of silk fibroin fibers dissolved in NaOH solution at the concentrations of 0.35 M (A), 0.55 M (B), 0.80 M (C), 1.00 M (D) and KOH solution at the concentrations of 0.40 M (E), 0.60 M (F), 0.85 M (G), 1.10 M (H), respectively.....	68

Figure	Page
4.22 Raman spectra of freshwater cultured pearl coated with silk fibroin solution prepared from 2 g (2 % w/v), 3 g (3 % w/v), 4 g (4 % w/v) and 5 g (5 % w/v) of silk fibroin fibers dissolved in NaOH solution at the concentrations of 0.35 M (A), 0.55 M (B), 0.80 M (C) and 1.00 M (D), respectively	70
4.23 Raman spectra of freshwater cultured pearl coated with silk fibroin prepared solution from 2 g (2 % w/v), 3 g (3 % w/v), 4 g (4 % w/v) and 5 g (5 % w/v) of silk fibroin fibers dissolved in KOH solution at the concentrations of 0.40 M (A), 0.60 M (B), 0.85 M (C) and 1.10 M (D), respectively.....	71
4.24 ATR FT-IR spectra of freshwater cultured pearl (A), coated with silk fibroin solution by dialysis method (B), by adjusting to neutral pH method using NaOH (C), KOH (D).....	73
4.25 ATR FT-IR spectra of freshwater cultured pearl soaked in acid solution (A) and alkaline solution (B).....	74
4.26 Optical images of freshwater cultured pearl (A), coated with silk fibroin solution by dialysis method (B), by adjusting to neutral pH method using NaOH (C), KOH (D), freshwater cultured pearl soaked in alkaline solution (E) and acid solution (F).....	75
4.27 ATR FT-IR spectra of freshwater cultured pearl coated with silk fibroin solution at room temperature (A), 50 °C (B) and 100 °C (C) for 30 min. Pearl soaked in water at room temperature (D), boiled in water at 50 °C (E) and 100 °C (F) for 30 min.....	77
4.28 ATR FT-IR spectra of freshwater cultured pearl (A) coated silk fibroin solution at room temperature for 30 (B), 60 (C) 90 min (D).....	79
4.29 ATR FT-IR spectra of freshwater cultured pearl (A) coated with silk fibroin solution at 50 °C for 30 (B), 60 (C) 90 min (D).....	80
4.30 ATR FT-IR spectra of freshwater cultured pearl (A) coated with silk fibroin solution at 100 °C for 30 (B), 60 (C) and 90 min (D).....	81

Figure	Page
4.31 ATR FT-IR spectra of freshwater cultured pearl (A), coated with silk fibroin solution plus isopropyl alcohol (2-propanol) (B), ethanol (C) and methanol treatment (D).....	83
4.32 Diagram of freshwater cultured pearl (A), coated with silk fibroin solution (B) boiled in water at 100 °C for 10 min (C). Pearl coated with silk fibroin solution plus methanol treatment (D) boiled in water at 100 °C for 10 min (E).....	84
4.33 ATR FT-IR spectra of freshwater cultured pearl (A) coated with silk fibroin solution (B) boiled in water at 100 °C 10 min (E). Pearl coated with silk fibroin solution plus methanol treatment (C) boiled in water at 100 °C 10 min (F).....	85
4.34 Raman spectra of freshwater cultured pearl (A) coated with silk fibroin solution (B) boiled in water at 100 °C 10 min (D). Pearl coated with silk fibroin solution plus methanol treatment (C) boiled in water at 100 °C 10 min (E).....	87
4.35 ATR FT-IR spectra of freshwater cultured pearl coated with silk fibroin solution (A) and polished surface (C). Pearl coated with silk fibroin solution and treated methanol (B) polishing surface (D).....	89
4.36 ATR FT-IR spectra of freshwater cultured pearl coated with silk fibroin solution plus methanol treatment polishing surface.....	90
4.37 Process of test the resistance to corrosion of pearl after the coating with silk fibroin solution on surface by solvents and detergents. Freshwater cultured pearl (A) tested heat, solvent and detergent (B). Pearl coated with silk fibroin solution (C) tested heat, solvent and detergent (D). Pearl coated with silk fibroin solution plus methanol treatment (E) tested heat, solvent and detergent (F).....	91
4.38 ATR FT-IR spectra of freshwater cultured pearl (A) boiled in water at 100 °C 10 min (B). Pearl coated with silk fibroin solution (C) boiled in water at 100 °C 10 min (E). Pearl coated with silk fibroin solution plus methanol treatment (D) boiled in water at 100 °C 10 min (F).....	93

Figure	Page
4.39 Raman spectra of freshwater cultured pearl (A) boiled in water at 100 °C 10 min (B). Pearl coated with silk fibroin solution (C) boiled in water at 100 °C 10 min (E). Pearl coated with silk fibroin solution plus methanol treatment (D) boiled in water at 100 °C 10 min (F).....	95
4.40 ATR FT-IR spectra of freshwater cultured pearl and soaked with tap water, NaOH solution pH 8, 9 and 10, HCl solution pH 4, 5 and 6, detergent, shower cream, body lotion, shampoo and perfume for 19 hours.....	97
4.41 Optical images of freshwater cultured pearl and soaked with tap water, NaOH solution pH 8, 9 and 10, HCl solution pH 4, 5 and 6, detergent, shower cream, body lotion, shampoo and perfume for 19 hours.....	98
4.42 ATR FT-IR spectra of freshwater cultured pearl coated silk fibroin solution and soaked with tap water, NaOH solution pH 8, 9 and 10, HCl solution pH 4, 5 and 6, detergent, shower cream, body lotion, shampoo and perfume for 19 hours.....	100
4.43 Optical images of freshwater cultured pearl coated silk fibroin solution and soaked with tap water, NaOH solution pH 8, 9 and 10, HCl solution pH 4, 5 and 6, detergent, shower cream, body lotion, shampoo and perfume for 19 hours.....	101
4.44 ATR FT-IR spectra of freshwater cultured pearl coated silk fibroin solution plus methanol treatment and soaked with tap water, NaOH solution pH 8, 9 and 10, HCl solution pH 4, 5 and 6, detergent, shower cream, body lotion, shampoo and perfume for 19 hours.....	103
4.45 Optical images of freshwater cultured pearl coated silk fibroin solution plus methanol treatment and soaked with tap water, NaOH solution pH 8, 9 and 10, HCl solution pH 4, 5 and 6, detergent, shower cream, body lotion, shampoo and perfume for 19 hours.....	104
4.46 Image of freshwater pearl coated silk fibroin solution plus methanol treatment.....	107

LIST OF TABLES

Table	Page
2.1 The four fundamental modes of CO_3^{2-} vibration.....	8
2.2 FT-IR band assignments of pearl.....	9
2.3 Raman band assignments of pearl.....	10
2.4 Amino acid composition of conchiolin protein in pearls.....	11
2.5 Amino acid composition of silk fibroins.....	19
2.6 The IRE materials used in ATR measurement.....	24
4.1 Band assignments of fibroin film by ATR FT-IR microspectroscopy....	45
4.2 Band assignments of fibroin film by Raman microspectroscopy.....	47
4.3 Band assignments of freshwater cultured pearl by ATR FT-IR microspectroscopy.....	49
4.4 Band assignments of freshwater cultured pearl by Raman microspectroscopy.....	51
4.5 The lowest amount of alkali for dissolving silk fibroin fibers.....	64
4.6 Summary of chemical and mechanical resistance test of silk fibroin coated pearls.....	105

LIST OF ABBREVIATIONS

ATR	: Attenuated Total Reflection
FT-IR	: Fourier Transform infrared
IRE	: Internal Reflection Element
SEM	: Scanning Electron Microscopy
SRU	: Sensor Research Unit
MCT	: Mercury-cadmium-telluride
MSEF	: Mean square electric field
CCD	: Charge Coupled Device
NIR	: Near Infrared
DI	: Deionized
approx.	: Approximately
kg	: kilogram (10^3 g)
g	: Gram
nm	: Nanometer (10^{-9} m)
μm	: Micrometer (10^{-6} m)
mm	: Millimeter (10^{-3} m)
cm^{-1}	: Wavenumber
kDa	: kilodaltons
kV	: Kilovolt (10^3 V)
M	: Molar
mL	: Milliliter (10^{-3} L)
min	: minute
pH	: Potential of Hydrogen ion
CaCO_3	: Calcium carbonate
CO_3^{2-}	: Carbonate ion
HCO_3^-	: Hydrogen carbonate ion
LiBr	: Lithium bromide
NaOH	: Sodium hydroxide
KOH	: Potassium hydroxide

CaCl_2	: Calcium chloride
ZnCl_2	: Zinc chloride
$\text{Ca}(\text{NO}_3)_2$: Calcium nitrate
Si	: Silicon
ZnSe	: Zinc selenide
Na_2CO_3	: Sodium Carbonate
HCl	: Hydrochloric acid
H_2O_2	: Hydrogen peroxide
Ge	: Germanium
KBr	: Potassium bromide
Gly	: Glycine
Ala	: Alanine
Ser	: Serine
MWCO	: Molecular weight cut off
m	: Medium band
s	: Strong band
v	: Volume
w	: Weak band
et al	: And others
$^\circ\text{C}$: Celsius
I_0	: Intensity of incident beam
I_R	: Intensity of reflected beam
I_S	: Intensity of scattered beam
I_T	: Intensity of transmitted beam
I_A	: Intensity of absorbed beam
I	: Light intensity
n_1	: Refractive index of the dense medium (IRE)
n_2	: Refractive index of the sample
θ	: Angle of incidence
θ_c	: Critical angle
ν	: Wavenumber

A	: Absorbance
l	: Film thickness
ε	: Absorption coefficient
d_p	: Penetration depth
c	: Concentration
λ	: Wavelength
D	: Diameter
d	: Spot size
f	: Focal length
α	: Alpha
β	: Beta
α_1	: Angle of incidence
α_2	: Angle of reflection
μ	: Micron (10^{-6} m)



ศูนย์วิทยทรัพยากร
จุฬาลงกรณ์มหาวิทยาลัย

CHAPTER I

INTRODUCTION

1.1 Background

Pearls are one of the popular organic gems due to the beauty of its natural lustrous and iridescent surface. The pearl begins its life as an irritant of the oyster. To protect itself, the oyster coats an intruding object or grains of sand with nacre, a crystalline calcium carbonate and conchiolin protein that builds up over time. This process becomes shimmering iridescent creation. It is important to note that pearls mainly consist of 95 wt% of calcium carbonate in the aragonite crystal form and 5 wt% of organic matrix called *conchiolin protein*. Basically, all pearls can be divided into natural pearls, cultured pearls and imitated pearls. In addition, natural pearls and cultured pearls can be listed in two types: *freshwater pearls and saltwater pearls*. It can also be divided into natural pearls, cultured pearls and imitated pearls.

The formation of pearl begins when the invaders intrude to the oyster. After that the oyster secreted calcium carbonate called *nacre* and *conchiolin protein* to coat the invader with deposition of multiple layers. Due to higher demand of pearls in the jewelry markets, natural pearls are insufficient. Therefore, human made the development of cultured pearls. The cultured pearls have mortality of 50% from surgical embedded nucleus procedures and cultivation. Approximately 5% of that is not born pearls because the nucleus does not be coated with nacre. Approximately 23% of middle quality of pearls is made as jewelry, which is nearly 5% of high quality pearls. The residues of pearls are low quality and must be sold as drugs or cosmetics. Industries of cultured pearls have high investment and risk, because high quality pearls are expensive. But the low quality pearls are very cheap and are in high volumes. Low quality pearls can be enhanced by bleaching, polishing, coating, filling, drying and irradiation in order to make more value of low quality pearls because high quality pearls are higher price.

Now, more than 99% of all pearls sold worldwide are cultured pearls because they have widely been cultivated. Factors in evaluating the quality and prices are luster, nacre thickness, color, size, lack of surface flaw and symmetry of shape. The luster is the most important differentiator of pearls quality and prices [1-8]. The luster depends on nacre thickness, calcium carbonate in the aragonite crystal form and conchiolin protein. Conchiolin protein mainly consists of amino acids which are glycine and alanine approximately 24.3% and 14%, respectively. The normal amino acid compositions of pearls are shown in Table 2.3 [6].

The conchiolin protein mainly consists of glycine and alanine amino acid which are the same as that of silk fibroin. Although the *Bombyx mori* silk fibroin protein consists of more than 16 amino acids. The major amino acid components are glycine and alanine approximately 44.6% and 29.4%, respectively. The normal amino acid compositions of silk *Bombyx mori* fibroin are shown in Table 2.4 [10]. Nowadays in Thailand, there are widely sericulture and producing silk fiber in both industry as well as community. The materials used in silk production are cocoons which can be sericultured in Thailand. In spite of widely sericulture and silk production, there are a large amount of low grade silk and cocoons that are not be profitably used; therefore in this work we prepared fibroin from low grade of silk and cocoon from industry and community. This method can be value-added of silk and freshwater pearls. It is of interest to modify pearl surfaces of economical aspects as well.

We are very proud to apply the knowledge of science that does not stay on the shelves any more; it becomes a major role in our way of life. Since now, as Thai citizen, we are very happy as well as appreciate for the know-how producing by Sensor Research Unit, SRU, Department of Chemistry, Faculty of Science, Chulalongkorn University, as a part of the contribution for promoting the prosperity of Thai economy.

It is obviously seen that the conchiolin protein and silk fibroin mainly consist of glycine and alanine amino acid. The properties of silk fibroin such as water insolubility, luster and thin film might be caused fibroin to be able to stick better on the pearl surfaces. In order to increase luster pearl surfaces, it is necessary to modify its surface by surface coating.

In this research, the development of coating on the surface of freshwater cultured pearls with silk fibroin is performed. The lusters of pearls are performed by Integrating Sphere Diffuse Reflectance technology by mean of UV-Visible spectrophotometer. Both ATR FT-IR and Raman microspectroscopy are used to investigate the molecular information of pearls and silk fibroin.

1.2 Literatures Review

Silk fiber has been used as textile for over 4000 years because of its high tensile strength, luster, and ability to bind chemical dyes. Silk fiber is still considered a premier textile material in the world today. Especially silk fiber produced by cultivated *Bombyx mori*. Mulberry silkworm mainly consists of two proteins—sericin and fibroin. The fibroin content is 66.5-73.5 wt% and the sericin content is 26.5-33.5 wt% of silk fiber. Silk proteins are due to the formation of anti-parallel beta-pleated sheets via hydrogen bonding and hydrophobic interactions. Silk fibroin has special properties for being used as cosmetics, healthy foods, cell culture medium, enzyme immobilizing materials, biosensor, artificial skin, artificial muscle, permeable membrane and drug release materials. The advantages of silk fibroin are several, such as biocompatible natural polymer, biodegradability, minimal inflammatory reaction and good water vapor permeability, the principal water insoluble protein and has a highly oriented and crystalline structure. Silk fibroin mainly consists of glycine, alanine and serine (approx. 85% in amino acid total), and amino acid sequence can be roughly expressed as (gly-ala-gly-ala-gly-ser)_n. The aqueous solution of *Bombyx mori* silk fibroin shows mainly random coil conformations. The dehydration of silk fibroin in the alcohol promotes solvent induced silk fibroin crystallization as the silk fibroin chains transform from random-coil to β -sheet conformation [10-13]. Now, more than 99% of all pearls sold worldwide are cultured pearls because they have widely been cultivated. Industries of cultured pearls have high investment and risk, because high quality pearls are expensive. But the low quality pearls are very cheap and are in high volumes. Low quality pearls can be enhanced by bleaching, polishing, coating, filling, drying and irradiation in order to make more value of low quality pearls because high

quality pearls are higher price. Imitation and simulated pearls are completely manmade from a variety of materials (beads of glass, plastic, or polished shells). Imitation pearls coated with pearly substance, lacquered wax and varnish so the surface of the pearl has been waxed to enhance its luster.

1.3 The objectives of this research

The objectives of this research are to prepare silk fibroin from silk fibers, and to apply silk fibroin solution into pearls for increasing the luster of low quality freshwater cultured pearls and to characterize the molecular characters of silk fibroin and pearls by means of ATR FT-IR microspectroscopy and Raman spectroscopy.

1.4 The scopes of this research

1. Prepare silk fibroin solution from silk fibers by dissolving in alkaline solution.
2. Prepare silk fibroin from alkaline solution by varying the condition of weights of silk fibroin dissolved in alkaline solution.
3. Coat surface freshwater cultured pearls with silk fibroin solution by varying the condition of time and temperature of the coating.
4. Study the molecular characteristics of silk fibroin and freshwater cultured pearls by means of ATR FT-IR microspectroscopy and Raman spectroscopy.
5. Study the luster of surface freshwater cultured pearls by means of Integrating Sphere Diffuse Reflectance technology and UV-Visible spectrophotometer.
6. Test resistance to corrosion of pearl surface by means of ATR FT-IR microspectroscopy, Raman microspectroscopy and Microscope.

CHAPTER II

THEORETICAL BACKGROUND

2.1 Pearl

Pearls are one of the popular organic gems worldwide. The procreation of pearl is invader into the mother of pearl. It responds by secreting a calcium carbonate substance called nacre and conchiolin protein coated the invader with deposits multiple layers and after that it becomes pearl. So pearls mainly consist of 95 wt% calcium carbonate in the aragonite crystal form and 5 wt% organic matrix that called conchiolin protein. Basically, all pearls can be listed in two types: freshwater pearls and saltwater pearls. It can also be divided into natural pearls, cultured pearls and imitated pearls [1-8].

2.1.1 Properties of pearls

2.1.1.1 Physical properties

- Fracture : Roughness
- Hardness : 2.5-4.5
- Specific gravity : Saltwater Pearls = 2.70 (+0.015 to -0.09)
: Freshwater Pearls = 2.72 (+0.06)

2.1.1.2 Optical properties

- Luster : Pearly
- Color : Pearl color is divided into 3 parts:
 - Body color : Underlying color
 - Overtone : Overlie the body color
 - Orient : Iridescent effect
- Refractive Index : 1.530-1.685
- Birefringence : 0.155
- Fluorescence : Inert to strong: yellow, green, light blue, pink in long-wave and short-wave UV radiation

2.1.1.2 Chemical properties

Pearls mainly consist of 95 wt% calcium carbonate in the aragonite crystal form and 5 wt% organic matrix that called conchiolin protein. The resulting fracture toughness 3,000 times greater than that of pure aragonite [14-27].



Figure 2.1 Structural assembly of pearl consisting of aragonite nanocrystal glued together by conchiolin protein (biopolymer) [20]

(1) Calcium carbonate

Pearls are calcium carbonate in the aragonite crystal form called nacre. Crystallized calcium carbonate contains millions of aragonite platelets, elastic biopolymers such as lustrin and chitin, and silk-like proteins at the same brick and mortar structure. Nacre is composed of hexagonal platelets of aragonite 5–15 μm in diameter and 250–500 nm thickness.

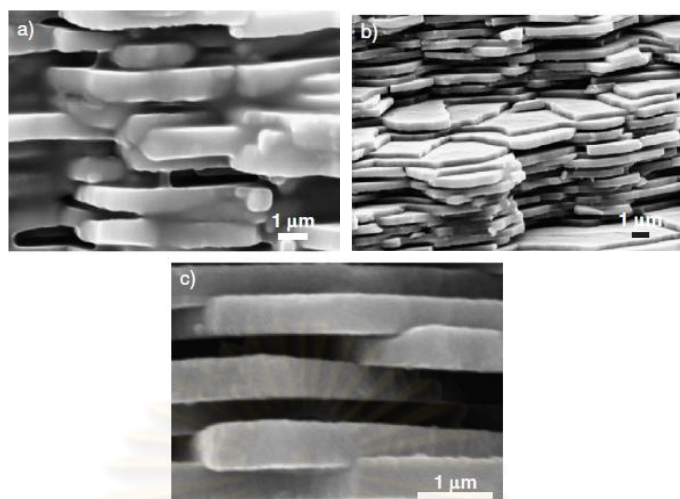


Figure 2.2 SEM images of fractured surface of nacre show important microstructural features responsible for mechanical response of nacre that large deformations in the organic phase [25].

As known before, calcium carbonate is polymorphous and occurs naturally in three crystalline forms: calcite, aragonite and vaterite. The formation of aragonite or calcite is very unstable phase of CaCO_3 that rarely occurred in nature. The free carbonate ion has D_{3h} symmetry and has four fundamental modes of vibration: a symmetric stretching (ν_1), an out of plane bending (ν_2), an asymmetric stretching (ν_3) and in of plane bending (ν_4). From the previous studies, it was demonstrated three majors of CaCO_3 which analyzed by FT-IR microspectroscopy as shown in Table 2.1 and the spectrum was shown in Figure 2.3 [29-33]. Furthermore, from the literatures review it is known that at 300-400 °C the aragonite can be transformed to the calcite and at 550-600 °C the calcite is transformed to calcium oxide (CaO) [34].

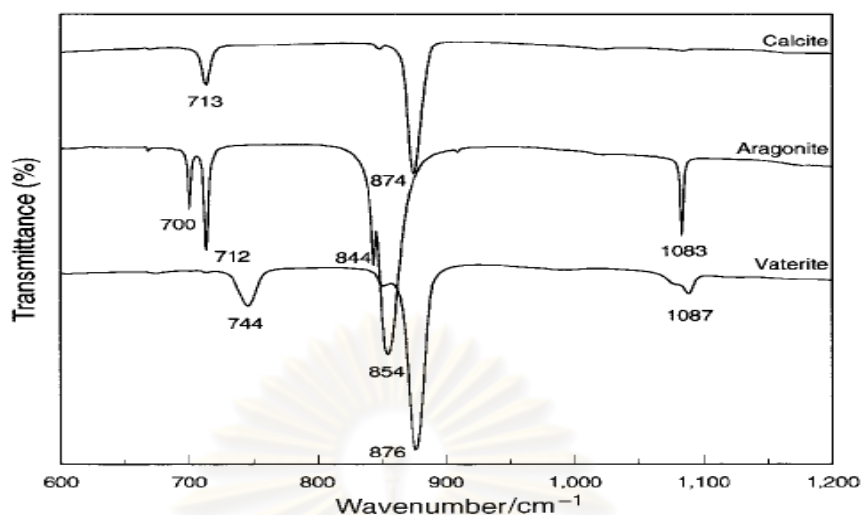


Figure 2.3 FT-IR spectra of CO_3^{2-} : calcite, aragonite and vaterite [32].

Table 2.1 The four fundamental modes of CO_3^{2-} vibration [34].

Calcium carbonate minerals	Vibrational frequencies of CO_3^{2-} ion			
	ν_1 (cm^{-1})	ν_2 (cm^{-1})	ν_3 (cm^{-1})	ν_4 (cm^{-1})
Calcite	-	875	1426	712
Aragonite	1082	859	1485	712, 699
Vaterite	1085, 1070	850, 830	1490, 1420	750
Lusterless pearl	1087, 1050	876, 830	1489, 1450, 1420	762, 743
High quality pearl	1082	859	1485	712, 699

The FT-IR spectra for the chemical compositions of cultured pearl by FT-IR spectroscopy studies are shown in Figure 2.4. The peaks at 700, 713, 862, 1083, 1469, 1788, 2499, 2522, 2547 and 2920 cm^{-1} as shown in Table 2.2 and the absorption peaks of 700, 713, 862 as well as 1083 cm^{-1} indicated the aragonite crystal form of CaCO_3 [35-39]. The paper reports a discovery of vaterite formation in low quality freshwater cultured pearls. The luster pearl tested by FT-IR spectra were assigned to be aragonite.

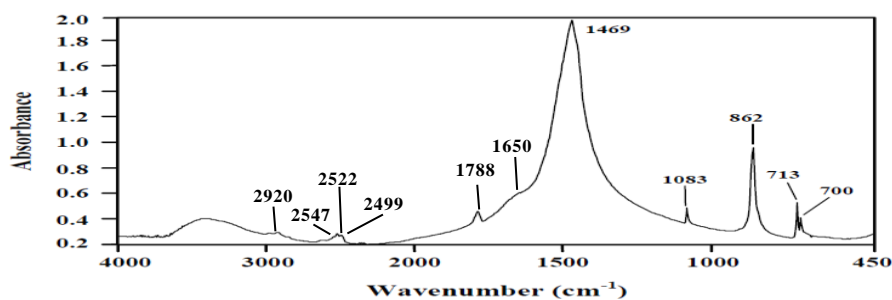


Figure 2.4 FT-IR spectra of naturally-coloured cultured pearl [36].

Table 2.2 FT-IR band assignments of pearl

Wavenumber (cm ⁻¹)	Band assignments
3446	OH stretching vibration of adsorbed water
2522, 2499, 2547	OH stretching vibration of HCO ₃ ⁻
2920	C-H stretching vibration
1788	C=O stretching vibration of CO ₃ ²⁻
1650	Amide I (C=O stretching, slightly coupled with CN stretching, CCN deformation and NH bending)
1469	Asymmetric stretching vibration of CO ₃ ²⁻
1083	Symmetric stretching vibration of CO ₃ ²⁻
862	Out of plane bending vibration of CO ₃ ²⁻
700, 712	Planar bending vibration of CO ₃ ²⁻

The Raman spectra characteristic peaks of CaCO₃ are as follows: 152, 205, 700 (v₄), 705 (v₄) and 1084 (v₁) cm⁻¹ of aragonite, 154, 280, 711 (v₄), 1085 (v₁) and 1435 (v₃) cm⁻¹ of calcite and 118, 268, 301, 738 (v₄), 750 (v₄), 1074 (v₁) and 1089 (v₁) cm⁻¹ of vaterite as shown in Figure 2.5 [40-45].

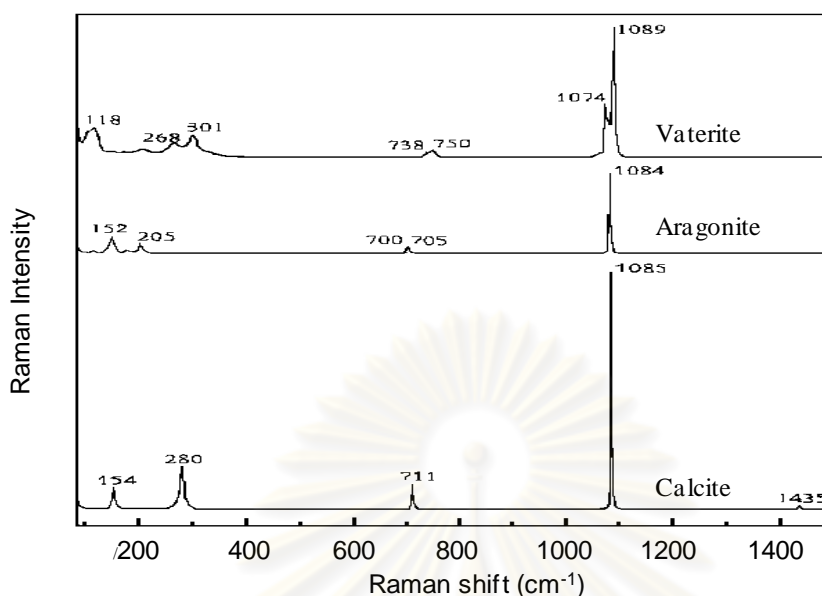


Figure 2.5 Raman spectra of CO_3^{2-} : calcite (A), aragonite (B) and vaterite (C) [40].

Table 2.3 Raman band assignments of pearl

Wavenumber (cm^{-1})	Band assignments
1083	Symmetric stretching vibration of CO_3^{2-}
702	In-plane bending vibration of C-O bonds of CO_3^{2-}

(2) Conchiolin protein

Organic matrix of pearl is called conchiolin protein. These layers are separated by sheets of conchiolin protein of 10-50 nm thickness. Conchiolin protein was destroyed at 550-600 °C. The conchiolin contains water soluble and water insoluble fractions. It is incorporated in each platelet, and silk fibroin-like proteins and the polysaccharide chitin form a water insoluble organic framework between the nacre layers and around each platelet. The conchiolin components are glycine and alanine approximately 24.3% and 14.0%, respectively were the major amino acid as shown in Table 2.3 [45-53].

Table 2.4 Amino acid composition of conchiolin protein in pearls [9].

Amino acid	Conchiolin protein*		
	Nacre of pearl	Nacreous substance of shell	Prismatic substance of shell
Leucines	9.2	13.6	9.0
Phenylalanine	1.1	0.0	16.9
Valine	2.1	0.5	1.0
Tyrosine	2.7	7.2	3.0
Proline	0.0	0.0	7.9
Alanine	14.0	16.3	4.6
Glutamic acid	3.1	1.5	1.5
Threonine	0.6	9.3	0.3
Aspartic acid	6.2	2.2	3.7
Serine	5.4	2.1	3.5
Glycine	24.3	12.8	16.8
Arginine	7.2	15.3	10.2
Lysine	7.4	3.3	1.5
Cystine/2	12.2	11.8	14.7

* Presented in gram of amino acid residue per 100 g of protein.

2.1.2 Type of pearls

Basically, all pearls can be listed in two categories: freshwater pearls and saltwater pearls [1-8].

Freshwater pearls are form in various species of freshwater mussels, which live in lakes, rivers, ponds and other bodies of freshwater.

Saltwater pearls can grow in several species of marine pearl oysters in the family *Pteriidae*.



Figure 2.6 Types of pearl: freshwater pearls and saltwater pearls [3].

Pearls can also be divided into natural pearls, cultured pearls and imitated pearls.

Natural pearls are formed randomly and really are simple accidents of nature. When a certain type of irritant, such as a parasite becomes lodged in the tissue of a mollusk, the animal responds by secreting a calcium carbonate substance called nacre to coat the intruder and protect the mollusk. Natural pearls are made by oysters and mollusks.

Cultured pearls formed by an oyster and composed of concentric layers of a crystalline substance called nacre deposited around an irritant placed in the oyster's body by human. Cultured pearls also are grown by mollusks with human intervention. That is an irritant introduced into the shells caused a pearl to grow.

Imitated pearls are man-made with shell, glass, plastic or organic materials.

2.2.3 Quality of pearls

The 6 factors that classify the quality of pearls are as follows: value and beauty of pearls: luster, nacre thickness, surface quality, size, color and shape.

Luster is the measure of quantity and quality of light that is reflected from the surface of pearl. The luster of good quality pearls is sharp and bright. One should be able to see the reflection clearly on the surface of a pearl.



Figure 2.7 Level of lustrous pearls [3].

Nacre thickness is more important factor in saltwater pearls than that of cultured freshwater pearls because it affects both the beauty and durability of the pearls.

Surface quality is completely clean with no scratches, pits, bumps or wrinkles visible to the naked eye and may be designated spotless.



Figure 2.8 The surface of pearl [3].

Size: Pearls are measured by their diameter in millimeters. The average pearl size sold today is between 6.5 mm and 7.0 mm. If all other quality factors equal, the size of a pearl will determine its value.



Figure 2.9 The size of pearls [3].

Color: Pearls have a variety in color, ranging from white to black and every shade in between. It is important to distinguish between the color and the overtone. For naturally pearls, the colors are white, champagne, aqua, green, golden, and black.



Figure 2.10 The color of pearls [4].

Shape: A perfectly round pearl is very rare in nature. The rounder the pearl is the more valuable. Baroque pearls are not symmetrical in shape but it can be lustrous and appealing. Pearls are not round have price less than round pearls.



Figure 2.11 The shape of pearls [3].

2.2.4 Enhancement of low quality pearls

Low quality pearls can be enhanced by bleaching, polishing, coating, filling, drying and irradiation in order to make more value of low quality pearls because high quality pearls are higher price [6].

Bleaching: Most white cultured pearls are bleached to purify their white color. This treatment also makes them easier to match because it makes the colors of the pearls more uniform and similar to each other.

Polishing: This technique is aimed to remove some surface blemishes and increase luster of natural and cultured pearls.

Coating: This technique is aimed to coat the surface of pearl in order to enhance its luster.

Filling: If a pearl has partially hollow or has a loose nucleus, people will fill the void with an epoxy substance. This will make the pearls more solid and improve their durability. Fillings can be detected with x-radiographs.

Irradiation: When light color pearls are bombarded with gamma rays, the irradiated pearls will achieve an iridescent bluish or greenish gray color.

Oiling is also used to improve pearl luster.

Dyeing is the most often used technique to get colorful pearls that people want. Dyed pearls do not fake, but people can get them easier than the pearls of natural color.

2.2 Silk fiber

Silk fiber is the natural protein polymer. It is produced by the silkworm so as to form cocoon. The silk fiber mainly component consists of two proteins, sericin and fibroin as well as various impurities: fats, waxes, dyes, and mineral salts. The fibroin content is 66.5-73.5 wt%, and the sericin content is 26.5-33.5 wt% of the total silk fiber [10-13]. Silk fibroin is the main structural protein of silk fiber and sericin is the water soluble glue-like protein. Raw silk fiber consists of two fibroin strands which sericin acts as gum for adhesive. The single fibroin strand is produced several microfibrils and stick together to form the microfibrils packs nanofibrils. The structure of single silk fiber is shown in Figure 2.12 [11].

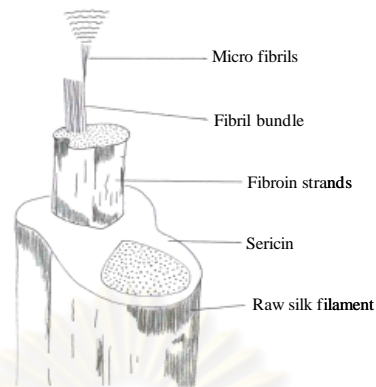


Figure 2.12 Structure of the silk fiber.

2.2.1 Silk fibroin structure

Silk fibroin composes of heavy chains (350 kDa) and light chains (25 kDa) [9]. The heavy chains are a major structural protein of silk fibroin which mainly consists of the recurrent amino acid sequence $(\text{Gly-Ala-Gly-Ala-Gly-Ser})_n$ [7-11]. The crystallinity of silk fibroin fiber consists of antiparallel β -sheet which is aligned along the axis of the fiber. However, silk fibroin protein is classified to four levels of protein structure [54-55].

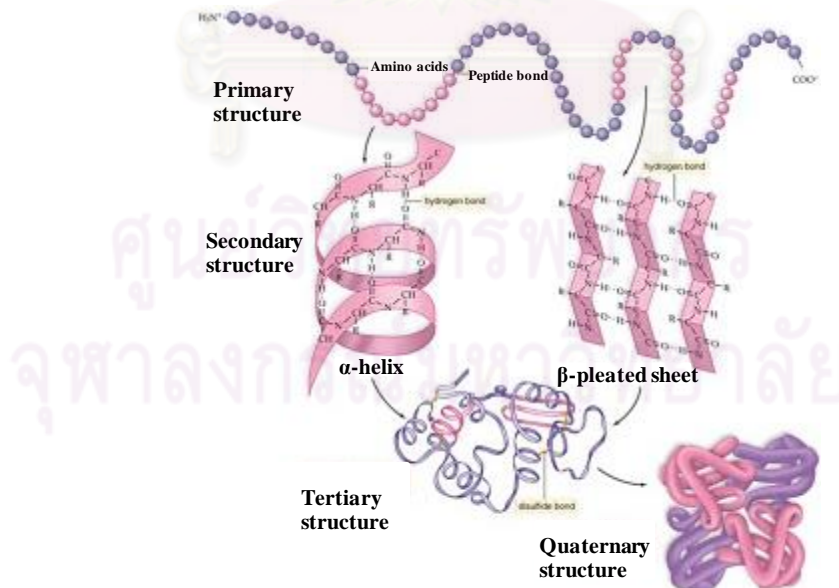


Figure 2.13 The four levels of protein structure [56].

Primary structure refers to the linear sequence of amino acid in the polypeptide chains. Repeating units of silk fibroin are mainly composed of glycine and alanine blocks that the sequences are $-(\text{Gly-Ala-Gly-Ala-Gly-Ser})_n$. The sequence of silk protein amino acids are non-polar side groups.

Secondary structure refers to the formation of a regular pattern of twists or kinks of the polypeptide chain. The major common types of protein are the β -pleated sheet and α -helix structures.

Tertiary structure refers to the three dimensional globular structure formed by bending and twisting of the polypeptide chain, which many secondary structures are organized into multiple domains. The domains are composed of the β -pleated sheet and α -helix structures are interacted via side group of non-polar amino acid with van der Waals force.

Quaternary structure refers to the complex of two or more globular/tertiary structures.

2.2.2 Secondary structure of silk fibroin

Silk fibroin has four common types of secondary structure that are random coil, α -helix, β -turns and β -pleated sheet structures. Silk fibroin consists of two phases: crystalline and amorphous regions. Crystalline regions are formed by the repetitive sequences of hydrophobic blocks $(\text{Gly-Ala-Gly-Ala-Gly-Ser})_n$ which identified as the β -pleated sheet structure as shown in Figure 2.14 a-b [7-11]. The β -pleated sheet consists of the multiple β -strands which refer to a single continuous polypeptide backbone of amino acids as shown in Figure 2.14. Multiple of adjacent β -strands are aligned along in the same direction from N or C terminus formed hydrogen bond between each other that is referred to parallel β -pleated sheet. The β -turn structure is found at turns of the β -pleated sheet which composed of four consecutive residues. The β -turn structure is classified to two types; Type I and Type II. Type I having side chain of amino acid was the same direction and Type II having side chain of amino acid was opposite direction as shown in Figure 2.14 c-d.

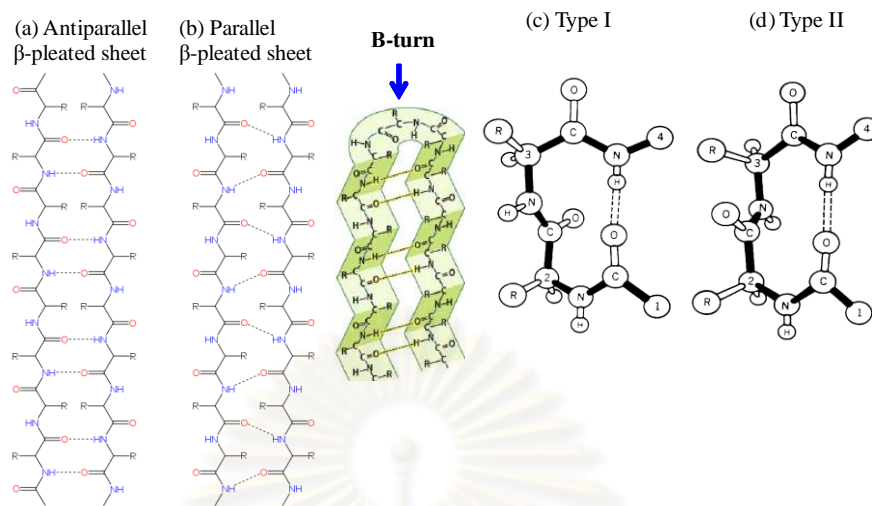


Figure 2.14 The antiparallel (a) and parallel β -pleated sheet structures (b) [57]. Then, the β -turn structure is classified to Type I (c) and Type II (d) [58].

The amorphous regions are identified as the α -helical structure and the random coil are shown in Figure 2.15. The α -helix structure refers to polypeptide chain twists itself to spiraling and form intra-molecular hydrogen bond. A random coil is randomly conformation which does not have the specific shape. It is the statistical distribution of shapes for all the chains in the population of macromolecules.

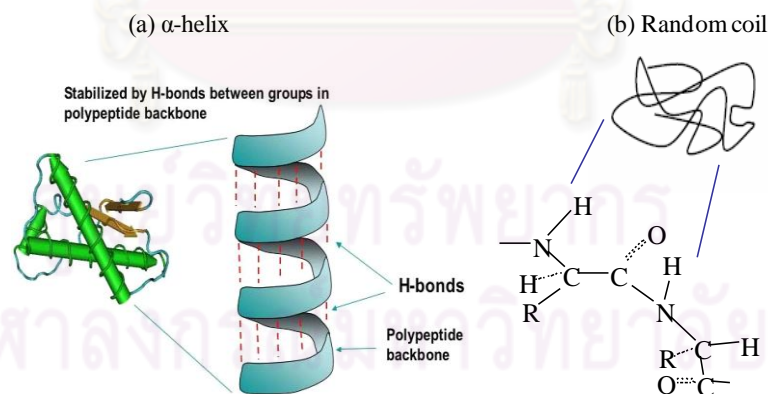


Figure 2.15 The secondary structure: (a) the α -helix and (b) random coil structure [59].

2.2.3 Chemical composition of silk fibroin

Bombyx mori silk fibroin consists of more than 16 amino acids which components are glycine, alanine, and serine (3:2:1 molar ratio) approximately 44.6%,

29.4%, and 12.1%, respectively [11-13]. The amino acid compositions of *Bombyx mori* silk fibroin is shown in Table 2.4.

Table 2.5 Amino acid composition of silk fibroins [10].

Amino acid	Composition*
Glycine	44.60
Alanine	29.40
Valine	2.20
Leucines	0.53
Isoleucine	0.66
Serine	12.10
Threonine	0.91
Aspartic acid	1.30
Glutamic acid	1.02
Lysine	0.32
Arginine	0.47
Histidine	0.14
Tyrosine	5.17
Phenylalanine	0.63
Proline	0.36
Tryptophan	0.11
Methionine	0.10
Cystein/2	0.20

* Presented in gram of amino acid residue per 100 g. of protein.

2.2.4 Preparation of silk fibroin solution

In general, silk fibroin solutions prepared from silk fibroin fibers dissolving in 9.3 M, 9.0 M and 9.5 M LiBr. Furthermore, it prepared from a mixed solution of calcium chloride, ethanol and water (1:2:8). Then, the solution was dialyzed against water using a cellulose dialysis membrane for 3 days. From the previous studies, it

was found that the silk fibroin solution prepared by using other chemicals such as LiBr, CaCl₂, ZnCl₂, Ca(NO₃)₂, NaOH and KOH [60-66].

In this research, the technique for the simple preparation of silk fibroin solution by dissolution in alkaline solution was developed. This method saves the cost and time of preparation of silk fibrin solution. The silk fibroin solutions are coated on the surface of freshwater cultured pearl and showed the sticking on pearl surface.

2.3 ATR FT-IR microspectroscopy

One of the most common spectroscopic techniques for chemical analysis is infrared spectroscopy. This technique can be determined the chemical functional groups in the sample which can be analyzed sample such as gases, liquids, and solids. Infrared spectroscopy measures the infrared intensity versus wavenumber when it passes through a sample. The frequencies of the infrared radiation are absorbed by the chemical functional group of a sample in specific wavenumber and leading the chemical bonds in the molecule to vibrate. Position of wavenumber and the chemical structure are related to the chemical functional group in a sample. So, infrared spectroscopy is the most popular technique for elucidating structure and identifying composition of the compound.

The molecular vibrations have two major types which are stretching and bending as illustrated in Figure 2.16. The change of the dipole moment during vibration is called *infrared active* that has the effect on the vibration of molecules.

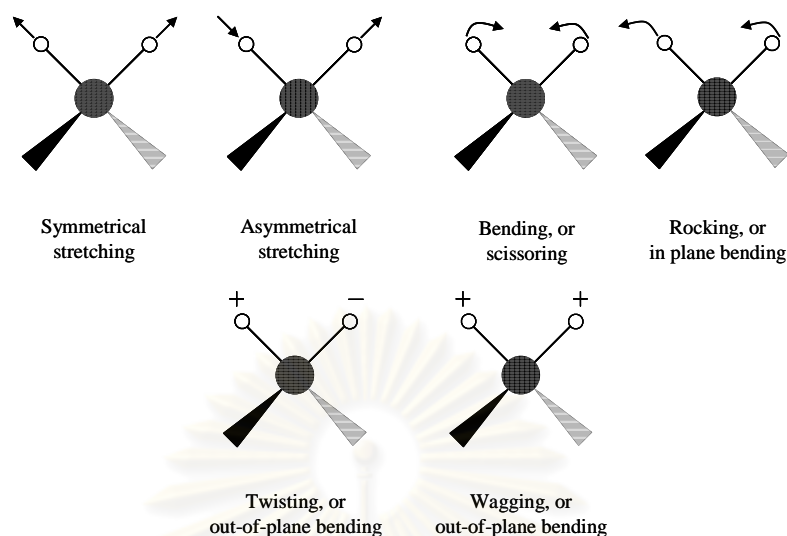


Figure 2.16 Modes of molecular vibration

2.3.1 Fundamental of infrared spectroscopy

Infrared spectroscopy is used to study the interaction of infrared light with matter. When infrared light or electromagnetic radiation impinges with a specimen, the incident beam can be reflected, scattered, transmitted, or absorbed as express by the following relationship [67].

$$I_0 = I_R + I_S + I_T + I_A \quad (2.1)$$

where I_0 is the intensity of the incident beam and I_R , I_S , I_T , and I_A are the reflected, scattered, transmitted, and absorbed beams, respectively. If the sample interpolates between light source and detector as shown in Figure 2.17, the incident beam will be absorbed by the sample which transmitted beam is detected, but reflected and scattered beam are not detected.

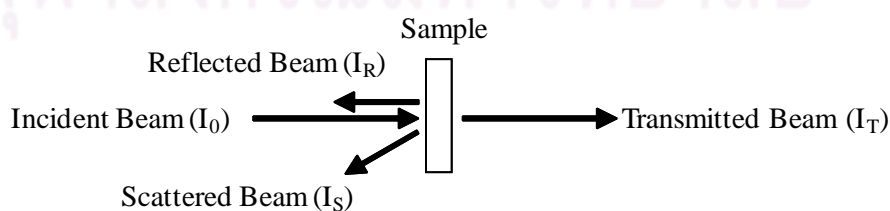


Figure 2.17 Position of beam after incident beam impinges on the sample.

After the transmitted beam is detected, the proportion of transmittance of sample is known by measuring the ratio of the sample attenuated (I_0) and non-attenuated (I) intensities which relationship with the **Beer-Lambert law** as [68].

$$I/I_0 = e^{-A(\bar{\nu})} = e^{-c_2 \varepsilon(\bar{\nu}) l} \quad (2.2)$$

where $A(\bar{\nu})$ is the absorbance of sample at given wavenumber $\bar{\nu}$, c_2 is the concentration of the absorbing functional group, $\varepsilon(\bar{\nu})$ is the wavenumber dependent absorption coefficient and l is the film thickness for the infrared beam at a normal incidence to the sample surface.

2.3.2 Attenuated Total Reflection Fourier Transform Infrared (ATR FT-IR) Microspectroscopy

ATR FT-IR microspectroscopy can analyze the surface of the materials which was the non-destructive technique. This technique is developed for studying the surface arrangement and resolved the problem of transmission technique. The sample is placed in contact with the internal reflection element (IRE), the light is totally reflected and a sample interacts with the *evanescent wave* which resulting in the absorption of radiation by a sample [69]. ATR method is suitable for this research more than the other method such as regular reflection and diffuse reflection method.

2.3.3 Principles of light reflection and refraction

The refraction and reflection occur when electromagnetic radiation passes a boundary between two media with different refractive indices. The equality of the incidence angle and reflection angle are required the process of reflection. In this case, reflection is specula. Electromagnetic radiation passed from one medium to another will suddenly change the direction of beam and it will be detected the difference in propagation velocity through two media. If light propagates through an incident medium with the refractive index n_1 and enters a medium with the refractive index n_2 as shown in Figure 2.18. The light path will be changed and extent of refraction is given by the following relationship known as *Snell's law* [67].

$$\frac{\sin \alpha_1}{\sin \alpha_2} = \frac{n_2(\bar{\nu})}{n_1(\bar{\nu})} \quad (2.3)$$

where α_1 is the incidence angle and α_2 is the refraction angle.

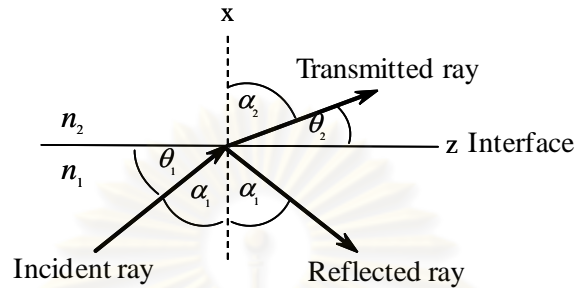


Figure 2.18 The reflection and refraction of the plane wave at the dielectric interface.

Total internal reflection is the travelling light through a high refractive index to a lower index medium (i.e., $n_1 < n_2$) at an incident angle greater than the critical angle. The critical angle can be derived from *Snell's law* and illustrated in Equation 2.4 [70].

$$\theta_c = \sin^{-1}(n_2(\bar{\nu})/n_1(\bar{\nu})) \quad (2.4)$$

Accordingly, total internal reflection spectroscopy can record the optical spectrum of the sample material that contacts an optically denser medium. The wavelength dependence the reflectivity of this interface can be measured introducing light into the denser medium. The reflectivity of this technique is measured the interaction of the electric field with the material.

2.3.4 Internal reflection element (IRE)

The internal reflection element (IRE) is the material of high refractive index material and is transparent throughout the mid-infrared spectral region [69]. Typical IREs are zinc selenide (ZnSe), silicon (Si), germanium (Ge), and diamond as shown in Table 2.5 which IRE material has an effect on the ATR measurement because the refractive index has affected the depth of the penetration.

Table 2.5 The IRE materials used in ATR measurement.

Material	RI at 1000 cm^{-1}	ATR spectral range (cm^{-1})	Hardness (kg m/m^2)	Depth of penetration at 45° , 1000 cm^{-1} (μm)
ZnSe	2.4	15000-650	120	2.01
Si	3.4	8900-1500, 360-120	1150	0.85
Ge	4.0	5500-675	550	0.66
Diamond	2.4	25000-100	5700	2.01

Two groups of IRE—single-reflection and multiple-reflection IRE are shown in Figure 2.19. The materials that have adequately strong or contrast absorption would be recorded the spectra by single-reflection IRE [70]. On the other hand, the multiple-reflection can be used to enhance the contrast that cannot be obtained with single-reflection. Designed IRE shapes have been developed such as hemi-cylinder, microhemicylinder, and hemisphere depending on simply instrumentation and nature of samples.

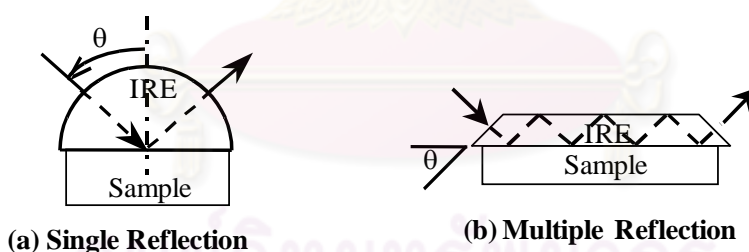


Figure 2.19 The illustration of IRE configurations used in ATR experimental setups: Single reflection hemispherical crystal (A), and Multiple reflections (B).

2.3.5 ATR spectral intensity and depth profiling

According to the critical angle (θ_c), the real portion of the complex refractive index is the ratio of refractivity from the high refractive index medium of IRE ($n_1(\nu)$) and the lower refractive index medium of sample ($n_2(\nu)$) at the frequency (ν). The

complex refractive index of medium consists of real and imaginary part as follows [71]:

$$\hat{n}(\nu) = n(\nu) + ik(\nu) \quad (2.5)$$

where $\hat{n}(\nu)$ and $n(\nu)$ are the complex refractive index and the refractive index of medium, respectively. i is equal to $\sqrt{-1}$, and $k(\nu)$ is the absorption index at frequency (ν).

ATR technique has two important phenomena—**total reflection phenomenon and attenuated total reflection (ATR) phenomenon**. These phenomena will occur when incident light travels from IRE and impinges at the interface. This interface is the zone between the IRE and sample with incident angle greater than the critical angle. The difference between these phenomena is the absorption capability of sample (lower refractive index medium). Interface of absorbing medium has strong electric field because no light travels across the boundary and it is interesting to note that the magnitudes of the interaction between light and sample can be expressed in term of absorbance. The absorptance of the ATR configuration is related to the reflectance as shown in equation.

$$A(\theta, \nu) = 1 - R(\theta, \nu) \quad (2.6)$$

where $A(\theta, \nu)$ is the absorbance and $R(\theta, \nu)$ is the reflectance.

Generally, the absorbance in ATR can be expressed in terms of the experimental conditions and material characteristic as shown in equation.

$$A_l(\theta, \nu) = \frac{4\pi\nu}{n_1 \cos\theta} \int_0^\infty n_2(\bar{\nu}) \langle \Sigma_{zi}^2(\theta, \nu) \rangle dz \quad (2.7)$$

where $A(\theta, \nu)$ is absorbance that l indicates the polarization of the incident beam. $\langle E_{zi}^2(\theta, \nu) \rangle$ is the mean square electric field (MSEF) at depth z , n_1 is the refractive index of the IRE, $n_2(\nu)$ is the refractive index and $k_2(\nu)$ is the absorption index of the sample.

Depth profiling can be determined by ATR FT-IR spectroscopy. It has MSEF under total internal reflection condition. An exponential function of distance from the

interface of IRE and sample is decayed as power of MSEF at interface. The decay pattern of MSEF can be expressed by:

$$\langle E_z^2(\theta, \nu) \rangle = \langle E_0^2(\theta, \nu) \rangle e^{-2z/d_p(\theta, \nu)} \quad (2.8)$$

where $\langle E_0^2(\theta, \nu) \rangle$ is the MSEF at the interface, $\langle E_z^2(\theta, \nu) \rangle$ is the depth z and $d_p(\theta, \nu)$ is the penetration depth.

Penetration depth of light into the sample can be determined by the decaying of the MSEF value to 1/e of its value at the interface. The experimental parameter of penetration depth is given by following equation:

$$d_p(\theta, \nu) = \frac{1}{2\pi\nu n_1 \left(\sin^2 \theta - (n_2/n_1)^2 \right)^{1/2}} \quad (2.9)$$

where $d_p(\theta, \nu)$ is the penetration depth, n_1 is the refractive index of the IRE and n_2 is the refractive index of the sample.

2.3.6 Principle of light entering the Ge μ IRE

Hemispherical dome of a miniature cone-shaped Ge IRE facilitates the coupling of focused radiation travelling into the IRE by minimizing the reflection loss at air/Ge interfaces. If nearly perfect coupling is assumed, the radiation will transmit through air/Ge interfaces of dome and impinges the Ge/air interface of tip without the significant change in the angle of incidence [72]. For ensuring the good contact, circular tip of the IRE should be the hemispherical surface. The contact area is $\leq 100 \mu\text{m}$ in diameter. Good contact was achieved with minimal force exerted on the tip. For the Ge μ IRE ($n_{\text{Ge}} = 4.0$), the critical angle for the total internal reflection (TIR) at interfaces with air ($n_{\text{air}} = 1.0$) is 14.48° and an organic medium ($n_{\text{organic}} = 1.5$) is 22.02° , respectively. As the result, parts of coupled radiation can be employed for ATR FT-IR investigation of the material having an optical contact with the miniature IRE tip. To eliminate interference from the internal reflection associated with a radiation having an angle of incidence smaller than the critical angle, an opaque circular adhesive tape is placed on the center of hemispherical dome. Due to an effective condensation of the coupled radiation and an efficient light-matter do

interaction under the ATR condition at the tip of the IRE. ATR FT-IR spectra of small specimen or small area can be acquired with the superb spectral quality.

In this experiment, the Ge IRE is designed the optical focusing radiation in range from 15° to 35° . The cause is that the coupling of these focused the radiations. It will make the angle of incidence at the sampling surface greater than the critical angle.

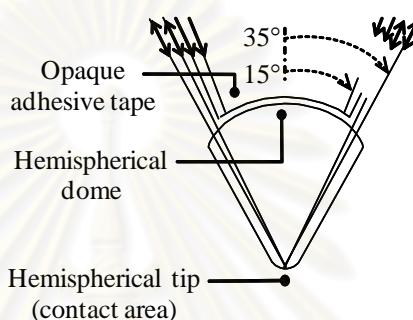


Figure 2.20 The ray tracing within the infrared objective focusing radiation travelling within the Ge μ IRE.

2.3.7 Homemade Slide-on Ge μ IRE Accessory

The homemade slide-on Germanium μ IRE accessory supplied with cone-shaped Ge μ IRE which is the small sampling area ($50 \times 50 \mu\text{m}^2$).

The homemade slide-on Ge μ IRE accessory is provided by *Sensor Research Unit, SRU, Department of Chemistry, Faculty of Science, Chulalongkorn University, Thailand*. The homemade slide-on Ge μ IRE consists of two parts as shown in Figure 2.21. The first component is the slide-on housing which is designed for placing slide-on Ge μ IRE into the continuum IR microscope. The second component is slide-on Ge μ IRE which is designed for the alignment adjusted to obtain high energy throughput. The slide-on Ge μ IRE is slidden into the position and locked by knob of slide-on housing which is located on built in 15x Schwarzschild-Cassegrain infrared objective as shown in Figure 2.22. Incident radiation from IR microscope is coupled into the dome-shaped Ge μ IRE which impinges on the tip when total internal reflection occurs at the Ge tip. The couple radiation can be employed for ATR FT-IR spectra acquisition as the tip of the Ge μ IRE contact the surface of sample.

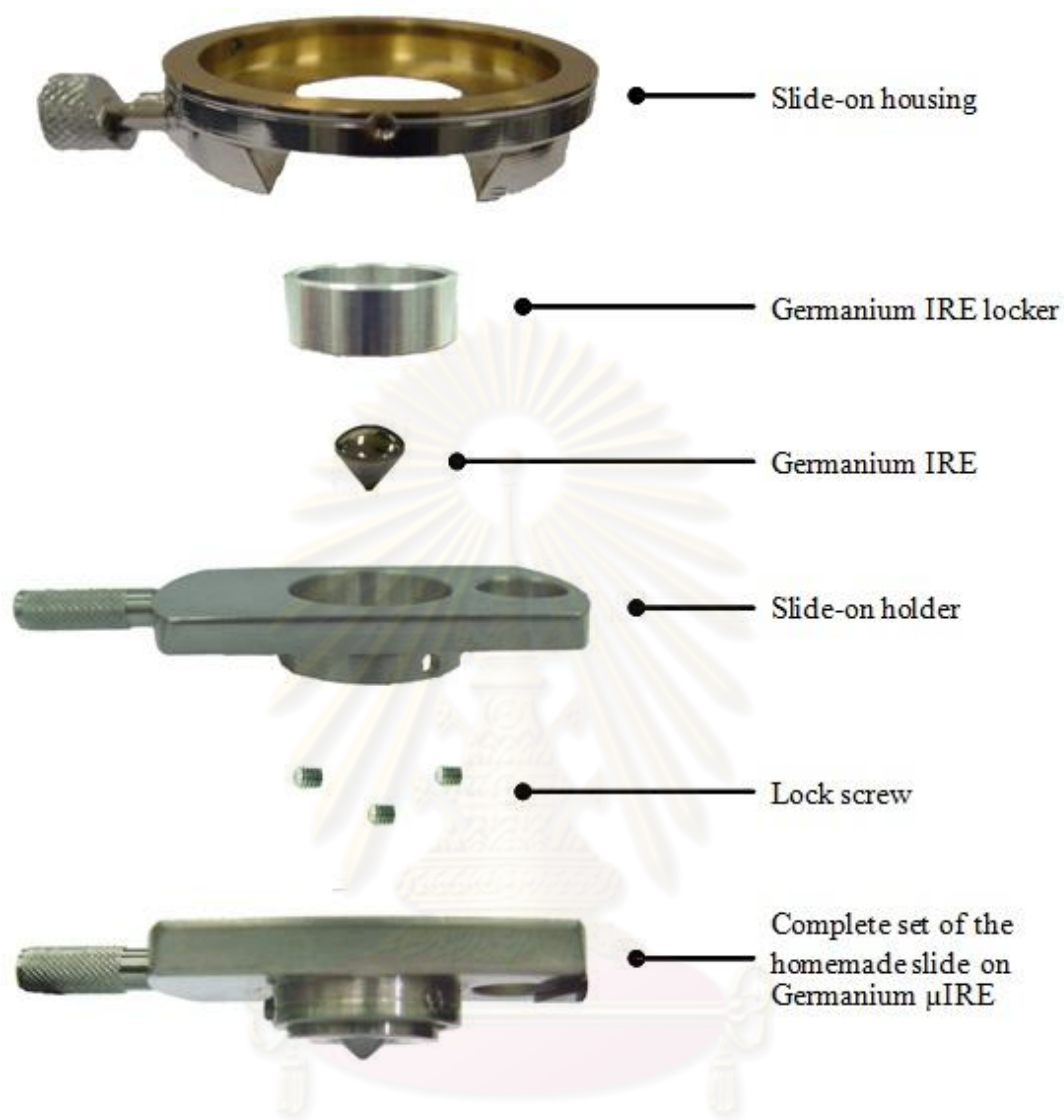


Figure 2.21 Slide-on housing and parts of the homemade ATR accessory with germanium μ IRE miniature.

2.4 Raman microspectroscopy

2.4.1 Theory

Raman scattering explains incident radiation of frequency (ν_0). Incident radiation of frequency is considered as the stream of particles (photons) undergoing collision with molecules. If the collision was perfectly elastic, there will be any exchange of energy between the photons and the molecule which will be exchanged of energy between the two if collision was inelastic. Molecule can gain or lose energy which is equal to the energy difference (ΔE) between any two of its allowed states. If molecule gains energy, the scattered photons will be had energy $\nu_0 - \nu_m$ which $\nu_m = \Delta E/h$ (*Stokes scatter*) and if it loses energy the scattered photon will have energy $\nu_0 + \nu_m$ (*anti-Stokes scatter*). The most of molecules of the system return to the original state from the virtual state giving the Rayleigh scatter. Different processes gives rise to Rayleigh, Stokes ad anti-Stokes scatter are illustrated in Figure 2.23 [76].

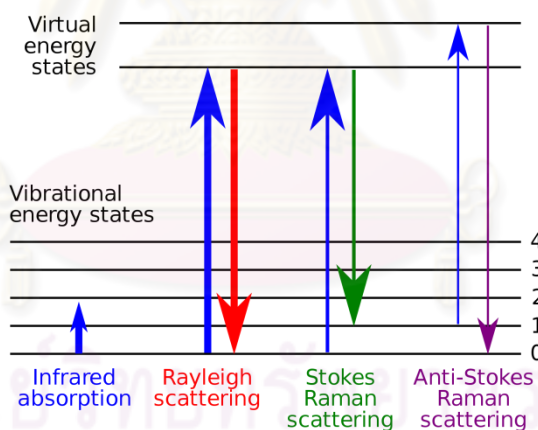


Figure 2.23 The energy level diagram for Raman spectra.

The vibrational spectroscopies provide key information of the molecular structure or determine the chemical identity of the sample.

2.4.2 Raman spectroscopy

Raman spectroscopy has major advantages over other analytical techniques that are very easy for sample preparation and the rich information content. This technique is non-destructive that is no need to dissolve solids, press pellets, compress the sample

against optical elements or otherwise alter the physical or chemical structure of a sample. Thus, Raman has been used extensively for analysis of such physical properties as crystallinity, phase transitions and polymorphs.

Raman spectroscopy is the light scattering technique that is collected the spectrum to place a sample into the excitation beam and collects the scattered light.

Basics of Raman spectrometer is divided into two technologies for collection of the spectra: dispersive Raman and Fourier transform Raman spectrometers. Each technique has unique advantages and is ideally suited to specific analyses.

2.4.3 Dispersive Raman spectroscopy

Dispersive Raman spectrometer is measured the wavelength and intensity of inelastically-scattered light which is used visible lasers, the grating, and charged-coupled detectors (CCD) to collect data. Dispersive Raman spectroscopy usually employs visible laser radiation of typical laser wavelengths of 780 nm, 633 nm, 532 nm and 473 nm although others are common. One advantage of using shorter wavelength lasers is the enhancement in the Raman scattering. Efficiency of Raman scattering is proportional to $1/\lambda^4$. So there is the strong enhancement as the excitation laser wavelength becomes shorter. Instrument throughput and sensitivity required the using single grating for more than one laser wavelength or more than one resolution. The gratings should be specifically matched to the laser and experimental conditions [75-79].

For dispersive Raman used the CCDs commonly are silicon devices with very high sensitivity. The detecting surface of the CCD in two dimensional arrays of light sensitive elements is called pixels which each pixel acts as the individual detector. So each dispersed wavelength is detected by a different pixel.

2.4.4 Raman Microscope

Raman spectroscopy with a microscope has the advantage on the couple of the strength with the flexibility that allows the analysis of very small samples. The aim of microscopy is to analyze the smallest samples and distinguish the substance of interest from its surroundings as spatial resolution in microscopy. The highest spatial resolution, it is attained by using small pinholes or “*apertures*” somewhere in the

microscope. To reach higher resolution is necessary to use smaller apertures, when light passes through these smaller apertures, diffraction becomes the limiting factor. Therefore, the spatial resolution is limited by diffraction limit of laser through objective as shown by the following equation:

$$D = \frac{1.22\lambda}{\text{n.a}}$$

where n.a. is the numerical aperture of the collection optics, λ is the wavelength of the radiation and D is the diameter of collimated beam.



CHAPTER III

EXPERIMENTAL SECTION

Generally, coating is applied to surface treatment in order to up-grade the low quality pearls to high-grade quality pearls. In this study, the silk fibroin are applied on pearl surfaces to protect the surface and increase the luster. The molecular conformation of silk fibroin coated on pearl surface was analyzed by ATR FT-IR microspectroscopy; homemade Ge μ IRE was employed to investigate ATR FT-IR spectra from pearl surfaces. The luster measurements after coating are performed by UV-Visible spectroscopy with Integrating Sphere Diffuse Reflectance technology.

3.1 Materials

1. *Bombyx mori* silk nests from Queen Sirikit Sericulture Regional Office (Northern Part: Phrae Province)
2. Sodium carbonate (Na_2CO_3) was purchased from Merck KGaA, Thailand.
3. Lithium bromide (LiBr) was purchased from Sigma-Aldrich Laborchemikalien GmbH, Thailand.
4. Sodium hydroxide (NaOH) was purchased from CARLO ERBA reagents, Thailand.
5. Potassium hydroxide (KOH) was purchased from CARLO ERBA reagents, Thailand.
6. Hydrochloric acid (HCl) was purchased from Merck KGaA, Thailand.
7. Methanol was purchased from Merck KGaA, Thailand.
8. Deionized (DI) water
9. Filter papers (Whatman Schleicher & Schuell, No.1), Thailand
10. Hydrogen peroxide was purchased from Merck KGaA, Thailand.

3.2 Experimental section

3.2.1 Preparation of *Bombyx mori* silk fibroin solution

The virgin silk fibers were degummed by 100mL of 0.02 M Na_2CO_3 at 60 °C until the solution changing from pale yellow to colorless. After that, the degummed silk fibroin was washed 2 times with DI water. Finally, we used degummed silk fibers in the preparation of silk fibroin solution.

For the other researches, the preparation of silk fibroin solution were performed by using 100 mL of 9.3 M LiBr solution in order to dissolve 5 g of silk fibroin fibers. This solution was filtered by a filter paper (Whatman[®] Schleicher & Schuell, No.1) to remove a small amount of insoluble silk. After that, the solution was dialyzed in DI water by dialysis tubing cellulose membrane for 3 days at room temperature for removing salts (LiBr) as shown in Figure 3.1.

In this work, silk fibroin solution were prepared by using methods as follows:

(1.) Two kinds of alkaline solution (NaOH and KOH) are used for the preparation of silk fibroin.

Getting started with NaOH solution; the silk fibroin fiber was dissolved in 100 mL of 0.2 M NaOH solution. If silk fibroin fiber did not dissolve, then each of the 0.2 g of solid NaOH is added to the solution until silk fibroin fiber was complete dissolved.

Repeat the above procedure by using KOH instead of NaOH and using 0.28 g of KOH in each adding instead of 0.2 g of NaOH.

After that, this solution was filtered by a filter paper (Whatman[®] Schleicher & Schuell, No.1) to remove a small amount of insoluble silk. Then, the solution was adjusted the pH in the range of 7 with HCl as shown in Figure 3.1.

(2.) The varying weight of silk fibroin fibers are as follows: 2, 3, 4 and 5 g were dissolved in NaOH and/or KOH solution.

These silk fibroin solutions coated on surface of freshwater cultured pearl.

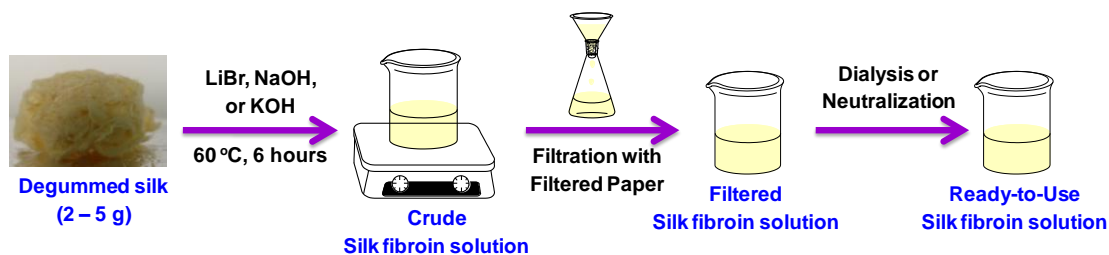


Figure 3.1 Preparation of *Bombyx mori* silk fibroin solution were performed by using LiBr, NaOH and/or KOH to dissolve 2 g (2 % w/v), 3 g (3 % w/v), 4 g (3 % w/v) and 5 g (5 % w/v) of silk fibroin fibers. Then, the solution was dialyzed in DI water by dialysis and/or was adjusted to the neutral pH.

3.2.2 Preparation of coated silk fibroin on pearl surfaces

Freshwater cultured pearls are washed with DI water or DI water plus 10% H₂O₂ for cleaning the surface of pearl. Then, the pearls were soaked in silk fibroin solution. The pearls soaked in silk fibroin solution at room temperature and boiled at 50 °C or 100 °C for 30, 60 and 90 min and then air dried at room temperature. After that, the alcohol (isopropyl alcohol (2-propanol), ethanol and methanol) treatment was performed as shown in Fig 3.2. The process of coating silk fibroin on pearl surfaces was shown in Fig 3.3 and the molecular conformation of silk fibroin coated on pearl surfaces was analyzed by ATR FT-IR and Raman microspectroscopy and the luster measurement of treated pearl was performed by UV-Visible spectroscopy.

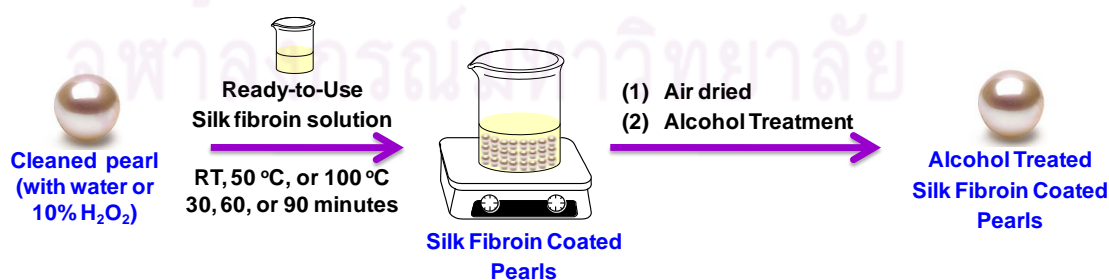


Figure 3.2 The cleaning surface of pearl and coated with silk fibroin solution plus alcohol treatment.

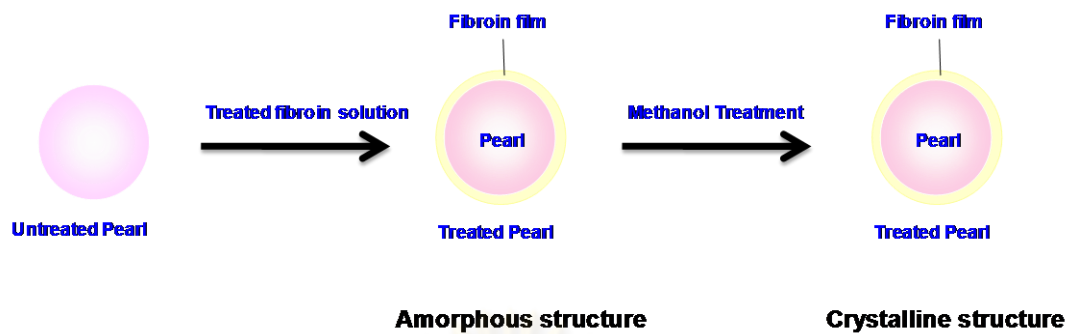


Figure 3.3 Process of silk fibroin coating on pearl surfaces.

3.2.3 Resistance to corrosion of pearl surface

In this work, resistance to corrosion of pearl surface were tested by using methods as follows: (Figure 3.4)

(i) Freshwater cultured pearl was boiled in water at 100 °C for 10 min. Then, pearl with soaked solvent and detergent (tap water, NaOH solution pH 8, 9 and 10, HCl solution pH 4, 5 and 6, detergent, shower cream, body lotion, shampoo and perfume) for 19 hours.

(ii) Freshwater cultured pearl coated with silk fibroin solution was boiled in water at 100 °C for 10 min. Then, they soaked with solvent and detergent for 19 hours.

(iii) Freshwater cultured pearl coated with silk fibroin solution plus alcohol treatment was boiled in water at 100 °C for 10 min. Then, they soaked with solvent and detergent for 19 hours.

(iv) After that, all kinds of pearls were analyzed by ATR FT-IR, Raman microspectroscopy and Microscope for resistance to corrosion of pearl surface and stuck of silk fibroin on pearl surface.

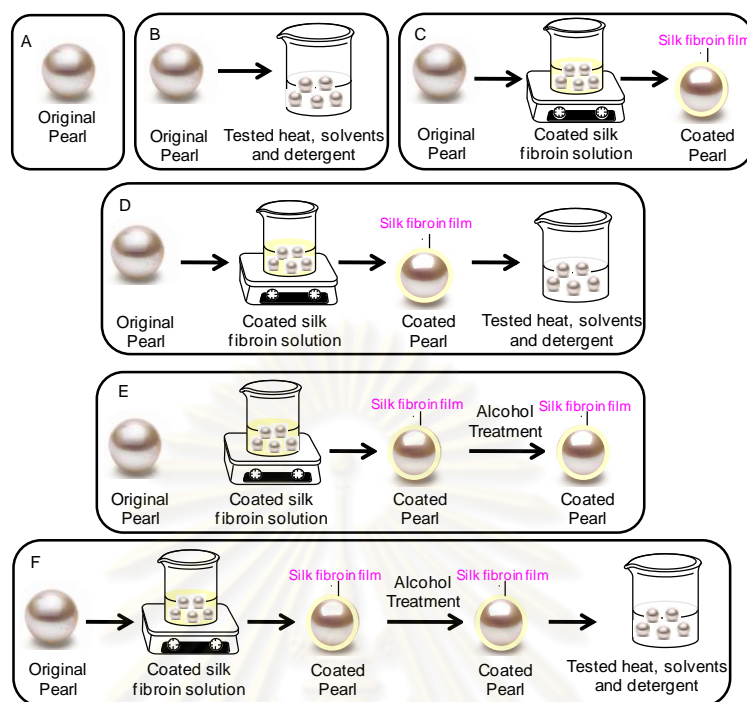


Figure 3.4 The method tested resistance to corrosion of pearl surface (freshwater cultured, coated silk fibroin pearl, alcohol treatment-coated silk fibroin pearl).

3.3 Characterization of coated silk fibroin on pearl surface

3.3.1 ATR FT-IR microspectroscopy

The molecular conformation of freshwater cultured pearls and silk fibroin coated on pearl surfaces was acquired by ATR FT-IR microspectroscopy. All ATR spectra were recorded in the frequency ranging from 750 to 4000 cm^{-1} on Nicolet 6700 FT-IR spectrometer with a mercury-cadmium-tellurium (MCT) detector at resolution of 4 cm^{-1} . All samples were collected at 128 co-addition times. The Ge μ IRE was placed on the objective microscope and pearls samples on holder were positioned on the microscope stage. After that, the stage of microscope was raised in order to contact Ge μ IRE probe and pearl. The ATR spectra of samples were acquired in the reflection mode of infrared microscope.

3.3.1.1 Instrument

1. Nicolet 6700 FT-IR spectrometer equipped with a mercury cadmium-telluride (MCT) detector.
2. Continuum™ infrared microscope with 15X Schwarzschild-Cassegrain infrared objective and 10X glass objective.
3. Homemade slide-on Ge μ IRE

3.3.1.2 Default Spectral Acquisition Parameter

Nicolet 6700 FT-IR Spectrometer

Instrumental Setup

Source	Standard Global™ Infrared Light Source
Detector	MCT
Beam splitter	Ge-coated KBr

Acquisition Parameters

Spectral resolution	4 cm^{-1}
Number of scans	128 scans
Spectral format	Absorbance
Mid-infrared range	4000-650 cm^{-1}

Advanced Parameters

Zero filing	none
Apodization	Happ-Genzel
Phase correction	Mertz

Continuum™ Infrared Microscope

Instrumental Setup

Detector	MCT
Objective	15X Schwarzschild-Cassegrain
Aperture size	150 μm x 150 μm



Figure 3.5 ATR FT-IR microspectroscopy: (A) Continuum™ infrared microscope attached to the Nicolet 6700 FT-IR spectrometer, (B) the holder of pearl and the slide-on Ge μ IRE is fixed on the position of slide-on housing on the infrared objective, and (C) Homemade slide-on Ge μ IRE.

3.3.2 Raman microspectroscopy

The molecular conformation of freshwater cultured pearls and silk fibroin coated on pearl surfaces were acquired by Raman spectroscopy. All Raman spectra were recorded in the frequency ranging from 50 to 3500 cm^{-1} on DXR Raman spectrometer with Charge Coupled Device (CCD) detector at resolution of 2 cm^{-1} . All samples were collected at 32 co-addition times.

3.3.2.1 Instrument

DXR Raman Microscope

3.3.2.2 Default Spectral Acquisition Parameter

DXR Raman spectrometer

Instrumental Setup

Spectrometer	Visible Raman Microscope
Source	Excitation source (Laser)
Detector	CCD
Laser polarization	Parallel
Laser	532 nm
Grating	900 lines/mm
Range	3500-50 cm^{-1}
Focusing objective	50X Long
Aperture size	150 μm x 150 μm
Spatial resolution	1 μm

Acquisition Parameters

Laser power	10
Spectral resolution	2 cm^{-1}
Number of scans	32 scans
Spectral format	Intensity
Spectrograph aperture	25 μm pinhole

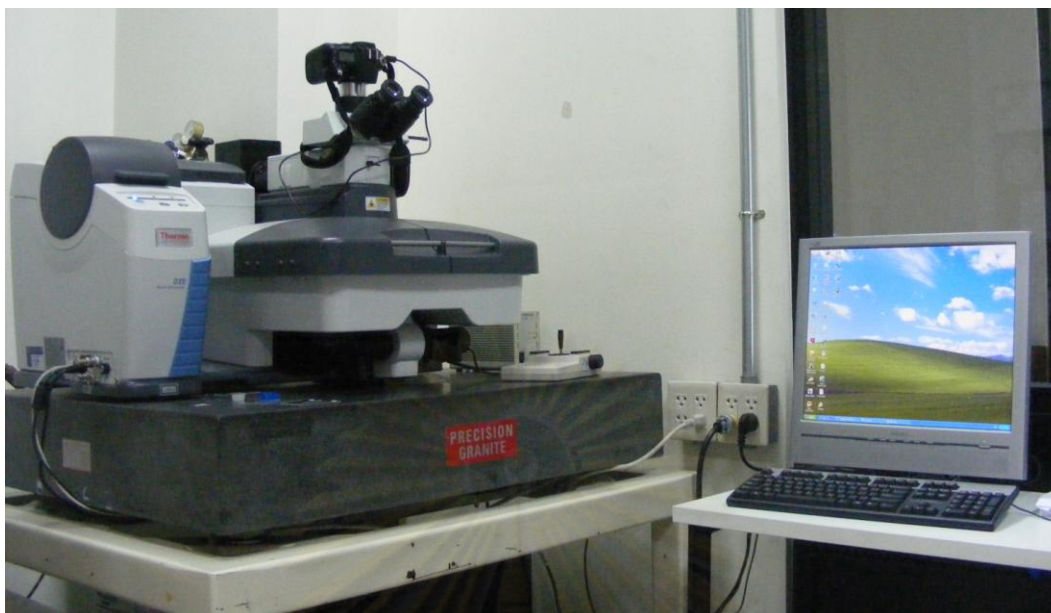


Figure 3.6 DXR Raman Microscope

3.3.3 UV-Visible spectroscopy

The luster is increased after coating with silk fibroin on pearl surfaces. The luster of pearl can be noticeably observed by looking at the treated pearl with your own eyes from the bright side that reflected on the surface of pearl. To confirm the luster of the pearl, it is practically analyzed by Ocean Optics Portable UV-Visible spectrometer with Integrating Sphere Diffuse Reflectance technology as shown in Figure 3.6.

Instrumental Setup

Model	USB4000
Source	Deuterium-Halogen light source DH 2000
Wavelength range	UV-Vis-NIR
Detector	Toshiba TCD1304AP, 3648-element linear silicon CCD array
Grating	600 Line Blazed at 300 nm
Bandwidth	200-1100 nm

Spectral Acquisition Parameter

Software	Ocean Optics Inc. Spectra Suit
Integration time	3-18 milliseconds
Scans to Average	10-25 milliseconds
Box car width	3 nm
Spectral format	Reflection
Spectra range	250-800 nm



Figure 3.6 UV-Visible spectrometer and Integrating Sphere.

CHAPTER IV

RESULTS AND DISCUSSION

Molecular structure and chemical composition of freshwater cultured pearl samples were investigated by ATR FT-IR and Raman microspectroscopy. The spectra manifested that the molecular structure of freshwater cultured pearls had been changed after coating with silk fibroin and elucidated the signature of silk fibroin protein and freshwater cultured pearl. After that, all kinds of pearls were analyzed by ATR FT-IR, Raman microspectroscopy and Microscope for resistance to corrosion of pearl surface and stuck of silk fibroin on pearl surface.

4.1 Chemical information by ATR FT-IR and Raman microspectroscopy

4.1.1 Silk fibroin film

Silk protein has three molecular conformations: random coil, α -helix and β -sheet conformations. We will study the molecular information of silk fibroin protein by ATR FT-IR and Raman microspectroscopy. Figure 4.1 showed ATR FT-IR spectra of silk fibroin film and silk fibroin film treated with methanol. Characteristic peaks at 3280 cm^{-1} (N-H stretching), 1622 cm^{-1} (Amide I), 1514 cm^{-1} (Amide II) and 1233 cm^{-1} (Amide III) assigned to the random coil and α -helix conformation (Figure 4.1 A). The spectrum of silk fibroin film (Figure 4.1 A) suggested the secondary structure of the random coil and α -helix conformation as amorphous form in solution and was water soluble. After methanol treatment, it occurred the shoulder peaks at 1705 cm^{-1} of Amide I and 1264 cm^{-1} of Amide III indicating that the secondary structure was anti-parallel β -sheet conformation (Figure 4.1 B). It indicated silk fibroin changed the secondary structure

from random coil and α -helix to β -sheet conformation as crystalline form after methanol treatment. Methanol extracted the water molecules from silk fibroin molecules due to their polar character and induced the rearrangement of molecular chain of silk fibroin from random coil and α -helix to β -sheet conformation. Further, methanol treatment induced a shift to higher amounts of crystalline β -sheets structures (crystalline structure) and higher hydrophobic.

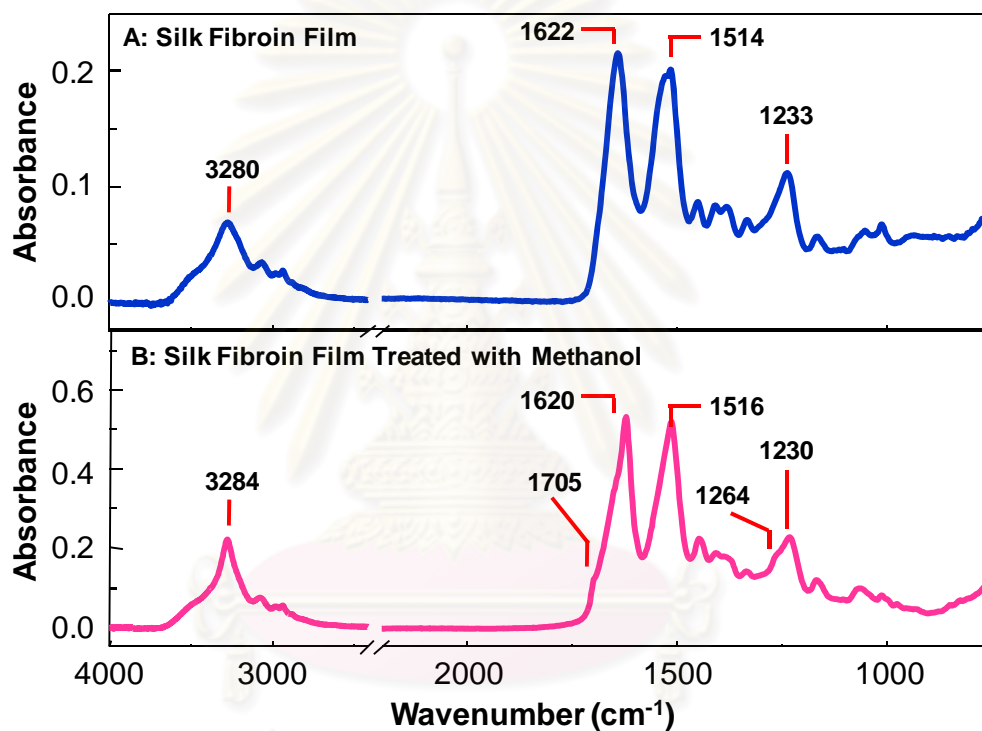


Figure 4.1 ATR FT-IR spectra of silk fibroin film (A) and silk fibroin film treated with methanol (B).

Table 4.1 Band assignments of silk fibroin film by ATR FT-IR microspectroscopy [80-87].

Wavenumber (cm ⁻¹)	Band assignments
3450-3160	<u>Amide A</u> N-H stretching
~ 3100	Overtone of Amide II
2975-2950	Asymmetric C-H stretching of CH ₃
2490-2915	Symmetric C-H stretching of CH ₂
2885-2865	Asymmetric C-H stretching of CH ₂
1698-1690	Anti-parallel <i>β-sheet</i>
1700-1600	<u>Amide I</u> C=O stretching
1540-1510	<u>Amide II</u> N-H bending (wagging) plus C-N stretching
1480-1440	C-H bending (scissoring) of CH ₂
1410-1350	C-H bending (scissoring) of CH ₃
1440-1260	C-H and O-H bending vibration
1300-1225	<u>Amide III</u> N-H bending (twisting) plus C-N stretching and the contribution from O=C-N bending
1175-1165	O-H bending of phenolic residue in Tyr
1100-1050	C-N stretching of RCH ₂ -NH ₂ , R ₂ CH-NH
1090-1000	C-OH stretching vibration
1000-945	C-C skeletal of Gly-Ala sequences

Figure 4.2 showed Raman spectra of silk fibroin film and silk fibroin film treated with methanol. Characteristic peaks at 3309 cm⁻¹ (N-H stretching), 2958 cm⁻¹ (C-H stretching), 1665 cm⁻¹ (Amide I), 1252 cm⁻¹ (Amide III) which Amide I and Amide III suggested the secondary structure of the random coil. The absorption peaks at 1102 and 641 cm⁻¹ (Amide V) indicated the secondary structure of the α -helix (Figure 4.2 A). The spectrum of silk fibroin film (Figure 4.2 A) suggested the secondary structure of the random coil and α -helix conformation as amorphous form in solution. After methanol treatment, it occurred the peaks at 3282 cm⁻¹ (N-H stretching), 2933 cm⁻¹ (C-H stretching),

1665 cm^{-1} (Amide I), and 1235 cm^{-1} (Amide III). The sharp peak at Amide I and Amide III indicated the secondary structure of the β -sheet. The absorption peaks at 1086 cm^{-1} (β -sheet) that was the crystalline structure (Figure 4.2 B). The spectrum (Figure 4.2 A) suggested that methanol changed the secondary structure from random coil and α -helix to β -sheet conformation as crystalline form after methanol treatment. The results of Raman microspectroscopy confirmed the results of ATR FT-IR microspectroscopy. Silk fibroin had the secondary structure of the random coil and α -helix conformation as amorphous form in solution. After methanol treatment, silk fibroin changed the secondary structure from random coil and α -helix to β -sheet conformation as crystalline form

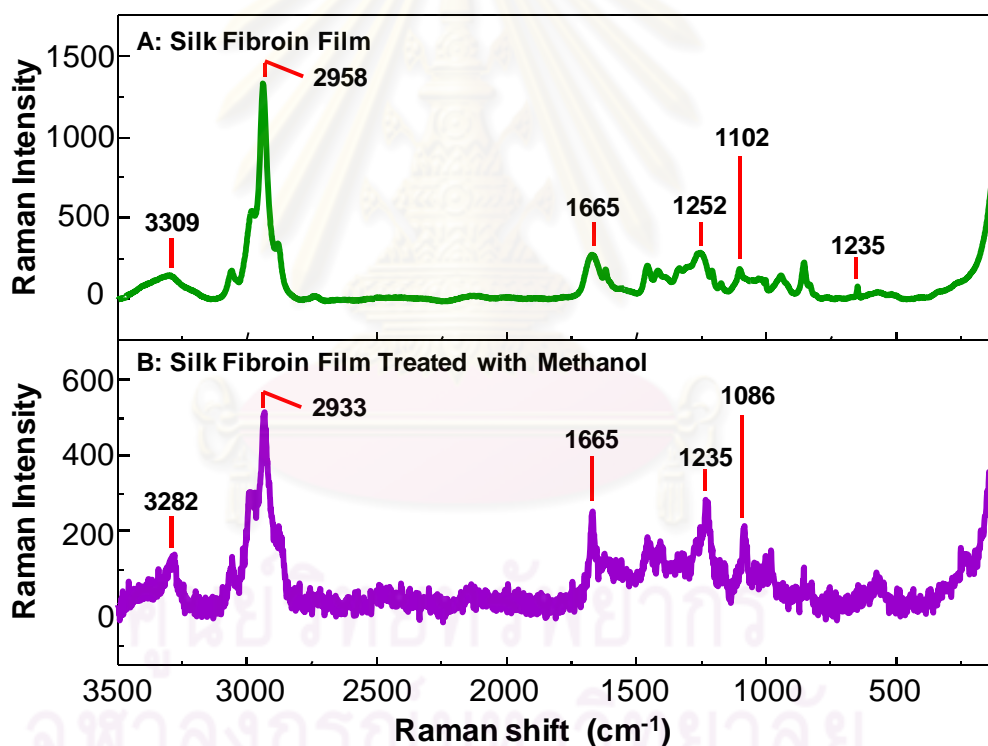


Figure 4.2 Raman spectra of silk fibroin film (A) and silk fibroin film treated with methanol (B).

Table 4.2 Band assignments of silk fibroin film by Raman microspectroscopy [88-90].

Wavenumber (cm ⁻¹)	Band assignments
3450-3160	<u>Amide A</u> N-H stretching
2975-2865	C-H stretching
1700-1600	<u>Amide I</u> C=O stretching
1670 ± 5	β -sheet
1660 ± 5	Random coil
1654 ± 5	α -helix
1500-1400	<u>Amide II</u> N-H bending (wagging) plus C-N stretching
1300-1200	<u>Amide III</u> N-H bending (twisting) plus C-N stretching and the contribution from O=C-N bending
800-500	<u>Amide V</u> N-H out of plane bending

The results of ATR FT-IR and Raman microspectroscopy can explain silk fibroin solution having secondary structure of the random coil and α -helix as the amorphous structure. When methanol was added to the solution, it attracted the water molecules from silk fibroin molecules due to their polar character and induced the rearrangement of molecular chain of silk fibroin from amorphous to crystalline structure and higher hydrophobic.

4.2.2 Freshwater cultured pearls

Having known the main component of freshwater cultured pearl, it is necessary to study the molecular information of freshwater cultured pearl by ATR FT-IR and Raman microspectroscopy.

4.2.2.1 Calcium Carbonate

Figure 4.3 showed ATR FT-IR spectrum of freshwater cultured pearl having characteristic peaks at 3370 cm^{-1} (O-H stretching), 2920 cm^{-1} (C-H stretching), 2520 cm^{-1} (O-H stretching vibration of HCO_3^-), 1788 cm^{-1} (C=O stretching vibration of the CO_3^{2-} ion), 1650 cm^{-1} (Amide I). The vibration of the CO_3^{2-} ion of the aragonite CaCO_3 showed the characteristic peaks at 1470 , 1442 , 1083 and 840 cm^{-1} as shown in Table 4.3. The reference ATR FT-IR spectra of CaCO_3 having three polymorphs was considered (Figure 4.4 A). The results indicated that freshwater cultured pearl was CaCO_3 in the aragonite crystal form (Figure 4.4 B). The results of ATR FT-IR microspectroscopy will be confirmed by Raman microspectroscopy.

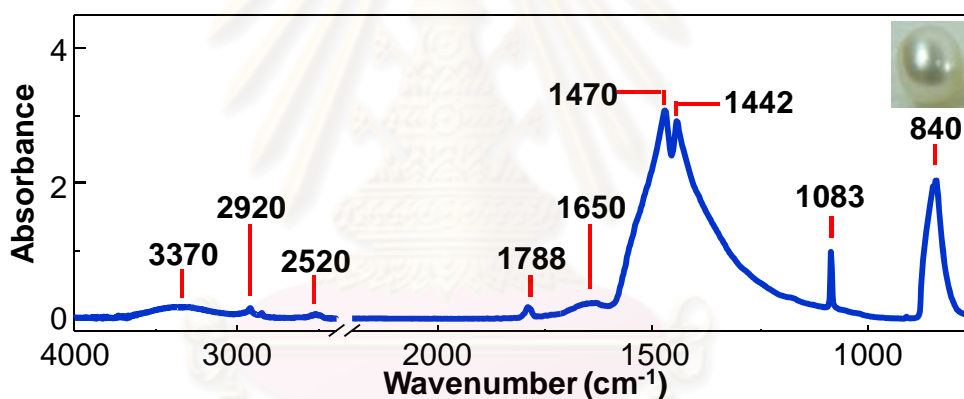


Figure 4.3 ATR FT-IR spectrum of freshwater cultured pearl.

ศูนย์วิทยทรัพยากร
จุฬาลงกรณ์มหาวิทยาลัย

Table 4.3 Band assignments of freshwater cultured pearl by ATR FT-IR microspectroscopy

Wavenumber (cm ⁻¹)	Band assignments
3370	O-H stretching vibration of adsorbed water
2920	C-H stretching
2520	O-H stretching vibration of HCO ₃ ⁻
1788	C=O stretching of CO ₃ ²⁻
1650	Amide I (C=O stretching and a small contribution from NH bending (scissoring))
1470 and 1442	Asymmetric in plane stretching of C-O bonds of CO ₃ ²⁻
1083	Symmetric stretching vibration of CO ₃ ²⁻
840	Out of plane bending vibration of C-O bonds of CO ₃ ²⁻

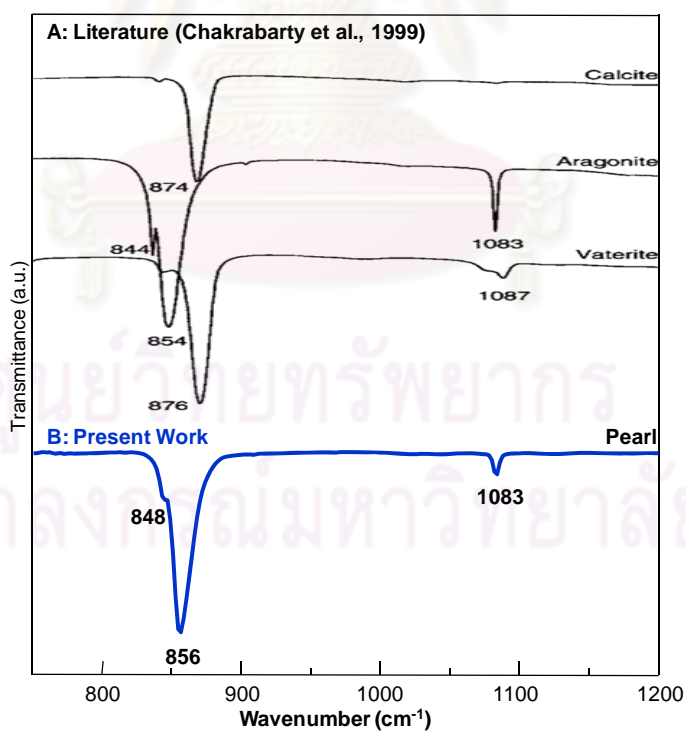
Figure 4.4 ATR FT-IR spectra of CaCO₃ different morphology (Chakrabarty et al., 1999) (A) and CaCO₃ of freshwater cultured pearl (B).

Figure 4.5 showed Raman spectrum of freshwater cultured pearl having the characteristic peaks at 1083, 702, 270 and 150 cm^{-1} which suggested the vibration of the CO_3^{2-} ion in the aragonite crystal form of the CaCO_3 having the same result as that of ATR FT-IR microspectroscopy.

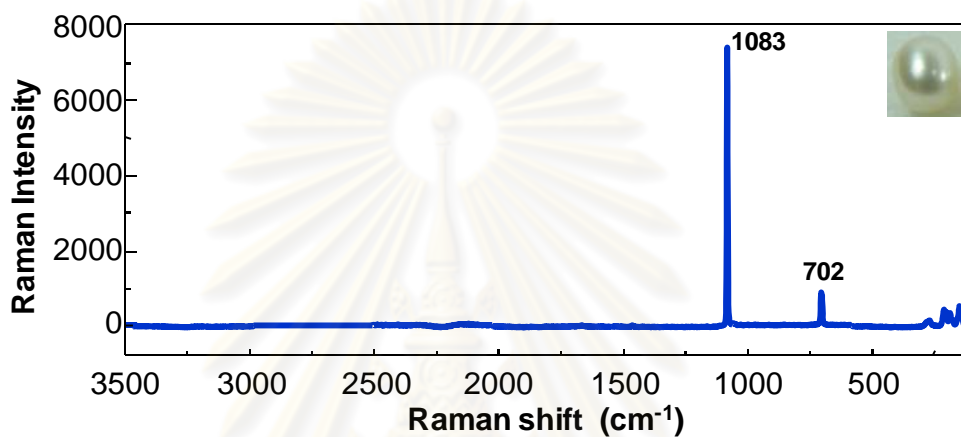


Figure 4.5 Raman spectrum of freshwater cultured pearl.

Figure 4.6 showed Raman spectra of CaCO_3 with different morphologies. Raman spectra showed characteristic peaks at 206, 703, and 1085 cm^{-1} of aragonite and calcite showing the peak position at 282, 712, and 1086 cm^{-1} of individual calcite crystal. The vaterite showed peak position at 713 and 1089 cm^{-1} .

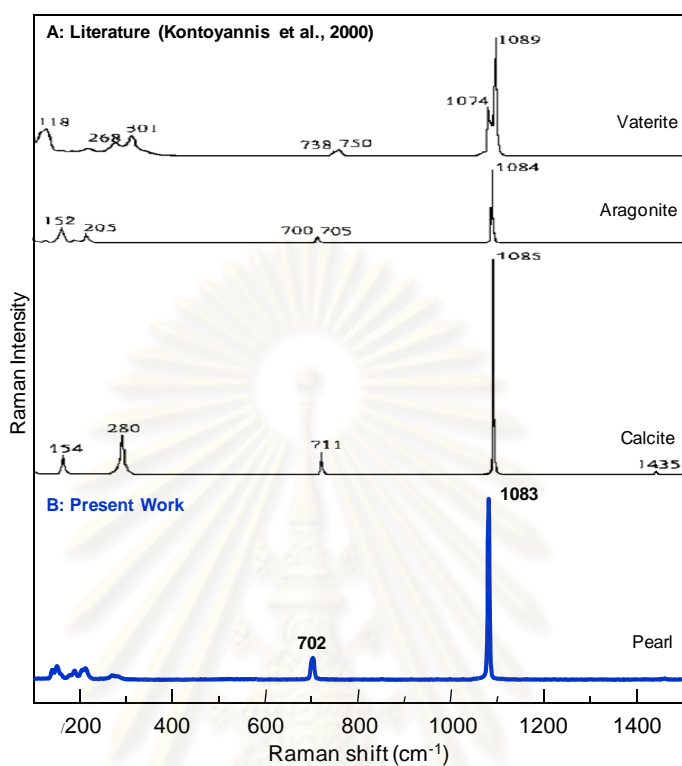


Figure 4.6 Raman spectra of CaCO_3 (Kontoyannis et al., 2000) of calcite, aragonite and vaterite crystal form (A) and CaCO_3 of freshwater cultured pearl (B).

Table 4.4 Band assignments of freshwater cultured pearl by Raman microspectroscopy.

Wavenumber (cm^{-1})	Band assignments
1083	Symmetric stretching vibration of CO_3^{2-}
702	In-plane bending vibration of C-O bonds of CO_3^{2-}

Optical image of the surface of freshwater cultured pearls showed the component of CaCO_3 and conchiolin protein (Figure 4.7).

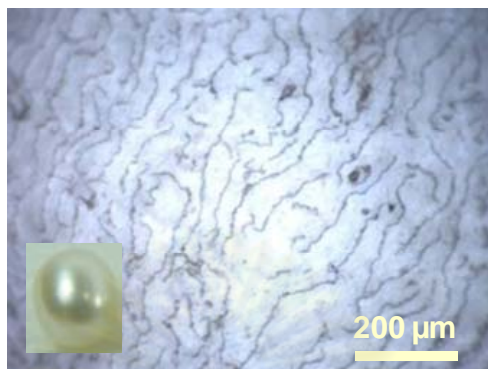


Figure 4.7 Optical image of freshwater cultured pearl surface.

The results from ATR FT-IR and Raman microspectroscopy indicated that freshwater cultured pearl was the structure of CaCO_3 in the aragonite crystal form.

4.2.2.2 Conchiolin protein

The conchiolin protein mainly consists of amino acids which are glycine and alanine approximately 24.3% and 14%, respectively. The silk fibroin protein mainly consists of amino acid are glycine and alanine approximately 44.6 % and 29.4 %, respectively. The conchiolin protein mainly consists of glycine and alanine amino acid which are the same as that of silk fibroin. Figure 4.8 showed the ATR FT-IR spectra of conchiolin protein of pearl and silk fibroin film of silk. The spectrum of conchiolin protein showed the characteristic peaks at 3280 cm^{-1} (N-H stretching), 1622 cm^{-1} (Amide I), 1514 cm^{-1} (Amide II) and 1233 cm^{-1} (Amide III) which indicated molecular information as shown in Figure 4.8 A. The molecular information is the same as that of silk fibroin as shown in Figure 4.8 B.

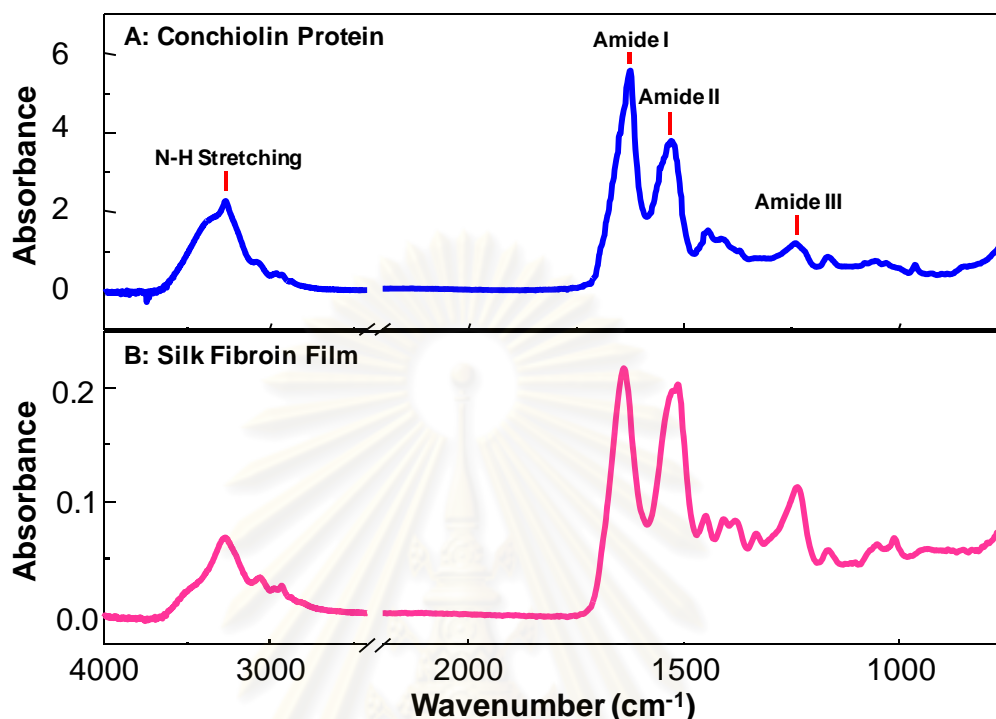


Figure 4.8 ATR FT-IR spectra of conchiolin protein of pearl (A) and silk fibroin film (B).

4.2.3 Freshwater culture pearls coated with silk fibroin solution on pearl surface

The freshwater cultured pearls coated with silk fibroin solution are performed by ATR FT-IR and Raman microscopy. Figure 4.9 showed ATR FT-IR spectra of silk fibroin film, freshwater cultured pearl and freshwater cultured pearl coated with silk fibroin solution. ATR FT-IR spectrum of silk fibroin film showed molecular information: backbone protein at N-H stretching, Amide I, Amide II and Amide III were observed (Figure 4.9 B). This meant that silk fibroin stuck on pearl surface. ATR FT-IR spectrum of freshwater cultured pearl coated with silk fibroin solution occurred the peak shape at 3280 cm⁻¹ (N-H stretching) but the ATR FT-IR spectrum of freshwater cultured pearl occurred broad peak at O-H stretching. Amide I at 1632 cm⁻¹ was higher intensity than that of the freshwater cultured pearl. ATR FT-IR spectrum of silk fibroin showed the

characteristic peaks of Amide I of very high intensity (main backbone protein), 1530 cm^{-1} (Amide II) and 1255 cm^{-1} (Amide III), which did not occur in freshwater cultured pearl (Figure 4.9 C). It showed the molecular information of silk fibroin stuck on pearl surface at N-H stretching and Amide I of the varied shape and the shoulder peaks at Amide II and Amide III. These results were confirmed by Raman microspectroscopy.

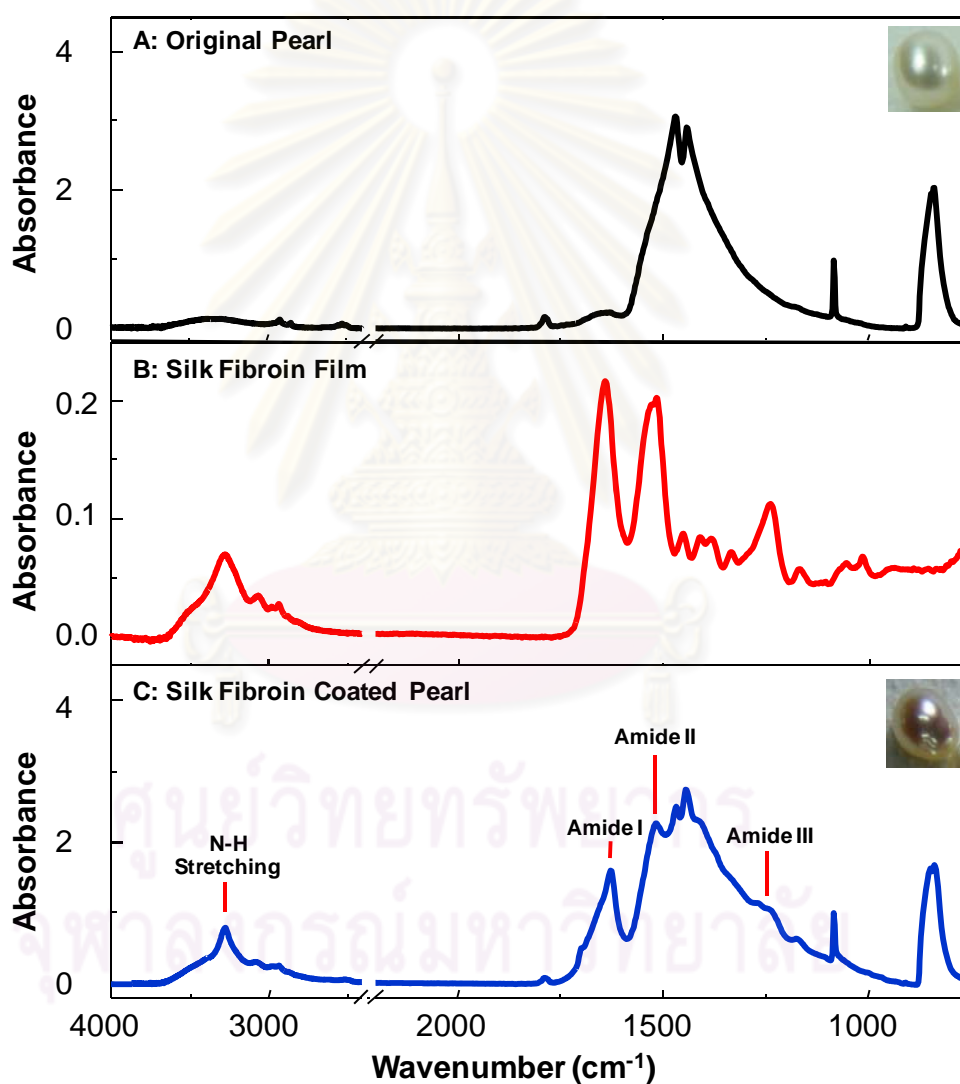


Figure 4.9 ATR FT-IR spectra of freshwater cultured pearl (A), silk fibroin film (B) and freshwater cultured pearl coated silk fibroin solution (C).

Figure 4.10 showed ATR FT-IR spectra of conchiolin protein coated on pearl surface and freshwater cultured pearl coated with silk fibroin solution on pearl surface. It showed the stick of silk fibroin on pearl surface which was able to imitate their conchiolin protein coated between aragonite platelets. Furthermore, the conchiolin protein mainly consists of glycine and alanine amino acid which are the same as that of silk fibroin.

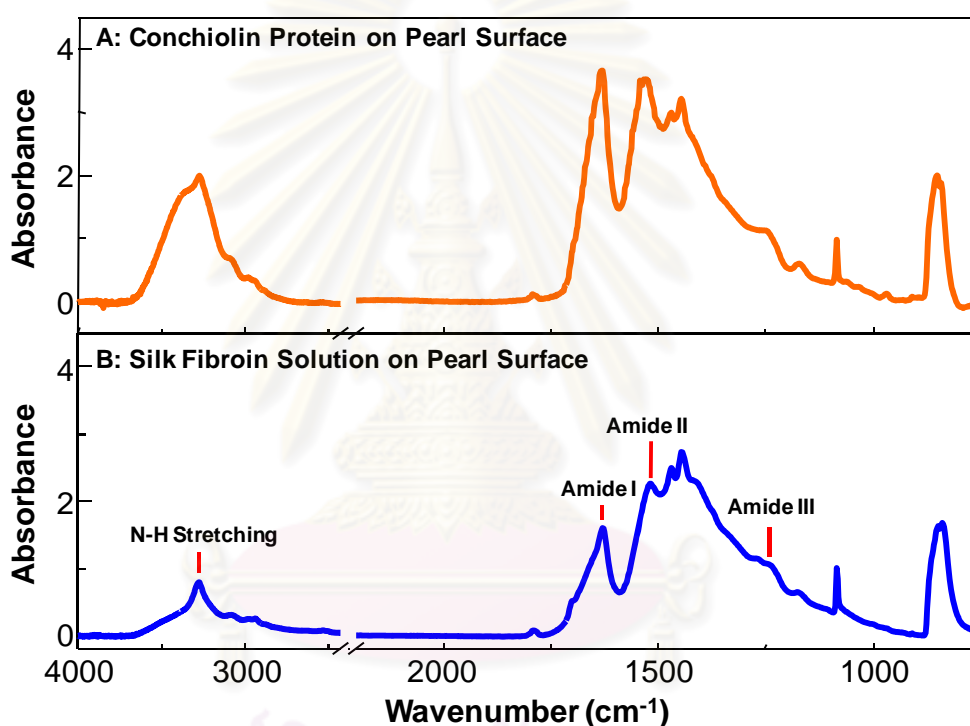


Figure 4.10 ATR FT-IR spectra of conchiolin protein of pearl (A), freshwater cultured pearl coated silk fibroin solution on pearl surface (B).

Figure 4.11 showed Raman spectra of silk fibroin film, freshwater cultured pearl, and freshwater cultured pearl coated with silk fibroin. Raman spectrum of freshwater cultured pearl coated with silk fibroin showed the characteristic peaks at 3280 cm⁻¹ (N-H stretching), 2934 cm⁻¹ (C-H stretching), 1664 cm⁻¹ (Amide I), 1527 cm⁻¹ (Amide II) and 1232 cm⁻¹ (Amide III) which Amide I, Amide II and Amide III indicated the secondary

structure of β -sheet conformation. Raman spectrum of silk fibroin coated pearl indicated the character of silk fibroin stuck on pearl surface the same as that of the result of ATR FT-IR microspectroscopy. The uniformity of silk fibroin film coated on surface of pearls was observed by means of Atomic Force Microscopy (AFM).

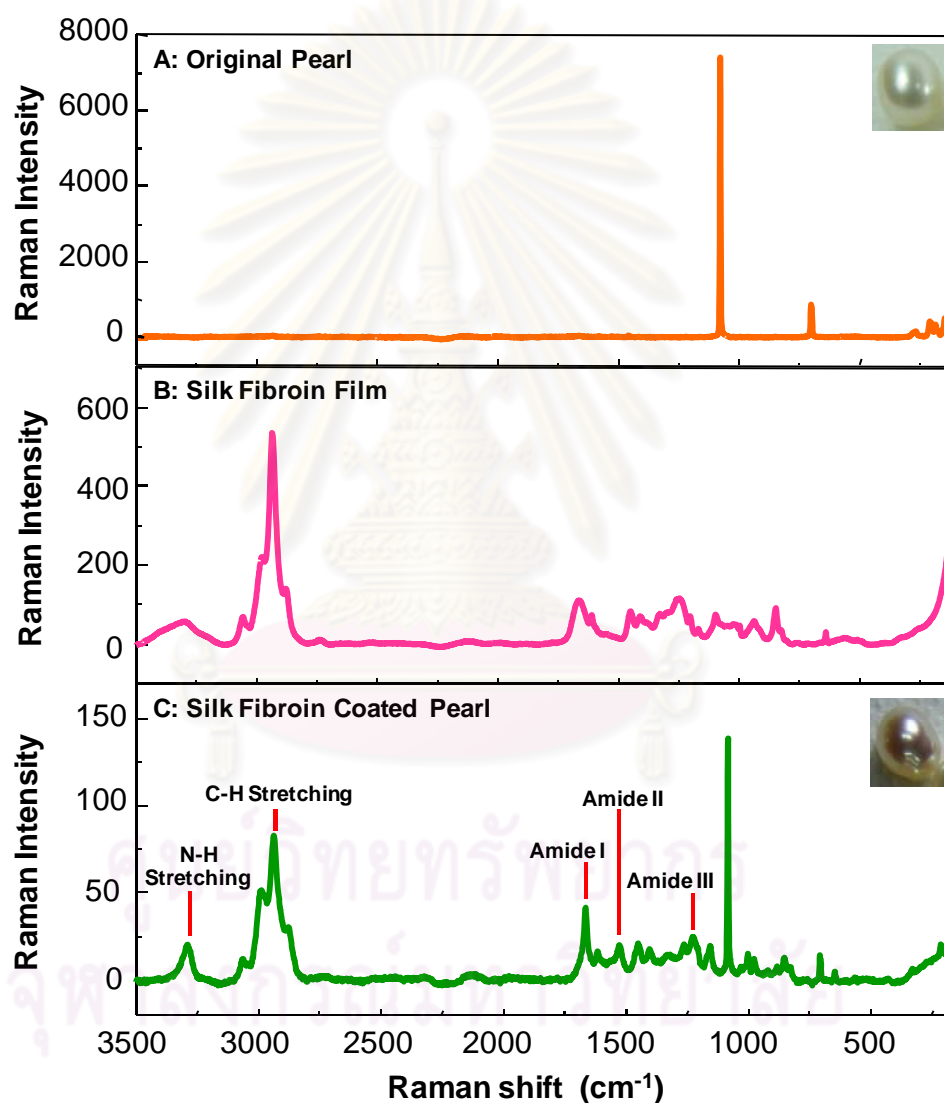


Figure 4.11 Raman spectra of freshwater cultured pearl (A), silk fibroin film (B) and pearl coated silk fibroin solution (C).

Figure 4.12 A showed Raman spectra of conchiolin protein coated on pearl surface and freshwater cultured pearl coated with silk fibroin solution on pearl surface (Figure 4.12 B). It showed the stick of silk fibroin on pearl surface which was able to imitate their conchiolin protein coated between aragonite platelets.

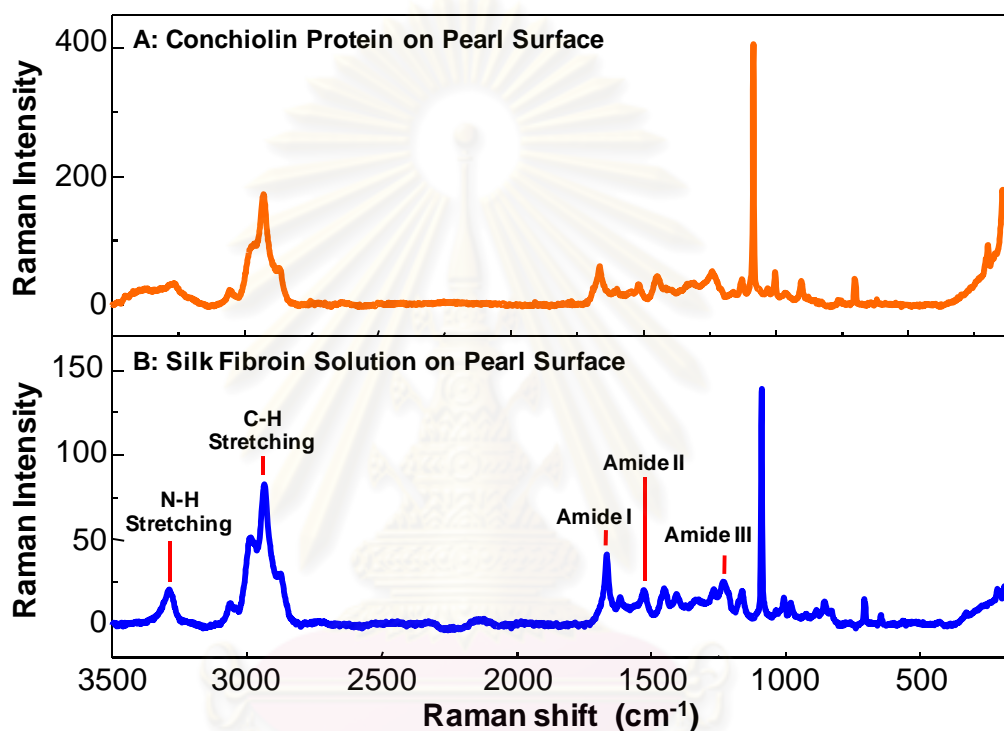


Figure 4.12 Raman spectra of conchiolin protein of pearl (A), freshwater cultured pearl coated silk fibroin solution on surface (B).

The optical image showed the distribution of short silk fibroin fibers on pearl surface coating with silk fibroin solution as shown in Figure 4.13. The size of short silk fibroin fibers was 11 μm in diameter and 96 μm in length and found depositing on the surface of treated pearls. According to Raman microspectroscopic technique, it was found that if the laser detected short silk fibroin fiber, it showed the molecular information of silk fibroin stuck on pearl surface. Using 50x long, the microscope which

had spot size of 1.1 μm , the analysis position of the sample can be evaluated. So, Raman microspectroscopy indicated qualitative analysis for this work.



Figure 4.13 Optical image of freshwater cultured pearl coated with silk fibroin solution.

The results of ATR FT-IR and Raman microspectroscopy confirmed that silk fibroin stuck on pearl surface. The observation peaks at the N-H stretching, Amide I, Amide II and Amide III demonstrated the character of silk fibroin stuck on pearl surface. It showed the stick of silk fibroin on pearl surface which was able to imitate their conchiolin protein coated between aragonite platelets.

4.2 Effect of the cleaning pearl surface for the sticking of silk fibroin on pearl surface

The cleaning surface of freshwater cultured pearl with DI water and DI water with 10 % H_2O_2 are analyzed by ATR FT-IR microspectroscopy. Figure 4.14 showed ATR FT-IR spectra of freshwater cultured pearl cleaned with DI water and DI water with 10 % H_2O_2 after that they coated with silk fibroin solution. ATR FT-IR spectra of freshwater cultured pearl cleaned with DI water and DI water with 10 % H_2O_2 showed the molecular information of the freshwater cultured pearl (Figure 4.14 A,C). ATR FT-IR spectrum of freshwater cultured pearl cleaned with DI water and 10 % H_2O_2 that coated with silk fibroin solution indicated silk fibroin stuck on pearl surface (Figure 4.14 D).

The observed peaks of N-H stretching, Amide I, Amide II and Amide III which distinctly confirmed silk fibroin stuck on pearl surface. Experimentally, H_2O_2 is the most powerful cleaning surface agent for our work.

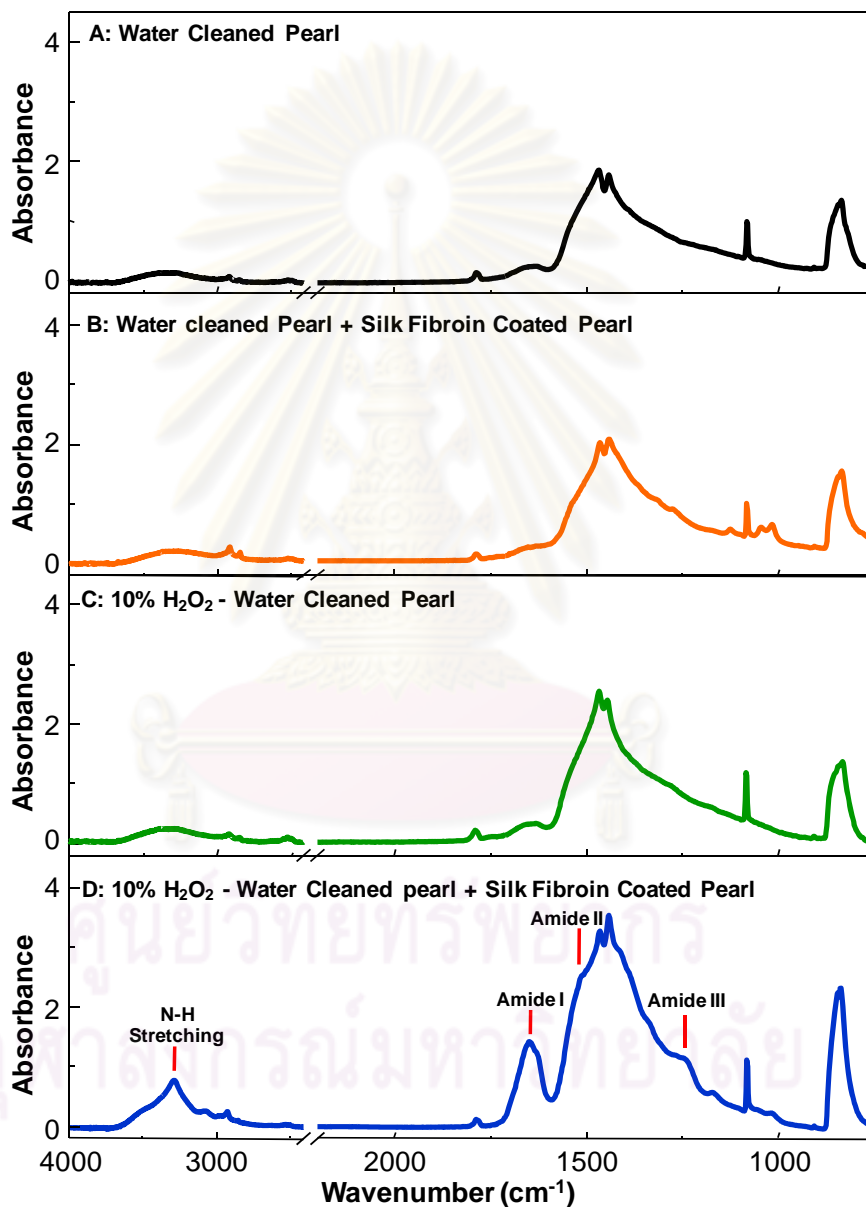


Figure 4.14 ATR FT-IR spectra of freshwater cultured pearl cleaned by DI water (A), and coated with silk fibroin solution (B). The pearls surface cleaned by DI water and 10% H_2O_2 (C), that coated with silk fibroin solution (D).

The optical image showed the surface of pearl coating with silk fibroin solution in Figure 4.15. The pearls surface cleaned by DI water, coated with silk fibroin solution and cleaned by DI water and 10% H₂O₂ clearly shown the texture of pearl surface (Figure 4.15 A-C). The pearls surface cleaned by DI water and 10% H₂O₂ that coated with silk fibroin solution unclearly shown the texture of pearl surface (Figure 4.15 D). It indicated that silk fibroin was stuck on pearl surface after the coating.

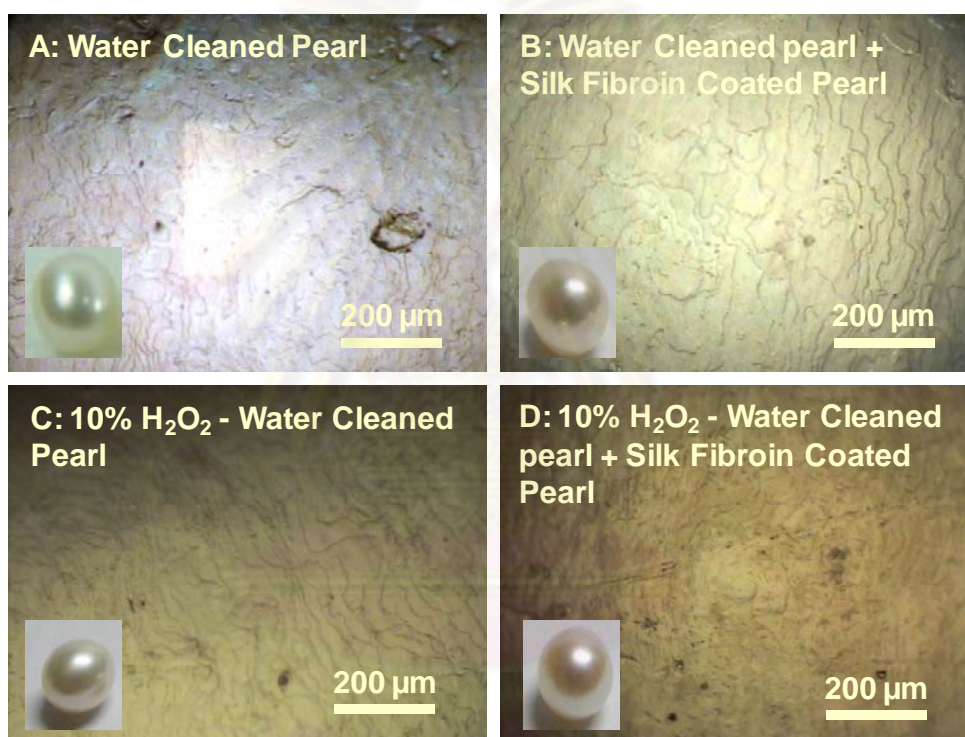


Figure 4.15 Optical image of freshwater cultured pearl cleaned by DI water (A), and coated with silk fibroin solution (B). The pearls surface cleaned by DI water and 10% H₂O₂ (C), that coated with silk fibroin solution (D).

The results of ATR FT-IR microspectroscopy suggested that the H₂O₂ cleaned the dirty on pearl surface that was increased the sticking performance which silk fibroin stuck on pearl surface.

4.3 Preparation of silk fibroin solution

The concentration of alkaline solution for dissolving silk fibroin fibers was minimized in order to reduce the cost of the preparation of silk fibroin solution. We proposed a new method instead of dialysis step.

4.3.1 Alkaline solution

It was found that the preparation of silk fibroin solution with high concentrations of LiBr, in general, were very expensive. So, we tried to reduce the cost of the solution preparation by using other chemicals such as LiBr, CaCl₂, ZnCl₂, Ca (NO₃)₂, NaOH and KOH. Experimentally speaking, using NaOH and KOH for the preparation of solution could reduce the cost of the preparation and used no other solvent in dissolving silk fibroin fiber. In this work, the preparation of silk fibroin solution was studied and compared the solubility of NaOH and KOH with that of LiBr.

From section 3.2, it was known that the alkaline solution using in the preparation of silk fibroin solution was 5 g of silk fibroin fibers dissolved in LiBr, KOH and NaOH solution. The conditions for the preparation were as follows: 9.3 M, 1.1 M, and 1.0 M, respectively. The solution using LiBr was dark yellow comparable to the colorless of the solutions using NaOH and KOH (Figure 4.16). However, the solutions prepared by using NaOH and KOH solution required less time in dissolving fiber. Prices of both NaOH and KOH were 7.5 times cheaper than that of LiBr and the concentration were 9 times lower than that of LiBr. Though, the suitable solution using NaOH for coating surface of freshwater cultured pearl because it required less time in dissolving silk fiber, low minimal concentration and the price was cheaper than both of LiBr and KOH.

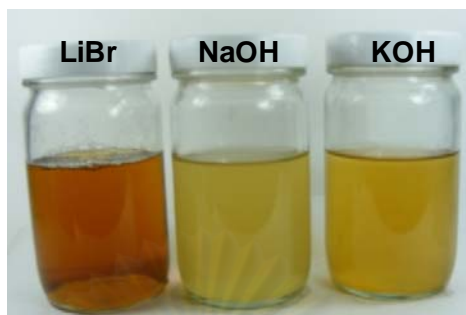


Figure 4.16 Silk fibroin solution are prepared from 5 g of silk fibroin fibers dissolved in LiBr, NaOH, and KOH at the concentrations of 9.3 M, 1.0 M, and 1.1 M, respectively.

After that, freshwater cultured pearl are coated with silk fibroin solution and are analyzed by ATR FT-IR microspectroscopy as shown in Figure 4.17. The spectra showed characteristic peaks at N-H stretching, Amide I and the shoulder peaks at Amide II and Amide III, which demonstrated the molecular information of silk fibroin stuck on pearl surface. Freshwater cultured pearl coated with silk fibroin solution prepared from NaOH showed the best result of the silk fibroin stuck on pearl surface observed by characteristic peaks of N-H stretching and Amide I which varied shape and the shoulder peaks of Amide II and Amide III as shown in Figure 4.17 (C).

ศูนย์วิทยทรัพยากร
จุฬาลงกรณ์มหาวิทยาลัย

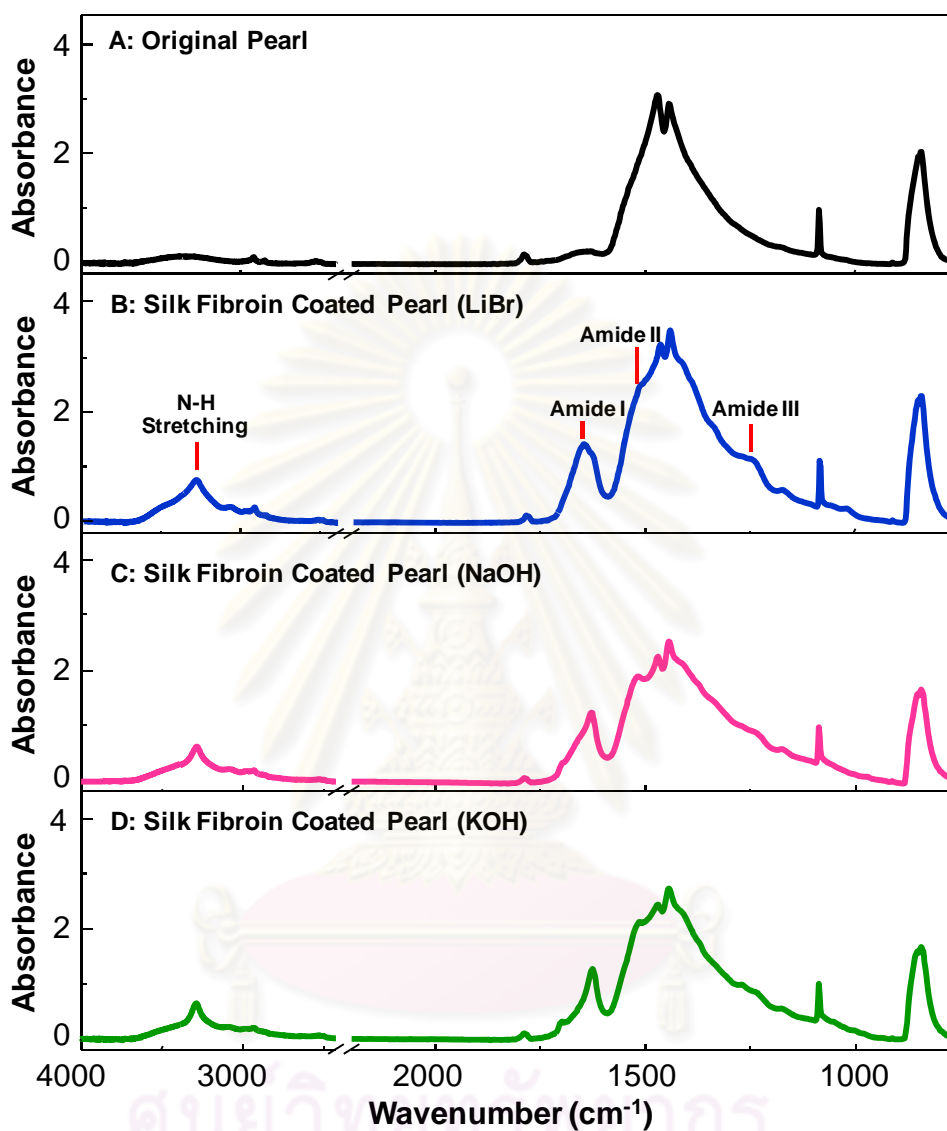


Figure 4.17 ATR FT-IR spectra of freshwater cultured pearl (A). Pearl coated with silk fibroin solution prepared from 5 g of silk fibroin fibers dissolved in 9.3 M LiBr (B), 1.0 M NaOH (C), and 1.1 M KOH (D).

The results of ATR FT-IR spectra demonstrated the stuck of silk fibroin on pearl surface. It confirmed that we used silk fibroin solution prepared from NaOH and KOH to replace LiBr for coating pearl surface.

4.3.2 Weight of silk fibroin fibers

The results from section 4.3.1 confirmed that silk fibroin solution prepared by using NaOH and KOH solution showing the stuck of silk fibroin on pearl the same as that of LiBr solution. Then, we used NaOH and KOH solutions for the preparation of silk fibroin solution on coating the surface of pearl.

Getting started with silk fibroin fibers are as follows: 2, 3, 4 and 5 g and performed the experiment as of section 3.2. Table 4.5 showed the condition of preparation of silk fibroin solution from NaOH and KOH solution. It was found that the preparation for the silk fibroin solution of 0.35 M NaOH for dissolving 2 g (2 % w/v) of silk fibroin fibers showing the minimal usage moles of alkali per 1 g of silk fibroin fiber that was 0.01750 mol/g.

The optimal silk fibroin solution prepared by using 0.35 M NaOH for dissolving 2 g (2 % w/v) of silk fibroin fiber used minimal alkali concentration and the usage mole of alkali for dissolving 1 g of silk fibroin fiber.

Table 4.5 The lowest amount of alkali for dissolving silk fibroin fibers

Type of alkali	Weight of silk fibroin fiber (g)	Amount of alkali (mol.)	Usage of alkali per silk fibroin fiber (mol/g)	Concentrations of alkali (M)	Weight of silk per volume of alkali solution (% w/v)
NaOH	2	0.035	0.01750	0.35	2
	3	0.055	0.01830	0.55	3
	4	0.080	0.02000	0.80	4
	5	0.100	0.02000	1.00	5
KOH	2	0.040	0.02000	0.40	2
	3	0.060	0.02000	0.60	3
	4	0.085	0.02125	0.85	4
	5	0.110	0.02200	1.10	5

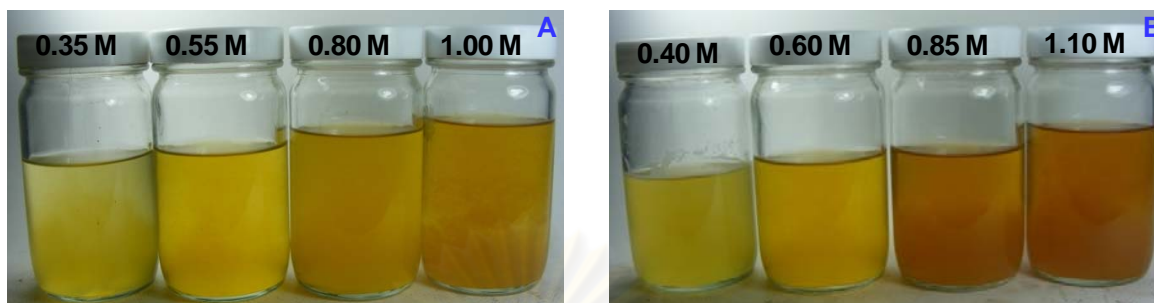


Figure 4.18 Silk fibroin solution prepared from 2 g (2 % w/v), 3 g (3 % w/v), 4 g (4 % w/v) and 5 g (5 % w/v) of silk fibroin fibers are dissolved in NaOH solution at the concentrations of 0.35 M, 0.55 M, 0.80 M, 1.00 M (A) and KOH solution at the concentrations of 0.40 M, 0.60 M, 0.85 M, 1.10 M (B), respectively.

After that, we used silk fibroin solution prepared by using NaOH and KOH solution for coating surface of pearl and analyzed by ATR FT-IR and Raman microspectroscopy. Freshwater cultured pearl coated with silk fibroin solution prepared from NaOH solution at the concentrations of 0.35 M (2 % w/v), 0.55 M (3 % w/v), 0.80 M (4 % w/v) and 1.00 M (5 % w/v), respectively (Figure 4.19). The spectra showed characteristic peaks at N-H stretching, Amide I and the shoulder peaks at Amide II and Amide III, which suggested the molecular information of silk fibroin stuck on pearl surface. It was found that silk fibroin solution prepared from NaOH solution at the concentrations of 0.35 M (2 % w/v) indicated the optimal stuck of silk fibroin on pearl surface.

จุฬาลงกรณ์มหาวิทยาลัย

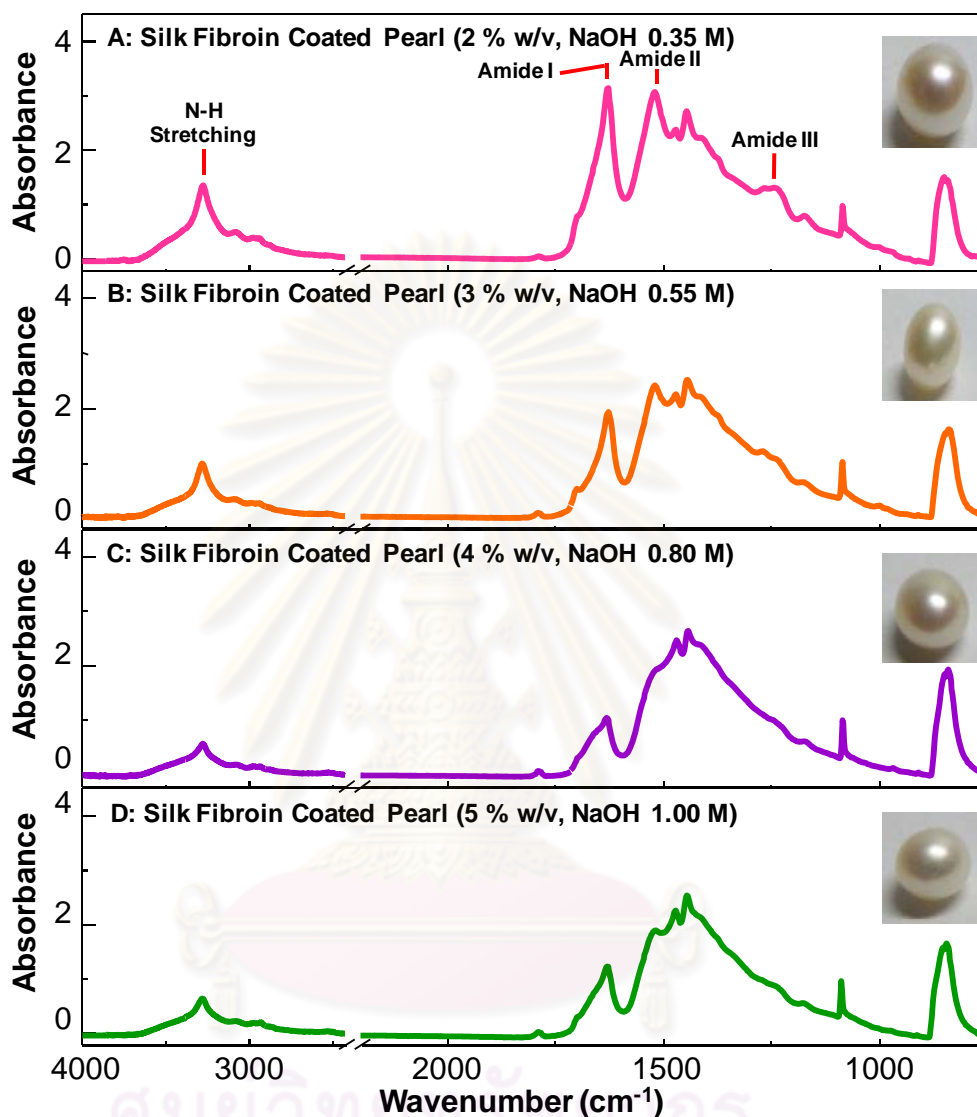


Figure 4.19 ATR FT-IR spectra of freshwater cultured pearl coated with silk fibroin solution prepared from 2 g (2 % w/v), 3 g (3 % w/v), 4 g (4 % w/v), and 5 g (5 % w/v) of silk fibroin fibers are dissolved in NaOH solution at the concentrations of 0.35 M (A), 0.55 M (B), 0.80 M (C) and 1.00 M (D), respectively.

Considering, freshwater cultured pearl coated with silk fibroin solution prepared from KOH solution at the concentrations of 0.40 M (2 % w/v), 0.60 M (3 % w/v), 0.85 M

(4 % w/v), 1.10 M (5 % w/v)), respectively (Figure 4.20). The spectrum manifested the character of silk fibroin stuck on pearl surface which silk fibroin solution prepared from KOH solution at the concentrations of 0.40 M displaying the stuck of silk fibroin better than at different concentrations.

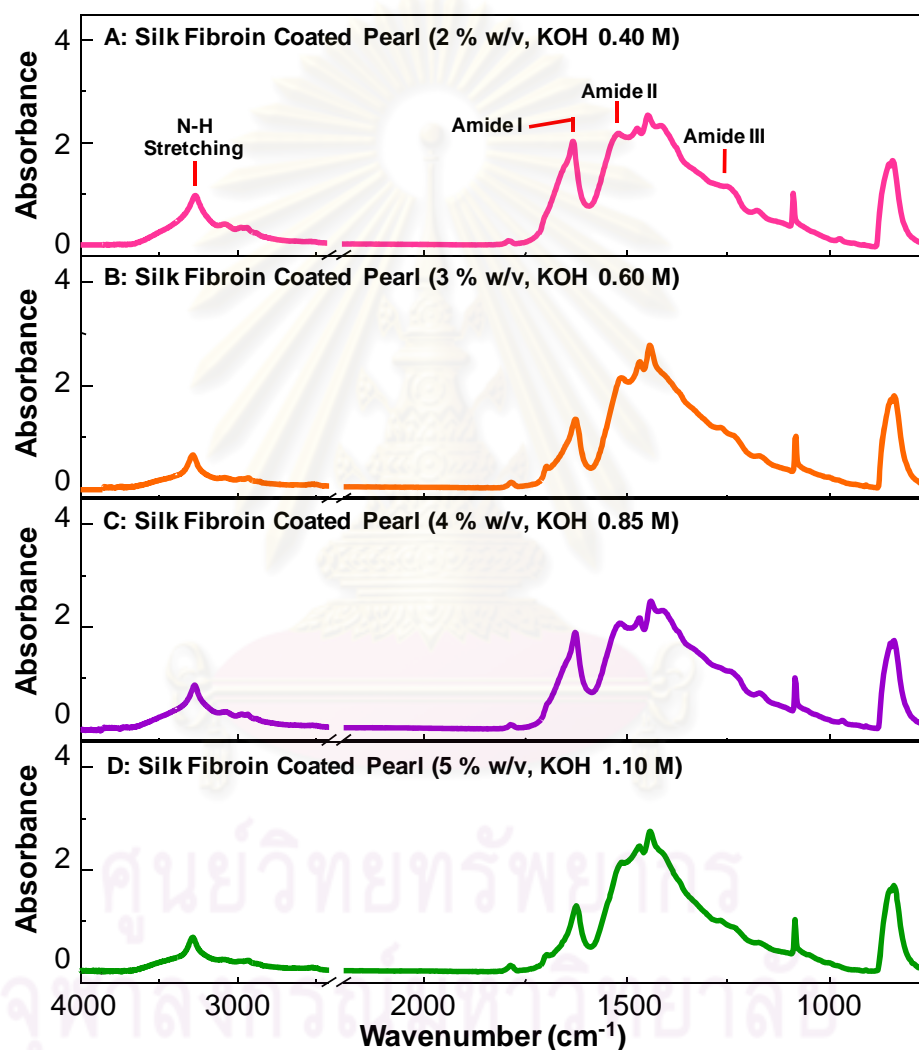


Figure 4.20 ATR FT-IR spectra of freshwater cultured pearl coated with silk fibroin solution prepared from 2 g (2 % w/v), 3 g (3 % w/v), 4 g (4 % w/v), and 5 g (5 % w/v) of silk fibroin fibers are dissolved in KOH solution at the concentrations of 0.40 M (A), 0.60 M (B), 0.85 M (C) and 1.10 M (D), respectively.

From the results, it was concluded that for the preparation of silk fibroin solution prepared from 2 g (2 % w/v) of silk fibroin fibers dissolved in 0.35 M NaOH solution was the suitable method because we used low concentration of NaOH which dissolved maximum amount of silk fibroin fiber and having the best stuck on pearl surface. Furthermore, the optical images showed the distribution of short silk fibroin fibers on pearl surface coating with silk fibroin solution as shown in Figure 4.21. The size of short silk fibroin fibers was 10 μm in diameter and 97 μm in length and found depositing on the surface of treated pearls. The results of ATR FT-IR microspectroscopy will be confirmed by Raman microspectroscopy.

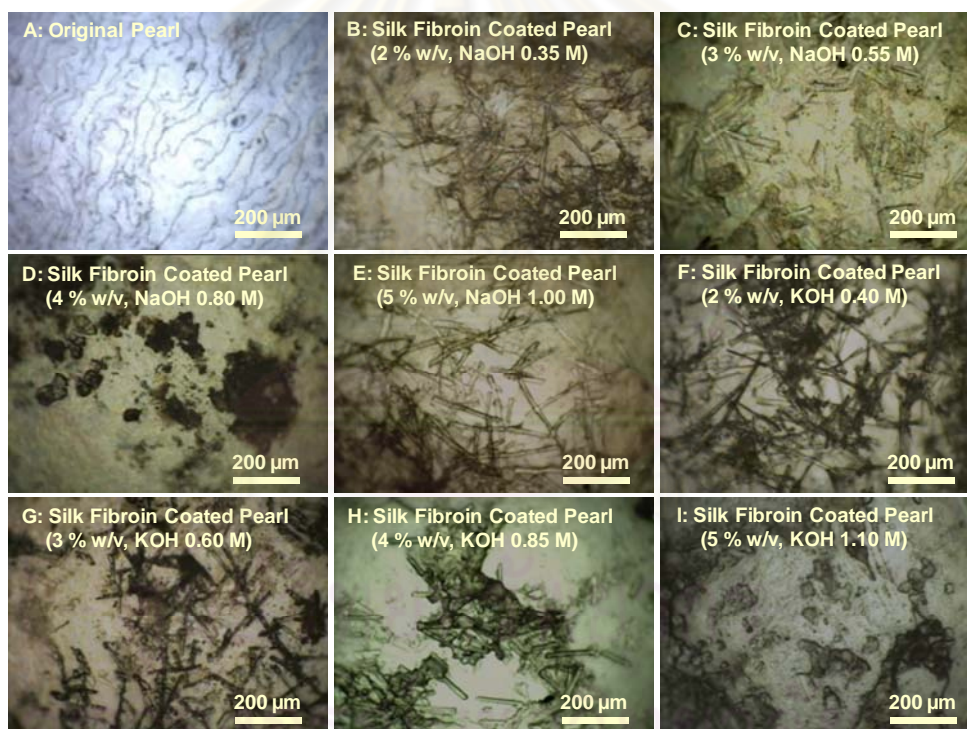


Figure 4.21 Optical images of freshwater cultured pearl (A) coated with silk fibroin solution prepared from 2 g (2 % w/v), 3 g (3 % w/v), 4 g (4 % w/v) and 5 g (5 % w/v) of silk fibroin fibers dissolved in NaOH solution at the concentrations of 0.35 M (B), 0.55 M (C), 0.80 M (D), 1.00 M (E) and KOH solution at the concentrations of 0.40 M (F), 0.60 M (G), 0.85 M (H), 1.10 M (I), respectively.

Raman spectra of freshwater cultured pearl coated with silk fibroin solution prepared from NaOH solution at the concentrations of 0.35 M (2 % w/v), 0.55 M (3 % w/v), 0.80 M (4 % w/v) and 1.00 M (5 % w/v), respectively, were shown in Figure 4.22. The observation of peak positions at N-H stretching, C-H stretching, Amide I, Amide II and Amide III suggested the molecular information of silk fibroin stuck on pearl surface having the same result as that of the spectra of freshwater cultured pearl coated with silk fibroin solution prepared from KOH solution at the concentrations of 0.40 M (2 % w/v), 0.60 M (3 % w/v), 0.85 M (4 % w/v), 1.10 M (5 % w/v), respectively (Figure 4.23). This results confirmed the stuck of silk fibroin on pearl surface which corresponding to the results of ATR FT-IR microspectroscopy.



ศูนย์วิทยทรัพยากร
จุฬาลงกรณ์มหาวิทยาลัย

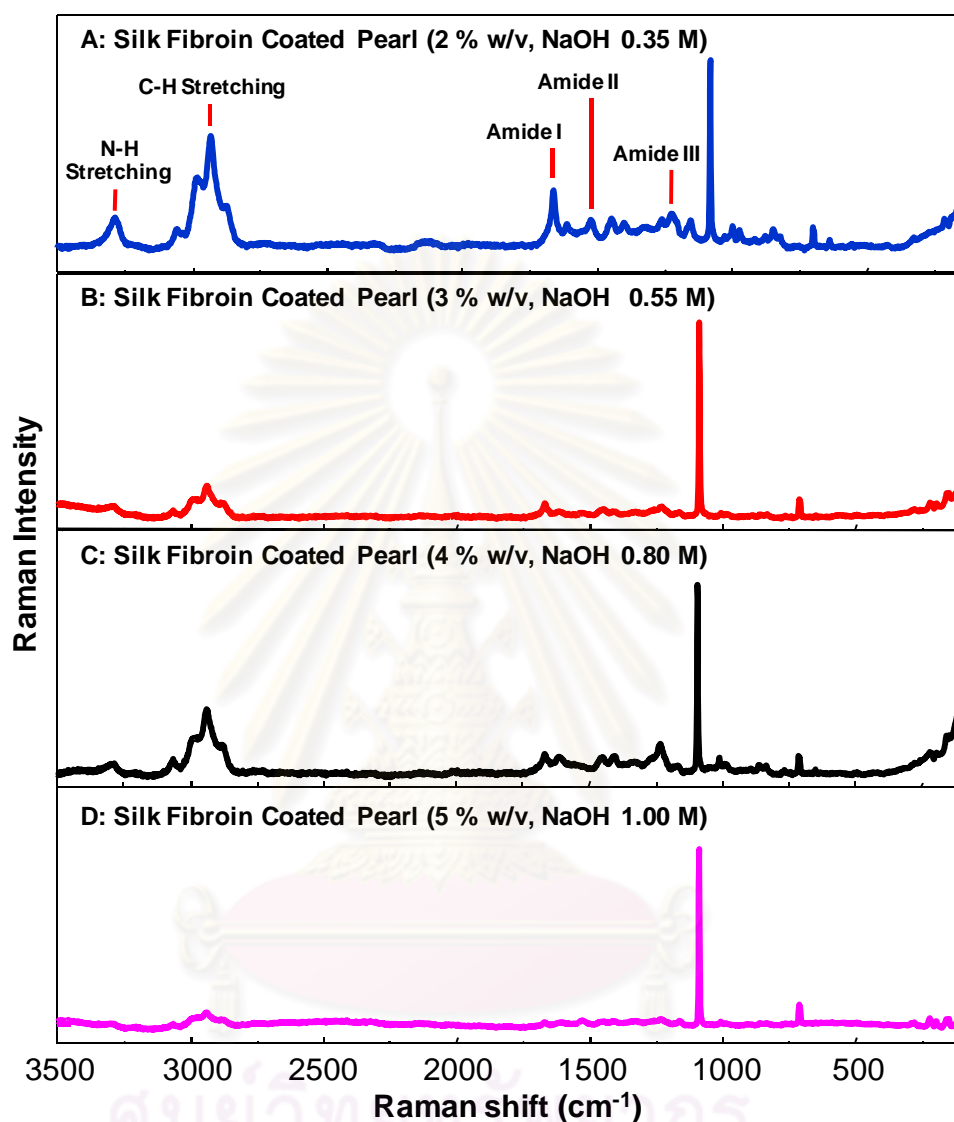


Figure 4.22 Raman spectra of freshwater cultured pearl coated with silk fibroin solution prepared from 2 g (2 % w/v), 3 g (3 % w/v), 4 g (4 % w/v), and 5 g (5 % w/v) of silk fibroin fibers dissolved in NaOH solution at the concentrations of 0.35 M (A), 0.55 M (B), 0.80 M (C) and 1.00 M (D), respectively.

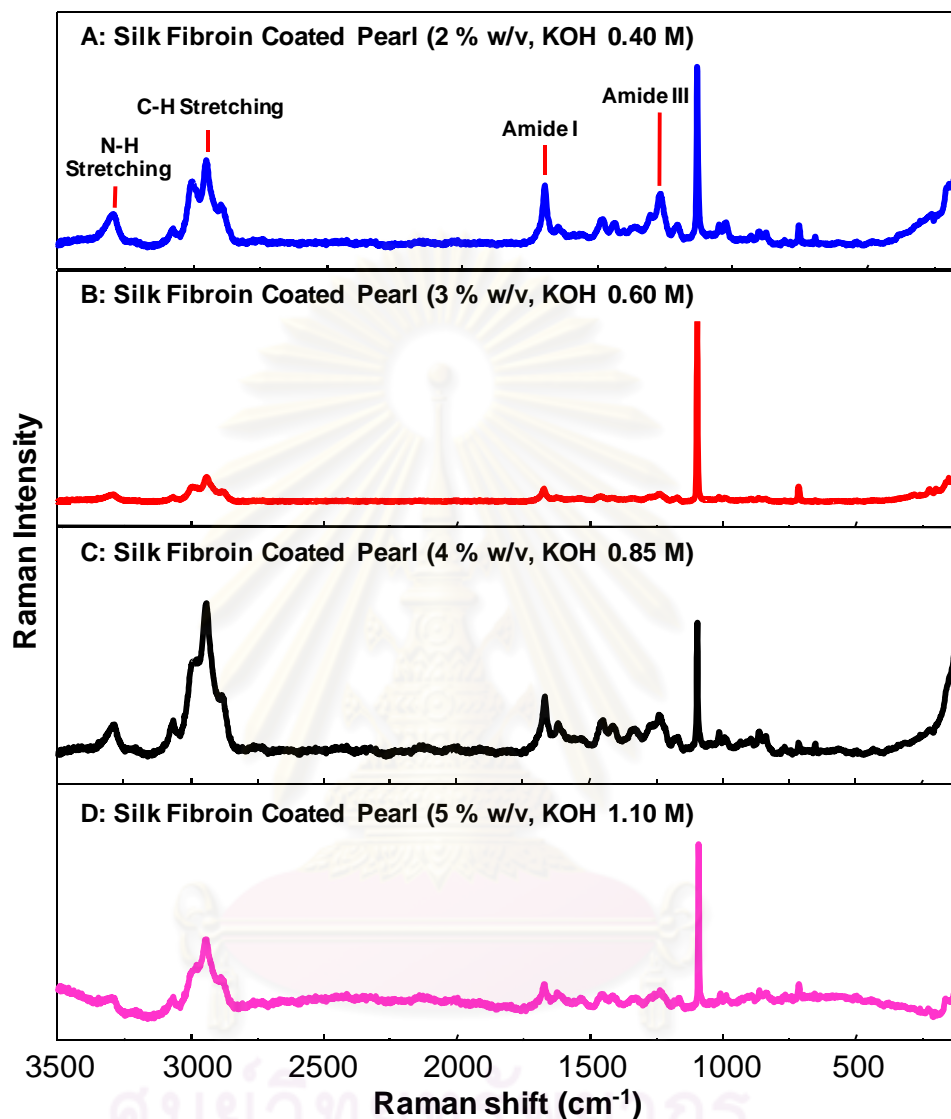


Figure 4.23 Raman spectra of freshwater cultured pearl coated with silk fibroin solution prepared from 2 g (2 % w/v), 3 g (3 % w/v), 4 g (4 % w/v), and 5 g (5 % w/v) of silk fibroin fibers dissolved in KOH solution at the concentrations of 0.40 M (A), 0.60 M (B), 0.85 M (C) and 1.10 M (D), respectively.

The results by ATR FT-IR microspectroscopy can be concluded that the most suitable preparative silk fibroin solution with 2 g (2 % w/v) of silk fibroin fibers dissolved in 0.35 M NaOH with low concentration in dissolving the maximum amount of

silk fibroin fibers and the ATR FT-IR spectra showed the sharp stuck of silk fibroin on pearl surface. The results of Raman microspectroscopy confirmed silk fibroin stuck on pearl surface as well.

The preparation of silk fibroin solution using NaOH reduces the cost, time, chemical, wastes and energy of production.

4.3.3 pH of silk fibroin solution

Formerly, the preparation of silk fibroin solution using LiBr solution, silk fibroin solution was dialyzed in DI water with dialysis tubing cellulose membrane for 3 days at room temperature for removing salt (LiBr). After that, freshwater cultured pearl coated with silk fibroin solution was analyzed by ATR FT-IR microspectroscopy. The spectra showed characteristic peaks at N-H stretching, Amide I and the shoulder peaks at Amide II and Amide III, that were the molecular information of silk fibroin stuck on pearl surface as shown in Figure 4.24 B.

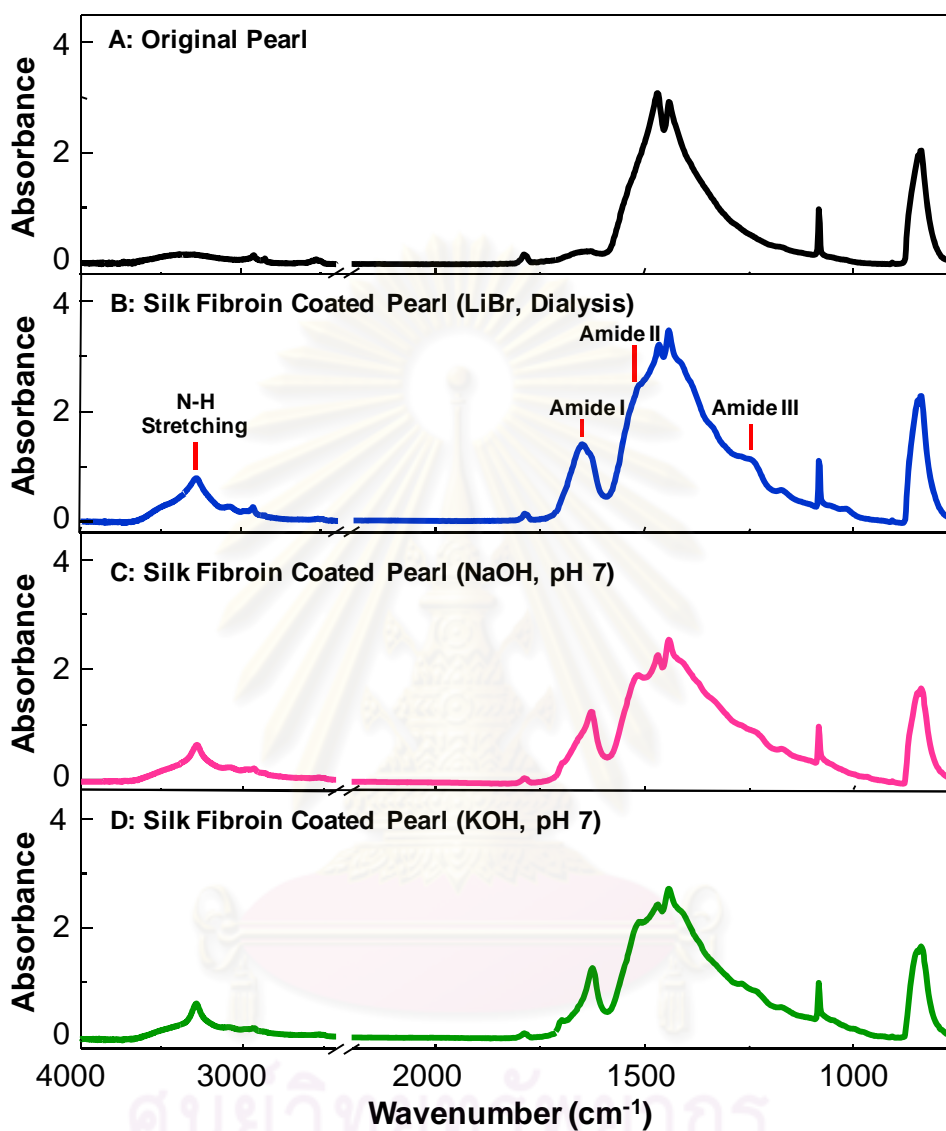


Figure 4.24 ATR FT-IR spectra of freshwater cultured pearl (A), coated with silk fibroin solution by dialysis method (B), by adjusting to neutral pH method using NaOH (C), KOH (D).

So, we adjusted the pH of solution in the range of 7 with HCl that making the coating on surface of pearl and then analyzed the coated sample by ATR FT-IR microspectroscopy. The spectra showed the character of silk fibroin stuck on pearl surface having the same result as that of dialysis method as shown in Figure 4.24 (C-D).

This method reduces the time of the dialysis for 3 days and the results of ATR FT-IR microspectroscopy showed the optimal stuck of silk fibroin on pearl surface with different result of the dialysis method.

Since, we adjusted the pH of solution in the range of 7 and analyzed by ATR FT-IR microspectroscopy. The spectrum of freshwater cultured pearl soaked in acid solution showed the peaks position of N-H stretching, Amide I and the shoulder peaks of Amide II and Amide III of conchiolin protein coated on pearl surface, and this indicated CaCO_3 was destroyed as shown in Figure 4.25 (A). Then, the spectrum of freshwater cultured pearl soaked in alkaline solution showed the characteristic peaks of CaCO_3 in the aragonite crystal form, this indicated conchiolin protein was destroyed as shown in Figure 4.25 (B). The alkaline and acid solution can dramatically dull the luster and surface of pearl.

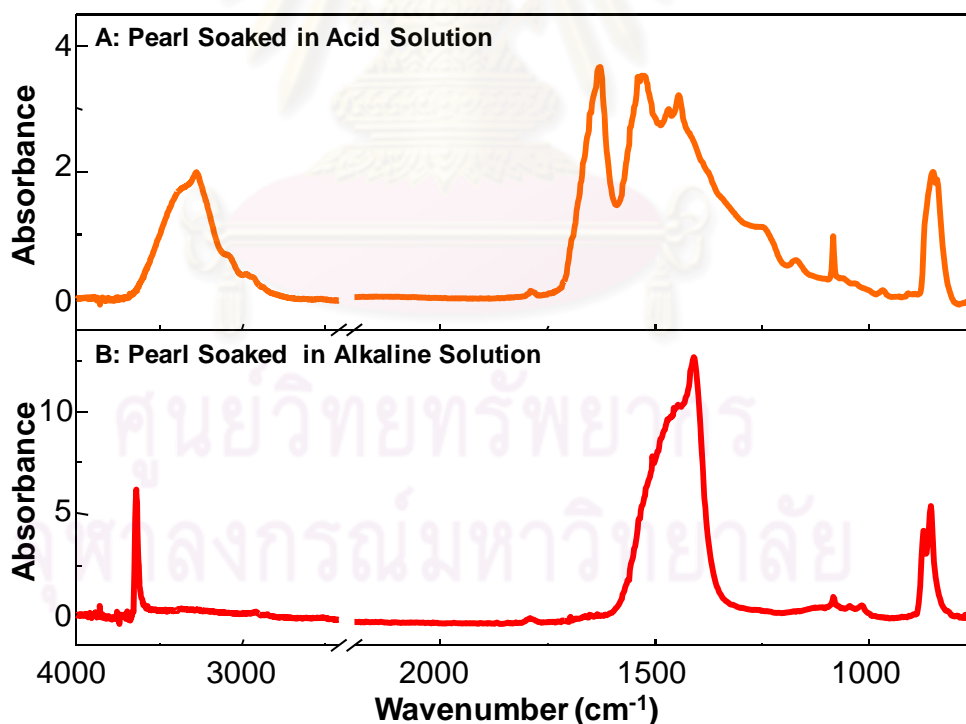


Figure 4.25 ATR FT-IR spectra of freshwater cultured pearl soaked in acid solution (A) and alkaline solution (B).

The optical images of freshwater cultured pearl soaked in acid solution showed conchiolin protein coated on pearl surface at different from original pearl surface as shown in Figure 4.26 E. It showed that calcium carbonate was destroyed. Then, freshwater cultured pearl soaked in alkaline solution showed gap between aragonite platelets which indicated conchiolin protein was destroyed as shown in Figure 4.26 F. The alkaline and acid solution destroyed surface and the luster of pearl.

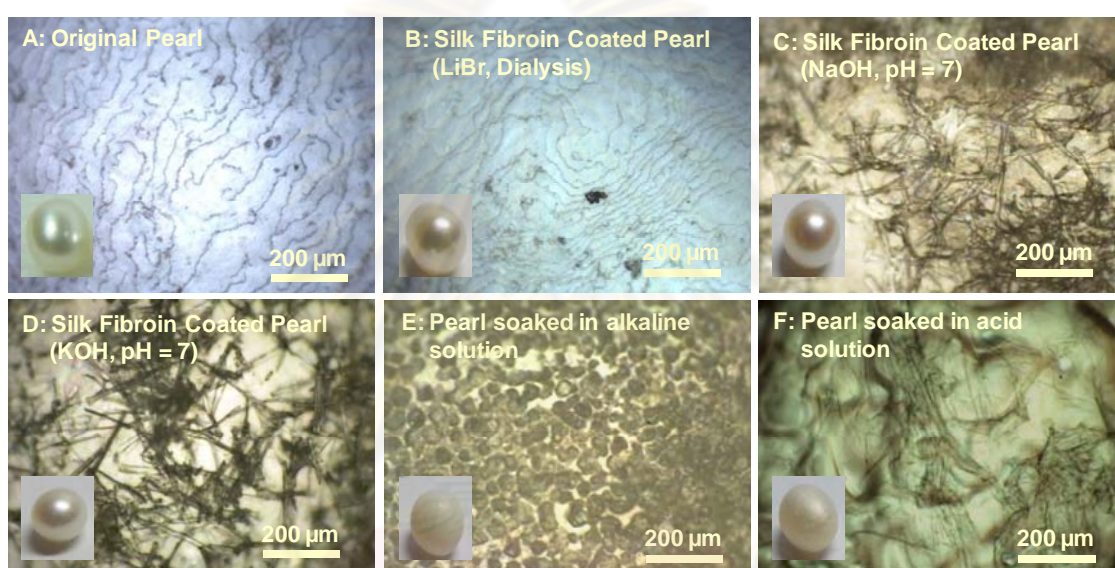


Figure 4.26 Optical images of freshwater cultured pearl (A), coated with silk fibroin solution by dialysis method (B), by adjusting to neutral pH method using NaOH (C), KOH (D), freshwater cultured pearl soaked in alkaline solution (E) and acid solution (F).

It is concluded that the optimal preparation of silk fibroin solution with 2 g (2 % w/v) of silk fibroin fibers dissolved in 0.35 M NaOH solution and adjusted the pH of solution in the range of 7 with HCl. This method reduced the time for dissolving fiber, costs of the preparation, chemicals, energy, waste from the preparation and time of the dialysis method.

4.4 Effect of the temperature for the sticking of silk fibroin on pearl surface

The coating silk fibroin solution on pearl surface are performed at room temperature, 50 °C and 100 °C (no higher temperatures and the energy will be saved). We did not use high temperatures because the solvent was water with its boiling point of 100 °C. After that, we analyzed freshwater cultured pearl coated with silk fibroin solution at different times by ATR FT-IR microspectroscopy as shown in Figure 4.27. The spectra of freshwater cultured pearl coated with silk fibroin solution at room temperature, 50 °C and 100 °C for 30 min showed the characteristic peaks of N-H stretching and Amide I which varied shape and the shoulder peaks of Amide II and Amide III at all temperature indicated that silk fibroin stuck on pearl surface. The stuck of silk fibroin increased with increasing temperatures. It was found that at 100 °C showing the character of silk fibroin stuck on pearl surface better than the other temperatures.

ATR FT-IR spectra of freshwater cultured pearl soaked in water at room temperature, boiled in water at 50 °C and 100 °C for 30 min. It showed that intensity of peaks at O-H stretching and Amide I were decreased at high temperature. From previous studies, the conchiolin protein in pearl component consists of soluble and insoluble fractions. The soluble proteins removed out at high temperatures that silk fibroin solution can be inserted to replace conchiolin protein. It was making the better stuck on pearl surface.

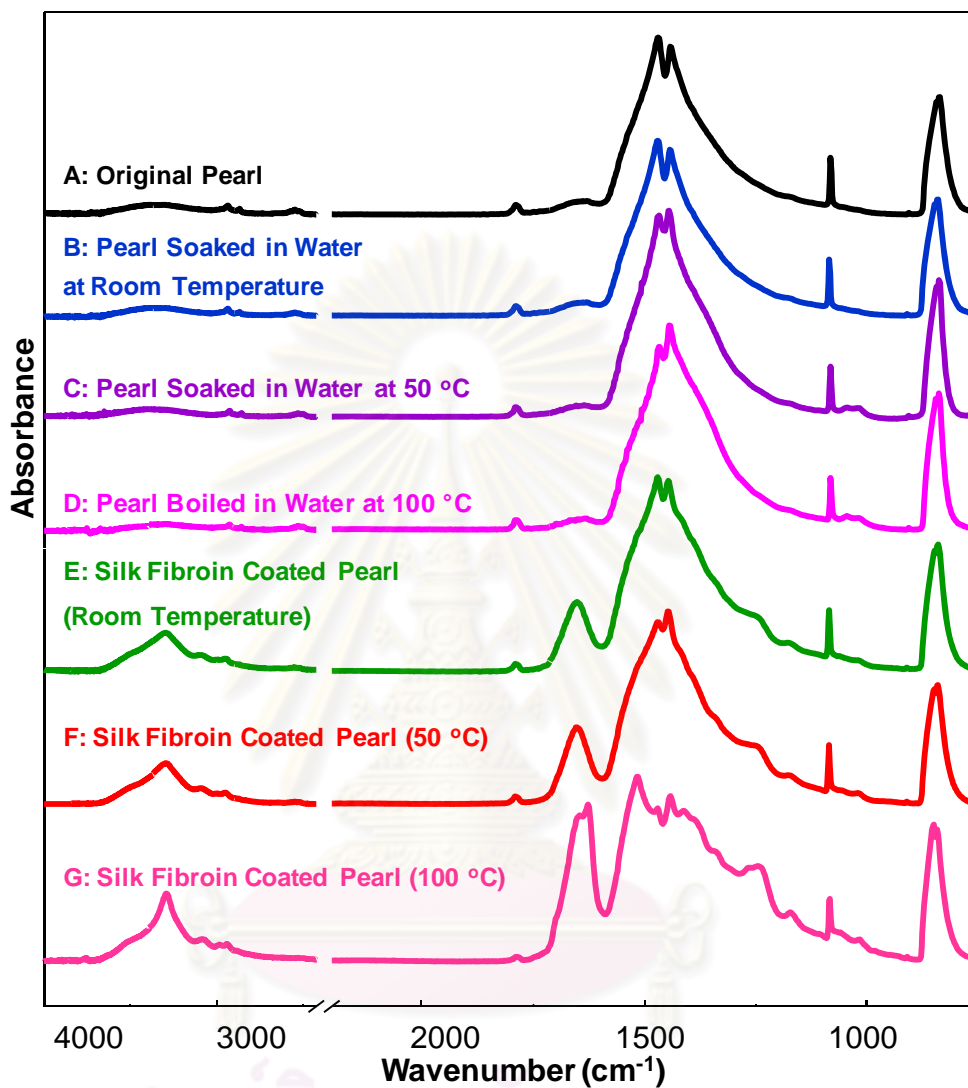


Figure 4.27 ATR FT-IR spectra of freshwater cultured pearl coated with silk fibroin solution at room temperature (A), 50 °C (B) and 100 °C (C) for 30 min. Pearl soaked in water at room temperature (D), boiled in water at 50 °C (E) and 100 °C (F) for 30 min.

The results of ATR FT-IR microspectroscopy showed that temperatures had nearly no effects for the sticking of silk fibroin on pearl surface. However, at 100 °C, it was

appropriate for coating because it displayed silk fibroin stuck on pearl surface as well. Since, the hot water washed conchiolin protein and silk fibroin solution can be inserted to replace conchiolin protein which showing the character silk fibroin stuck on pearl surface.

4.5 Effect of the time for the sticking of silk fibroin on pearl surface

In order to observe the role of the time for the sticking of silk fibroin solution on pearl surface, the time was adjusted in the coating process as follows: 30, 60 and 90 min at room temperature, 50 °C and 100 °C. After that, the treated samples were performed by ATR FT-IR microspectroscopy.

It was found that the ATR FT-IR spectra of freshwater cultured pearl coated with silk fibroin solution at room temperature for 30, 60 and 90 min showed the characteristic peaks of N-H stretching and Amide I which varied shape and the shoulder peaks of Amide II and Amide III. It suggested the molecular information of silk fibroin stuck on pearl surface. Furthermore, it was found that for 90 min; it had sharper peak at N-H stretching and highest intensity of Amide I. It showed the character of silk fibroin stuck on pearl surface better than that for 30 and 60 min as shown in Figure 4.28. The stuck of silk fibroin increased with increasing times.

ศูนย์วิทยทรัพยากร
จุฬาลงกรณ์มหาวิทยาลัย

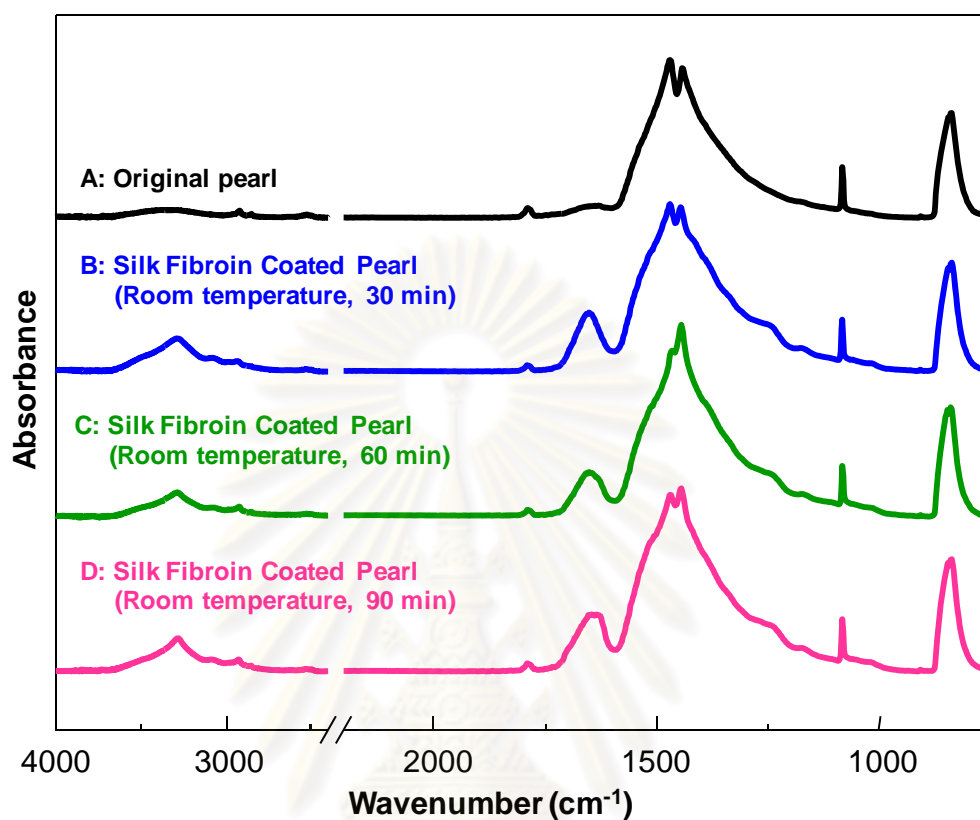


Figure 4.28 ATR FT-IR spectra of freshwater cultured pearl (A) coated silk fibroin solution at room temperature for 30 (B), 60 (C) 90 min (D).

After that, freshwater cultured pearl coated with silk fibroin solution at 50 °C for 30, 60 and 90 min were analyzed by ATR FT-IR microspectroscopy. ATR FT-IR spectra showed the characteristic peaks of N-H stretching and Amide I which varied shape and the shoulder peaks of Amide II and Amide III indicated the silk fibroin stuck on pearl surface (Figure 4.29). Furthermore, it was found that the coating sample for 90 min showed the character of silk fibroin stuck on pearl surface better than that for 30 and 60 min.

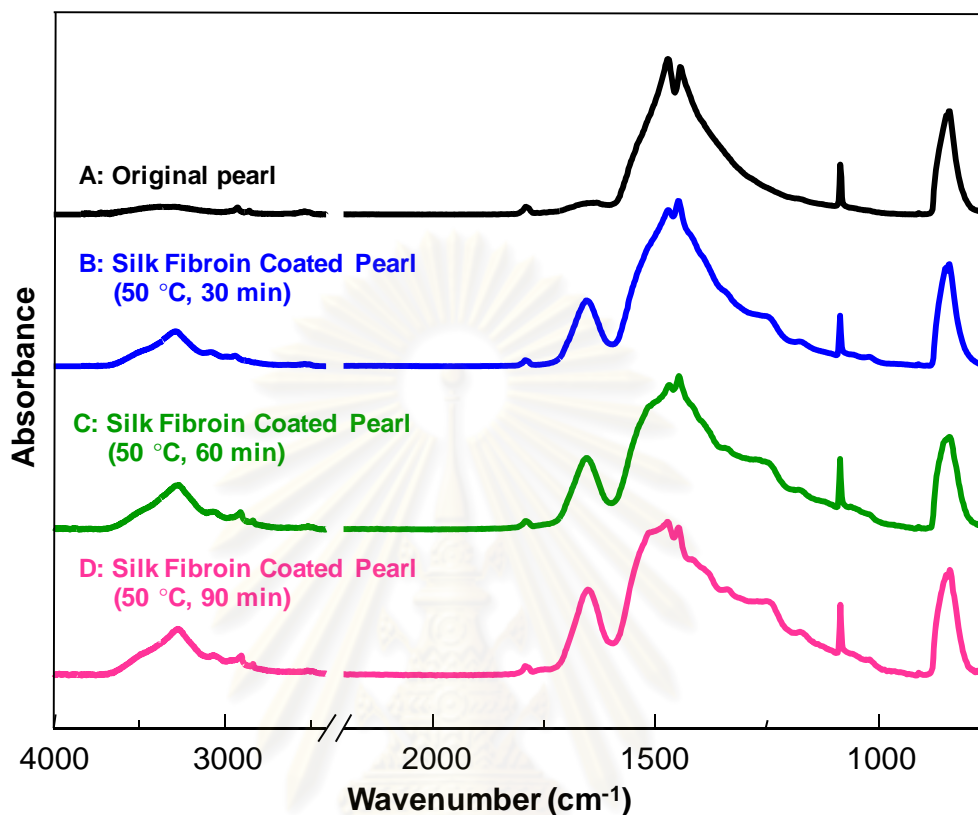


Figure 4.29 ATR FT-IR spectra of freshwater cultured pearl (A) coated with silk fibroin solution at 50 °C for 30 (B), 60 (C) 90 min (D).

Freshwater cultured pearl coated with silk fibroin solution at 100 °C for 30, 60 and 90 min were analyzed by ATR FT-IR microspectroscopy. ATR FT-IR spectra showed the characteristic peaks of N-H stretching and Amide I which the varied shape and the shoulder peaks of Amide II and Amide III indicated silk fibroin stuck on pearl surface (Figure 4.30). It was found that the sample for 30 min showed the character of silk fibroin stuck on pearl surface better than that for 60 and 90 min. At 100 °C due to the increasing time, silk fibroin solution will be destroyed by heat that caused silk fibroin performing degradation. At room temperature and 50 °C showed ATR FT-IR spectra indicates the stuck of silk fibroin increased with increasing time but at 100 °C that indicated the stuck of silk fibroin decreased with increasing time.

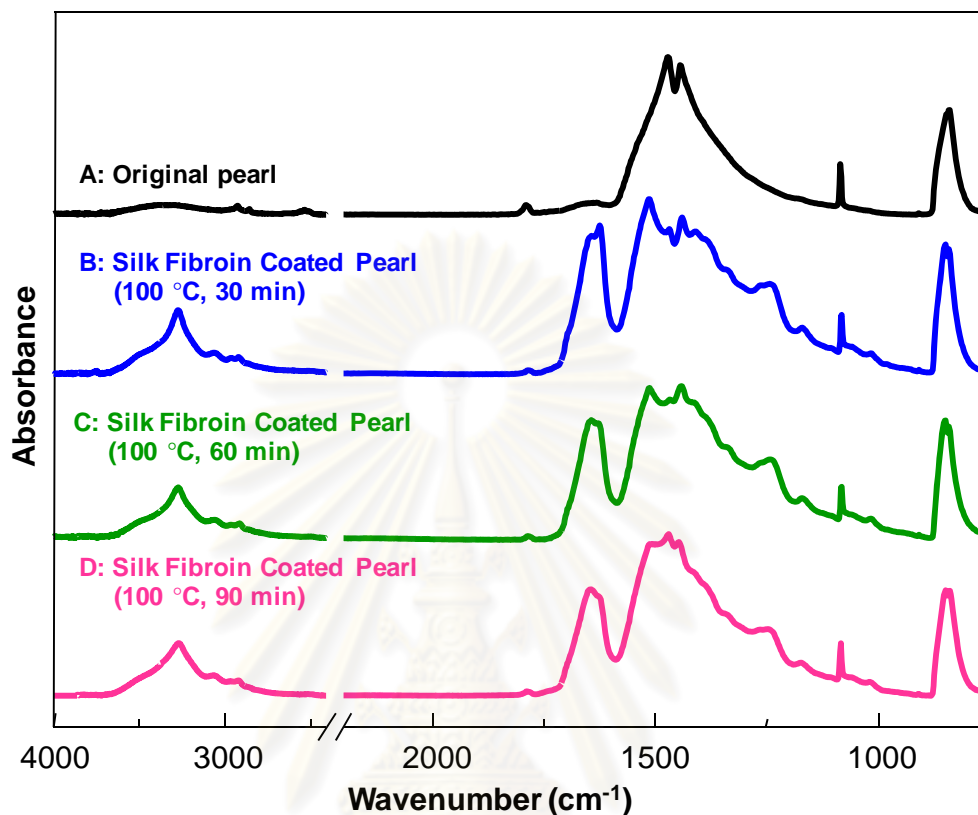


Figure 4.30 ATR FT-IR spectra of freshwater cultured pearl (A) coated with silk fibroin solution at 100 °C for 30 (B), 60 (C) and 90 min (D).

All in all, the comparisons of the ATR FT-IR spectra of freshwater cultured pearl coated with silk fibroin solution at room temperature, 50 °C and 100 °C for 30, 60 and 90 min, it was found that the coating at 100 °C for 30 min showing the optimal stick of silk fibroin on pearl surface and saved the time and vice versa.

4.6 Effect of the alcohol treatment for the sticking of silk fibroin on pearl surface

In order to observe the role of the alcohol treatment for the sticking of silk fibroin solution on pearl surface, it was getting started with the performance of alcohol which had effectiveness of extracting into water from the molecular structure of silk fibroin and

changed structure from amorphous to crystalline. Since, freshwater cultured pearl coated with silk fibroin solution treated methanol, ethanol and isopropyl alcohol (2-propanol). All of the alcohols treatment samples are analyzed by ATR FT-IR microspectroscopy. ATR FT-IR spectra of freshwater cultured pearl coated with silk fibroin solution and treated alcohol showed the characteristic peaks of N-H stretching, Amide I and the shoulder peaks of Amide II and Amide III (Figure 4.31). It was found that freshwater cultured pearl coated with silk fibroin solution treated methanol showed character of silk fibroin optimal stuck on pearl surface (Figure 4.31 E). Methanol extracted water from the molecular structure better than that of ethanol and isopropyl alcohol (2-propanol) because methanol has the smallest size. Methanol changed secondary structure of silk fibroin from random coil and α -helix to β -sheet which showed the amorphous changed to crystalline structure causing water insoluble and has been to more difficult to remove from the pearl surface.



ศูนย์วิทยทรัพยากร
จุฬาลงกรณ์มหาวิทยาลัย

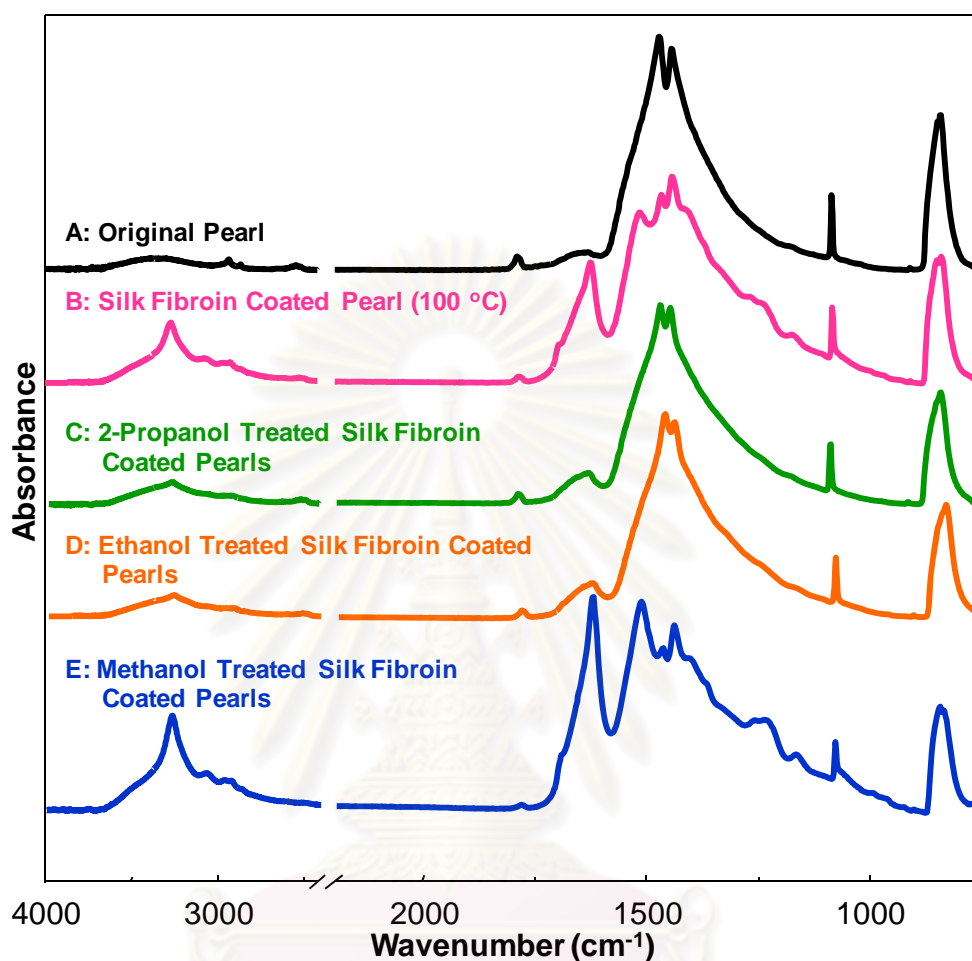


Figure 4.31 ATR FT-IR spectra of freshwater cultured pearl (A), coated with silk fibroin solution plus isopropyl alcohol (2-propanol) (B), ethanol (C) and methanol treatment (D).

4.7 Effect of the methanol treatment for the sticking of silk fibroin on pearl surface

In order to observe the role of the methanol treatment for the sticking of silk fibroin solution on pearl surface, it was getting started with freshwater cultured pearl coated with silk fibroin solution and treated methanol, then analyzed by ATR FT-IR microspectroscopy. From the analysis, the spectra showed the characteristic peaks of N-H stretching, Amide I

and the shoulder peaks of Amide II and Amide III indicated silk fibroin stuck on pearl surface for both cases (Figure 4.33 B, D).

So, it will be tested the permanent of silk fibroin solution stuck on pearl surface by boiling in water at 100 °C for 10 min (Figure 4.32 C, E) and then analyzed. The spectrum of freshwater cultured pearl coated with silk fibroin solution showed characteristic peaks were decreased, that indicated silk fibroin fall off from pearl surface. Silk fibroin in the solution had the secondary structure of random coil and α -helix conformation which showed amorphous structure causing water soluble well (Figure 4.33 C). Freshwater cultured pearl coated with silk fibroin solution plus methanol treatment showed character of silk fibroin stuck on pearl surface (Figure 4.33 E). After that, the results of ATR FT-IR microspectroscopy will be confirmed by Raman microspectroscopy.

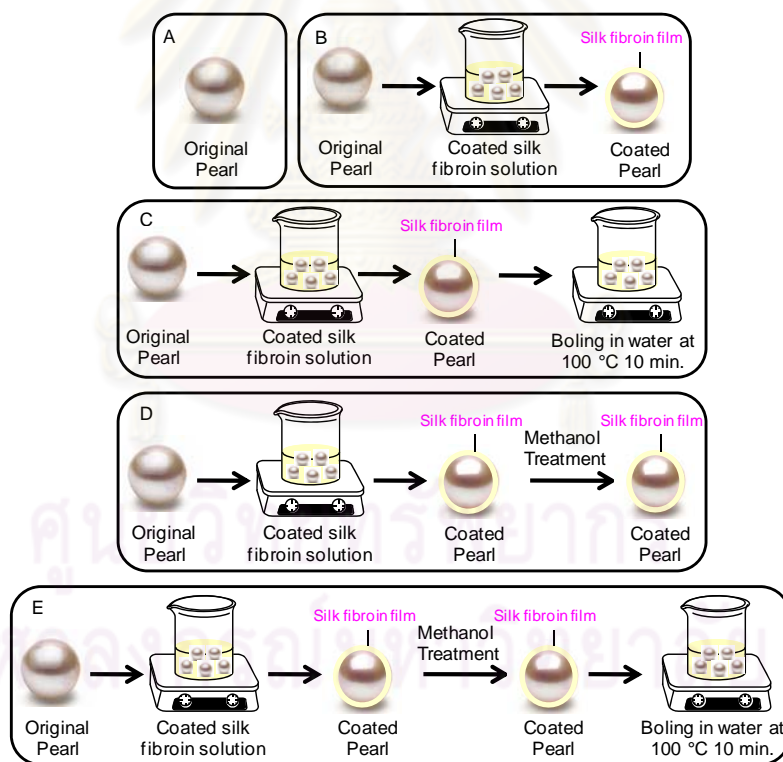


Figure 4.32 Diagram of freshwater cultured pearl (A), coated with silk fibroin solution (B) boiled in water at 100 °C for 10 min (C). Pearl coated with silk fibroin solution plus methanol treatment (D) boiled in water at 100 °C for 10 min (E).

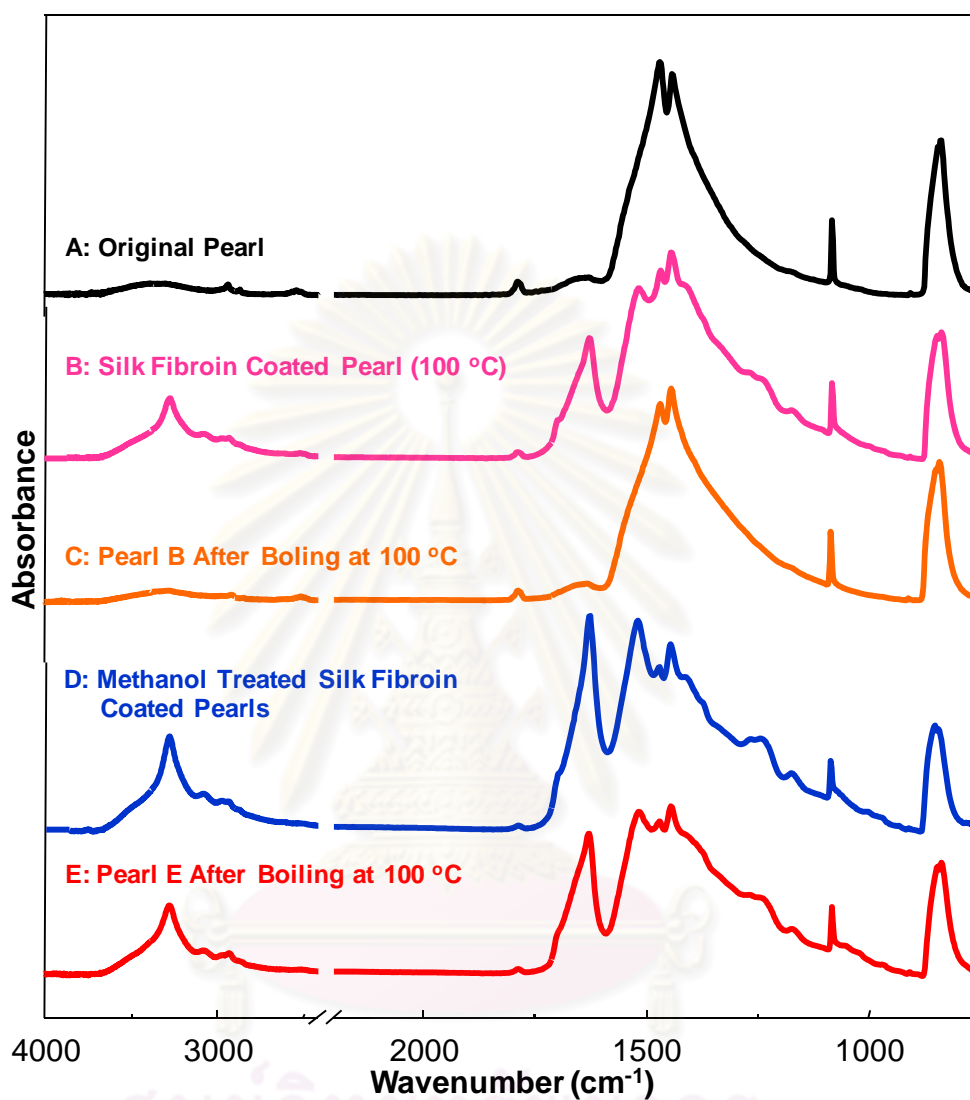


Figure 4.33 ATR FT-IR spectra of freshwater cultured pearl (A) coated with silk fibroin solution (B) boiled in water at 100 °C 10 min (D). P coated with silk fibroin solution plus methanol treatment (C) boiled in water at 100 °C 10 min (E).

Raman spectra of freshwater cultured pearl coated with silk fibroin solution plus methanol treatment showed the characteristic peaks at N-H stretching and Amide I which

varied shape and Amide III of both as shown in Figure 4.34 (B, D), which indicated silk fibroin stuck on pearl surface.

After that, the test of the permanent of silk fibroin solution stuck on pearl surface was performed by boiling in water at 100 °C for 10 min. The spectrum of freshwater cultured pearl coated with silk fibroin solution did not show the characteristic peaks of N-H stretching, Amide I and Amide III, which indicated silk fibroin fall off from pearl surface (Figure 4.34 C). Raman spectrum of freshwater cultured pearl coated with silk fibroin solution plus methanol treatment showed character of silk fibroin stuck on pearl surface (Figure 4.34 E).



ศูนย์วิทยทรัพยากร
จุฬาลงกรณ์มหาวิทยาลัย

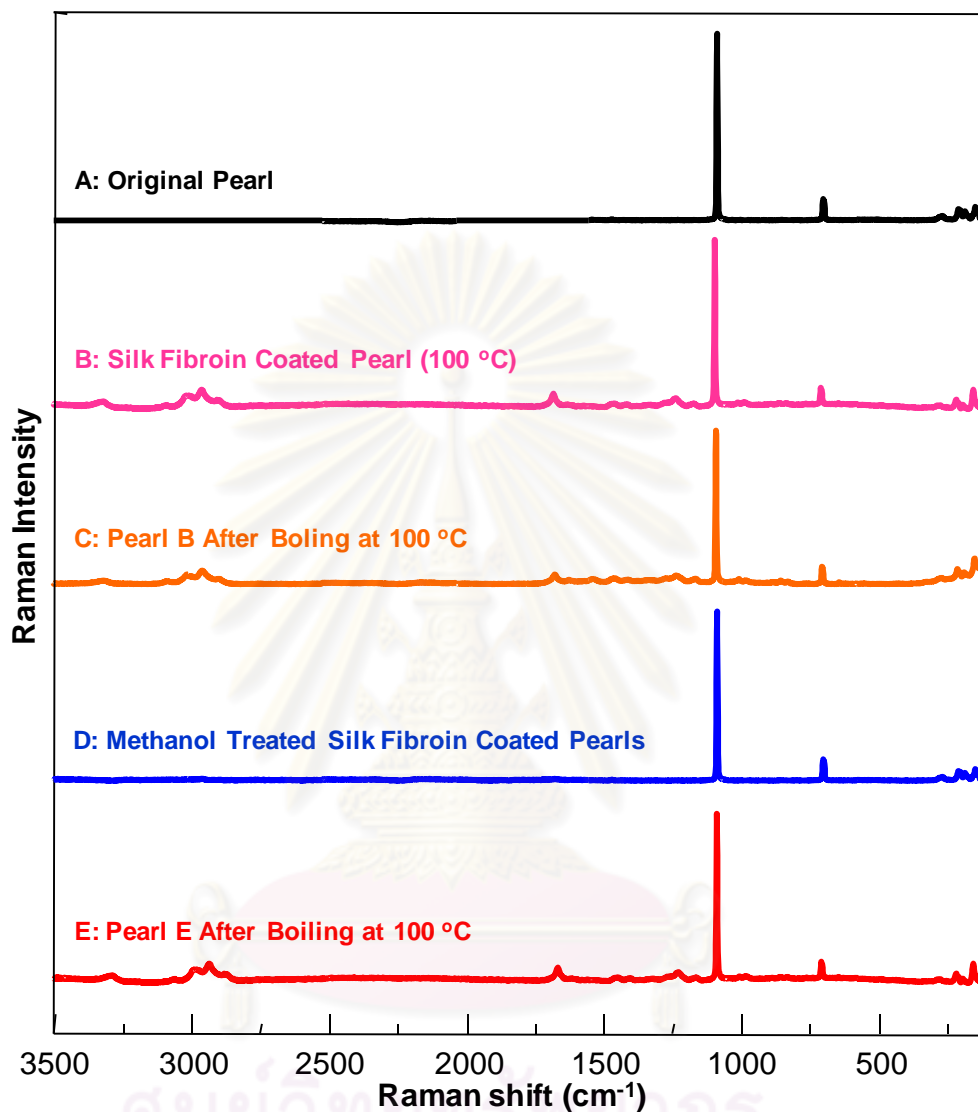


Figure 4.34 Raman spectra of freshwater cultured pearl (A) coated with silk fibroin solution (B) and boiled in water at 100 °C 10 min (C). Pearl coated with silk fibroin solution plus methanol treatment (D) and boiled in water at 100 °C 10 min (E).

The results of ATR FT-IR and Raman microspectroscopy indicated that silk fibroin solution plus methanol treatment stuck on pearl surface more permanent and it protected pearl surface as well. Methanol treatment improved the performance of silk fibroin stuck on pearl surface, increased luster and protected surface from heat.

4.8 Effect of the polishing for the sticking of silk fibroin on pearl surface

Freshwater cultured pearl coated with silk fibroin solution plus methanol treatment and cleaned surface by polishing, are analyzed by ATR FT-IR microspectroscopy. The spectra of pearl treated after methanol treatment showed the characteristic peaks of N-H stretching and Amide I which varied shape and the shoulder peaks of Amide II Amide III indicated silk fibroin stuck on pearl surface (Figure 4.35 B-C). After polishing pearl surface, it was found that the spectra showed the intensity of peaks were decreased significantly as shown in Figure 4.35 (D-E) comparable to Figure 4.35 (B-C). The results indicated that the polishing affect the stuck of silk fibroin solution on pearl surface, thus it should be wiping pearl surface instead of polishing pearl surface as shown in Figure 4.36.

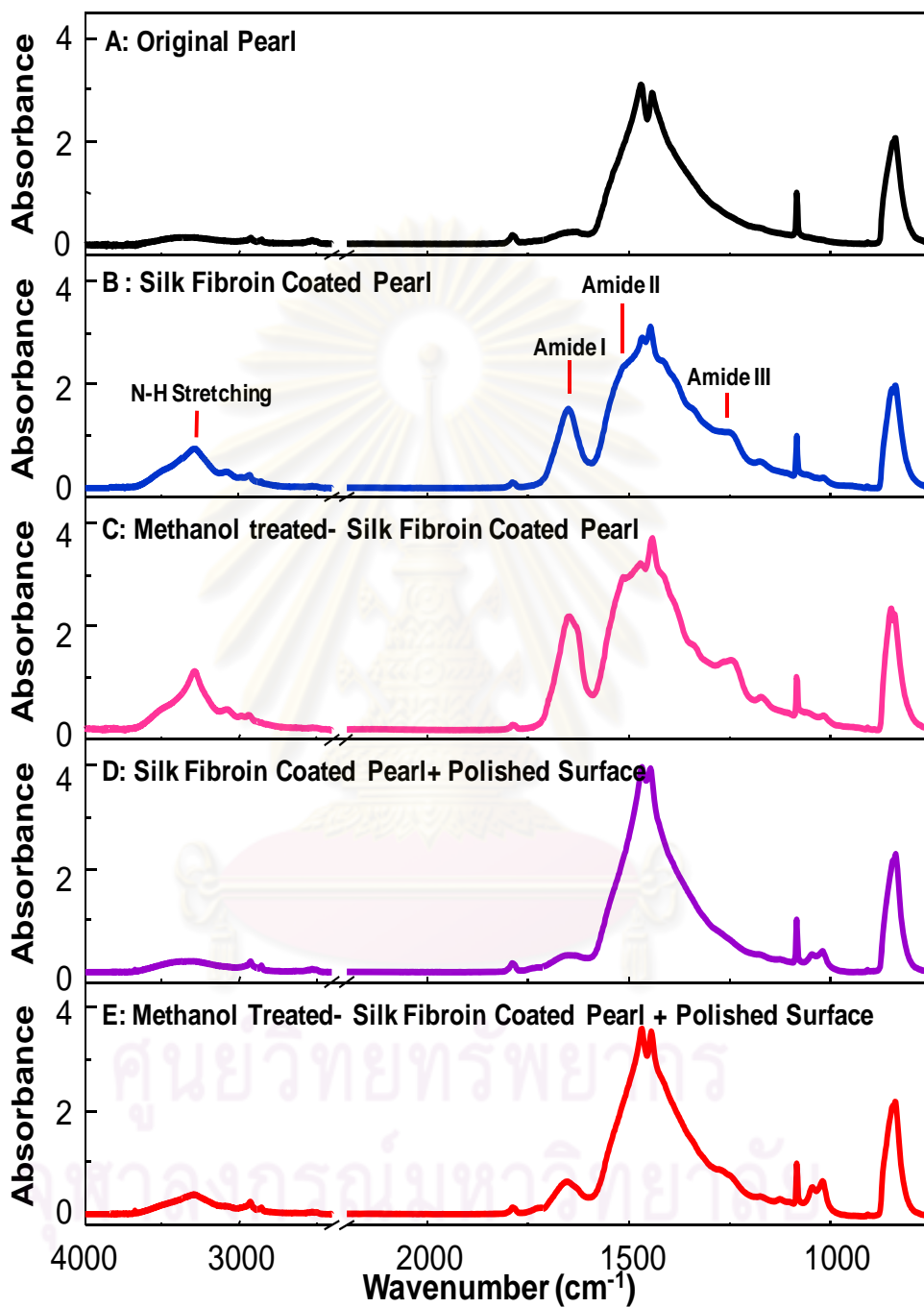


Figure 4.35 ATR FT-IR spectra of freshwater cultured pearl (A) coated with silk fibroin solution (B) and polished surface (D). Pearl coated with silk fibroin solution plus methanol treatment (C) and polishing surface (E).

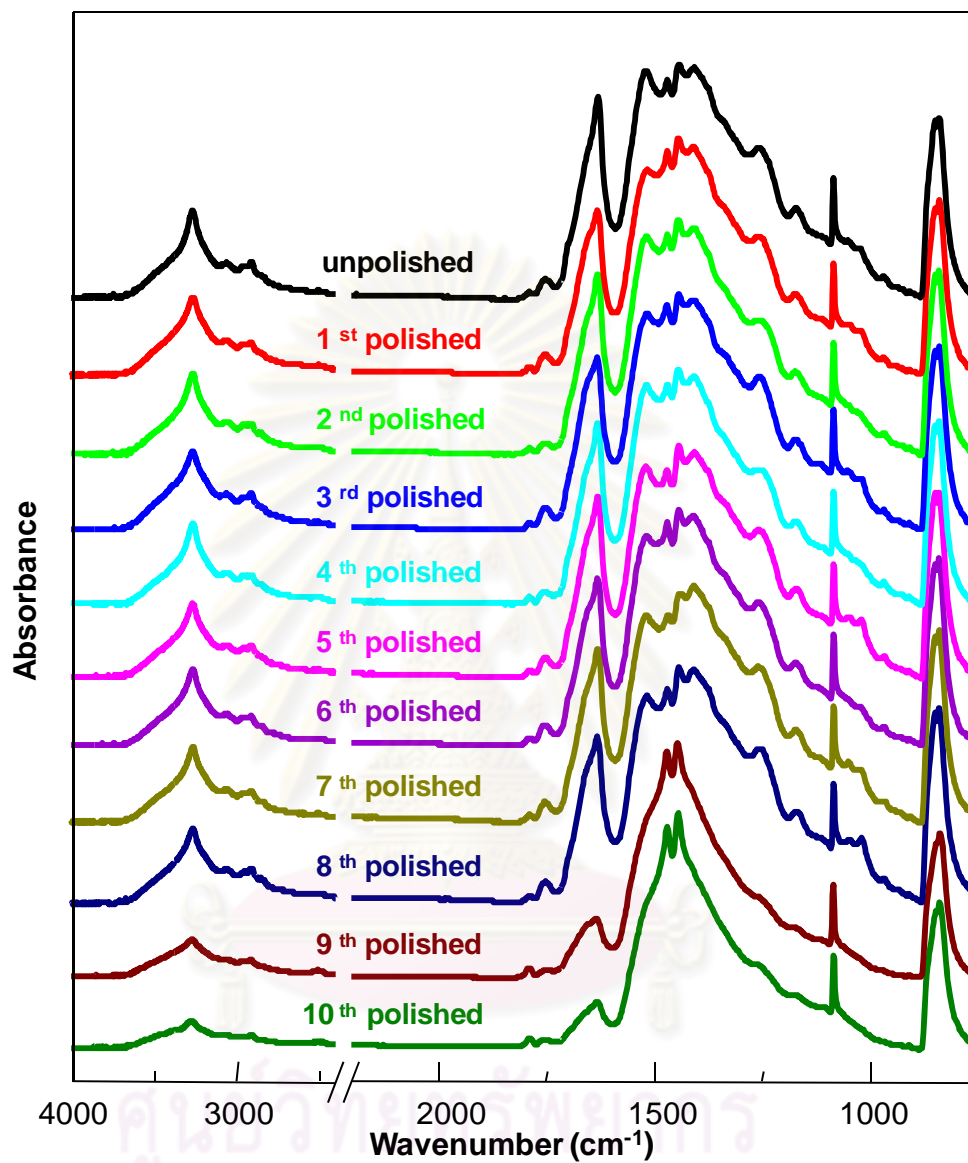


Figure 4.36 ATR FT-IR spectra of freshwater cultured pearl coated with silk fibroin solution plus methanol treatment polishing surface.

The results of ATR FT-IR microspectroscopy suggested the removal of silk fibroin on pearl surface after polishing. So the polishing affected the stuck of silk fibroin on pearl surface thus, it should be wiped pearl surface instead of polishing it.

4.9 Resistance to corrosion of pearl after coated with silk fibroin solution on surface

Pearls are organic gems that are vulnerable to alkaline, acid, different humidity levels and heat. Lotion, shower cream, shampoo, detergent and perfume all contain chemicals that can dramatically dull the luster of pearl surface. It is best to put your pearls on at least 30 min after applying any personal care products which are important tip to care for your pearls. We test the resistance to corrosion of pearl after coating with silk fibroin solution on surface by heat, solvents and detergents. They were analyzed by ATR FT-IR microspectroscopy. Figure 4.37 showed process of test the resistance to corrosion of pearl after coating with silk fibroin solution on surface by heat, solvents and detergents.

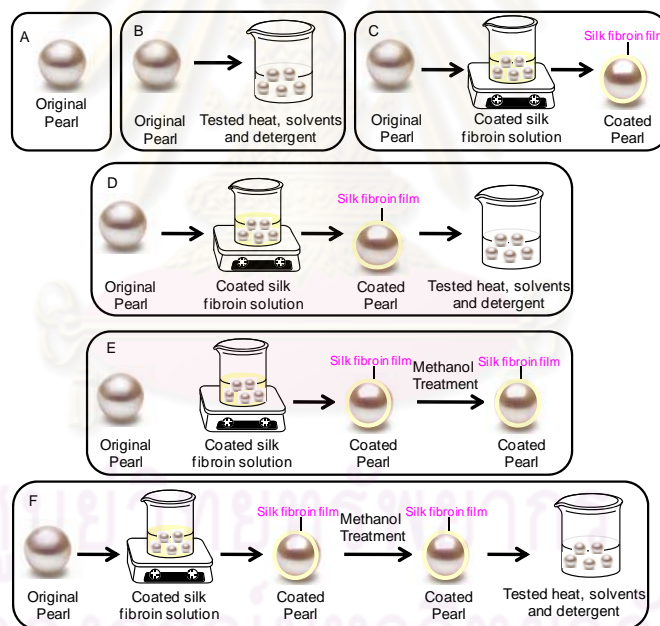


Figure 4.37 Process of test the resistance to corrosion of pearl after coating with silk fibroin solution on surface by solvents and detergents. Freshwater cultured pearl (A) tested heat, solvent and detergent (B). Pearl coated with silk fibroin solution (C) test heat, solvent and detergent (D). Pearl coated with silk fibroin solution plus methanol treatment (E) test heat, solvent and detergent (F).

4.9.1 Heat

The effect of heat for the sticking of silk fibroin solution on pearl surface was analyzed by ATR FT-IR and Raman microspectroscopy (Figure 4.38). ATR FT-IR spectrum of freshwater cultured pearl boiled in water at 100 °C for 10 min showed the molecular information of pearl the same as that of original pearl (Figure 4.38 A-B). It was found that the decreased in luster from original pearl because the heat destroyed the luster of pearl. From previous studies, the conchiolin protein in pearl component consists of soluble and insoluble fractions. The soluble protein removed out when high temperature water damaged the pearl structure that caused the decrease of luster.

The results of ATR FT-IR microspectroscopy of freshwater cultured pearl coated with silk fibroin solution demonstrated the characteristic peaks of N-H stretching and Amide I which varied shape and the shoulder peaks of Amide II and Amide III indicated silk fibroin stuck on pearl surface (Figure 4.38 C). After that, boiled freshwater cultured pearl coated with silk fibroin solution in water at 100 °C for 10 min and was performed by ATR FT-IR microspectroscopy. ATR FT-IR spectrum indicated silk fibroin removed from pearl surface when heating (Figure 4.38 E). The result showed that the heat will remove amorphous structure but it did not destroy the surface of pearl.

Furthermore, the spectrum of freshwater cultured pearl coated with silk fibroin solution plus methanol treatment showed character silk fibroin stuck on pearl surface (Figure 4.38 D). ATR FT IR spectrum of sample was boiled in water at 100 °C for 10 min demonstrated that silk fibroin stuck on pearl surface (Figure 4.38 F). It was found that the heat did not destroy silk fibroin stuck on pearl surface because silk fibroin film protected surface which the heat did not damage surface of pearl. Heat did not affect silk fibroin of crystalline structure and film coating protected pearl surface that did not destroy, so the luster of pearl still remains.

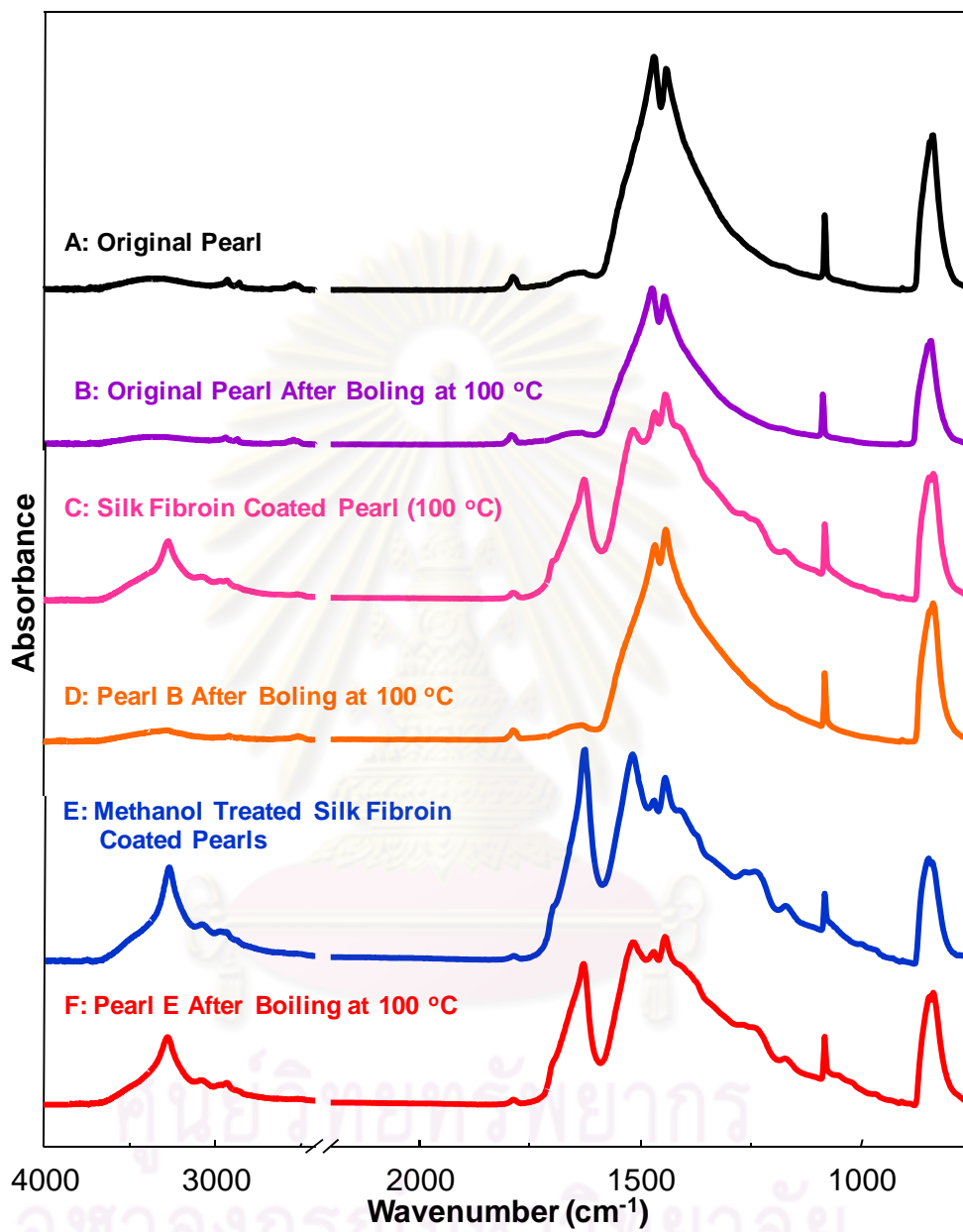


Figure 4.38 ATR FT-IR spectra of freshwater cultured pearl (A) boiled in water at 100 °C 10 min (B). Pearl coated with silk fibroin solution (C) boiled in water at 100 °C 10 min (E). Pearl coated with silk fibroin solution plus methanol treatment (D) boiled in water at 100 °C 10 min (F).

Raman spectrum of freshwater cultured pearl boiled in water at 100 °C for 10 min showed the molecular information of pearl the same as that of original pearl (Figure 4.39 A-B). However, Raman spectrum of freshwater cultured pearl with coated silk fibroin showed the character of silk fibroin stuck on pearl surface as shown in Figure 4.38 C. If the tested object boiled in water at 100 °C for 10 min, Raman spectrum indicated silk fibroin removed from pearl surface when received the heat (Figure 4.39 D). The result showed the luster of the original pearl because the heat directly destroyed silk fibroin and had a very little chance to destroy pearl surface. Vice versa, Raman spectrum of freshwater cultured pearl coated with silk fibroin solution plus methanol treatment showed the character of silk fibroin stuck on pearl surface (Figure 4.39 E). After boiling in water at 100 °C for 10 min that Raman spectrum still showed silk fibroin stuck on pearl surface as shown in Figure 4.39 F. Raman spectra confirmed the results of ATR FT-IR microspectroscopy which suggested the heat did not destroy silk fibroin stuck on pearl surface after methanol treatment because silk fibroin film changed amorphous to crystalline structure which water insoluble.

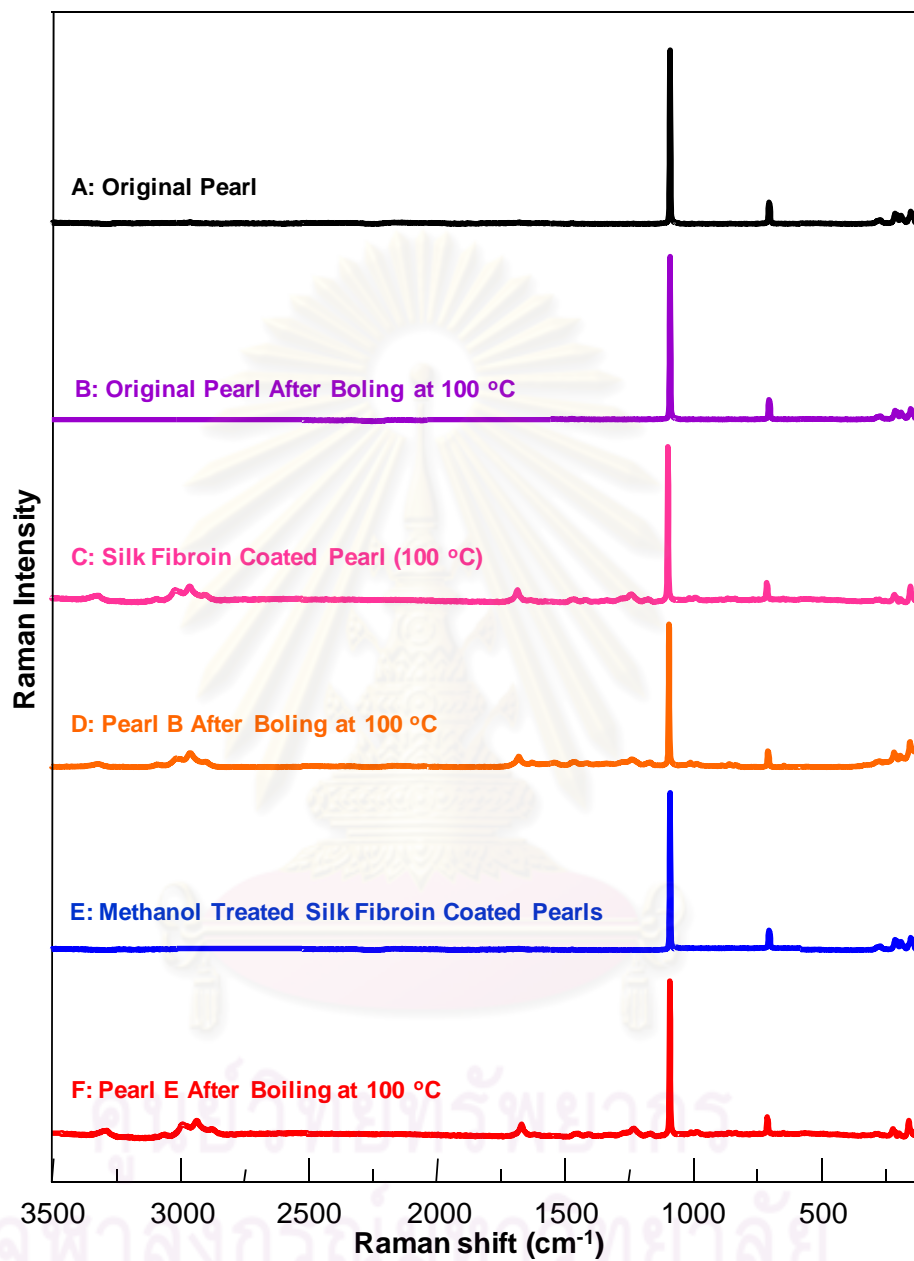


Figure 4.39 Raman spectra of freshwater cultured pearl (A) boiled in water at 100 °C 10 min (B). Pearl coated with silk fibroin solution (C) boiled in water at 100 °C 10 min (D). Pearl coated with silk fibroin solution plus methanol treatment (E) boiled in water at 100 °C 10 min (F).

The results of ATR FT-IR and Raman microspectroscopy suggested that the heat did not destroy silk fibroin stuck on pearl surface after methanol treatment. The coating of silk fibroin protected pearl surface from the heat.

4.9.2 Detergent and solvent

The method tested the resistance to corrosion of pearl (Figure 4.37). ATR FT-IR spectra of freshwater cultured pearl soaked with tap water, NaOH solution pH 8, 9 and 10, acid solution pH 4, 5 and 6, detergent, shower cream, body lotion, shampoo and perfume for 19 hours showed the molecular information of pearl the same as that of original pearl (Figure 4.40).



ศูนย์วิทยทรัพยากร
จุฬาลงกรณ์มหาวิทยาลัย

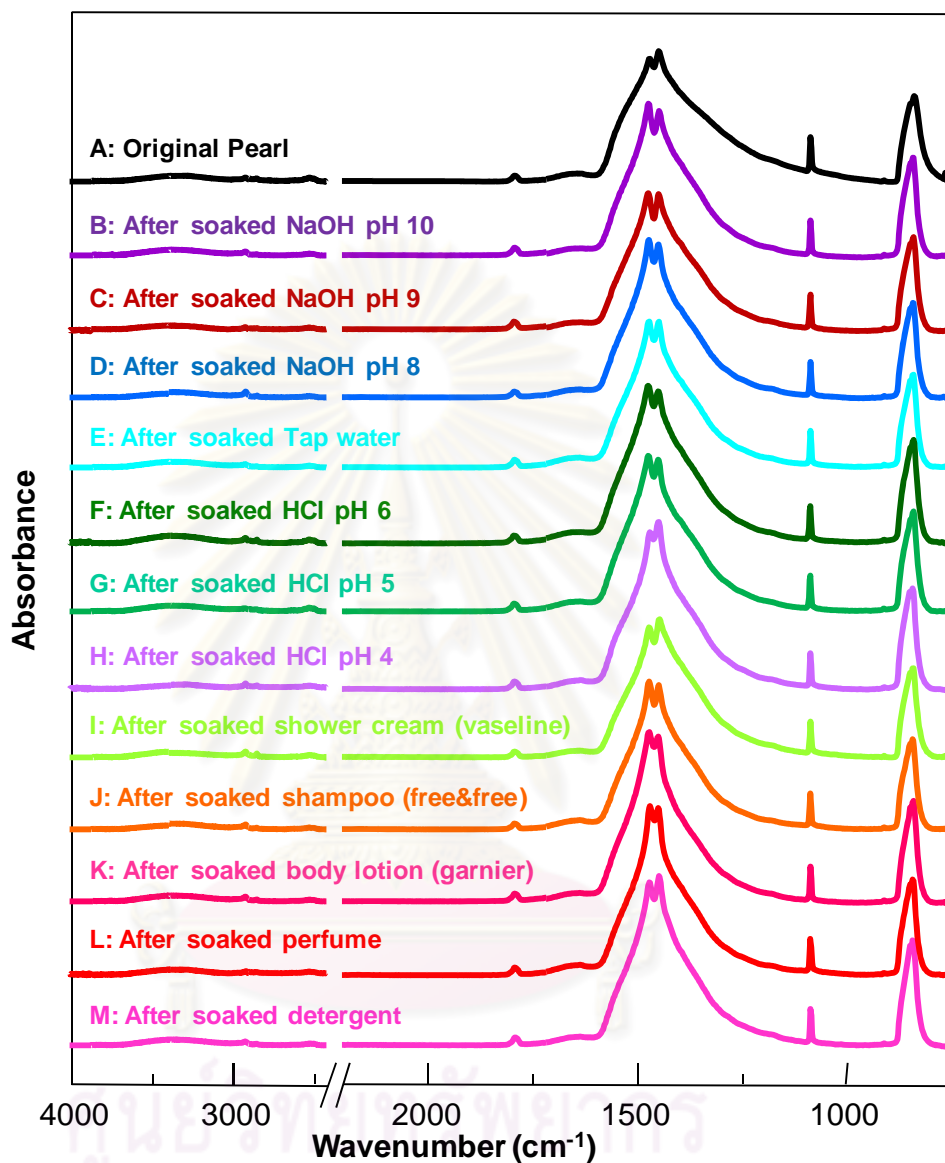


Figure 4.40 ATR FT-IR spectra of freshwater cultured pearl and soaked with tap water, NaOH solution pH 8, 9 and 10, HCl solution pH 4, 5 and 6, detergent, shower cream, body lotion, shampoo and perfume for 19 hours.

Figure 4.41 showed optical images of freshwater cultured pearl soaked with tap water, NaOH solution pH 8, 9 and 10, acid solution pH 4, 5 and 6, detergent, shower cream, body lotion, shampoo and perfume for 19 hours. It indicated pearl surface

destroyed after that soaked in solvents and detergents. It was found that the decreased in luster from original pearl because the solvent and detergent destroyed the luster of pearl. From previous studies, the pearls keep away from chlorine bleaching powder, detergent, vinegar, ammonia, hair spray, cosmetics, perfume and sunblock, as these substances will damage the pearl surface.

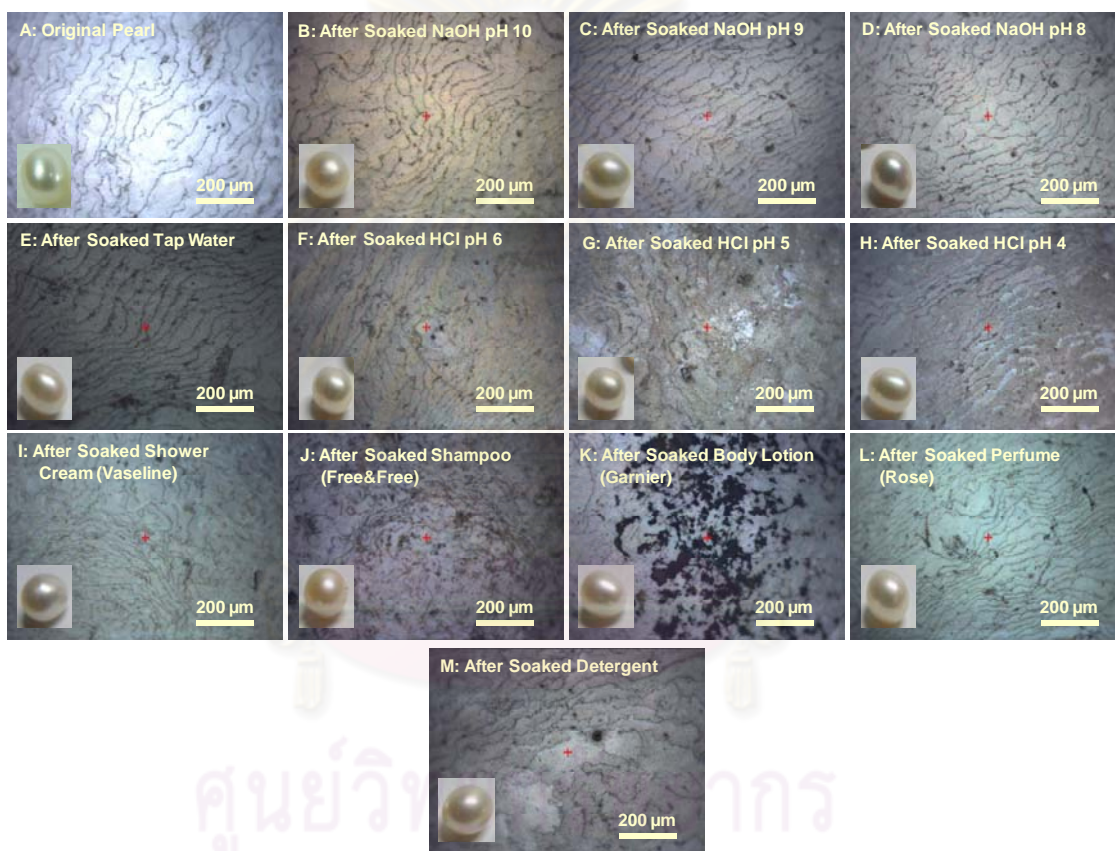


Figure 4.41 Optical images of freshwater cultured pearl and soaked with tap water, NaOH solution pH 8, 9 and 10, HCl solvent pH 4, 5 and 6, detergent, shower cream, body lotion, shampoo and perfume for 19 hours.

The results of ATR FT-IR microspectroscopy of freshwater cultured pearl coated with silk fibroin solution demonstrated the characteristic peaks of N-H stretching and

Amide I which varied shape and the shoulder peaks of Amide II and Amide III indicated silk fibroin stuck on pearl surface (Figure 4.42). After that, soaked with tap water, NaOH solution pH 8, 9 and 10, HCl solvent pH 4, 5 and 6, detergent, shower cream, body lotion, shampoo and perfume for 19 hours and was performed by ATR FT-IR microspectroscopy. ATR FT-IR spectrum indicated the stick performance of silk fibroin decreased from pearl surface after soaked with tap water NaOH solution pH 8, 9 and 10, HCl solvent pH 4, 5 and 6, detergent, shower cream, body lotion, shampoo and perfume for 19 hours (Figure 4.42). The result showed that the solvents and detergents will remove silk fibroin of amorphous structure but it did not destroy the surface of pearl.



ศูนย์วิทยทรัพยากร
จุฬาลงกรณ์มหาวิทยาลัย

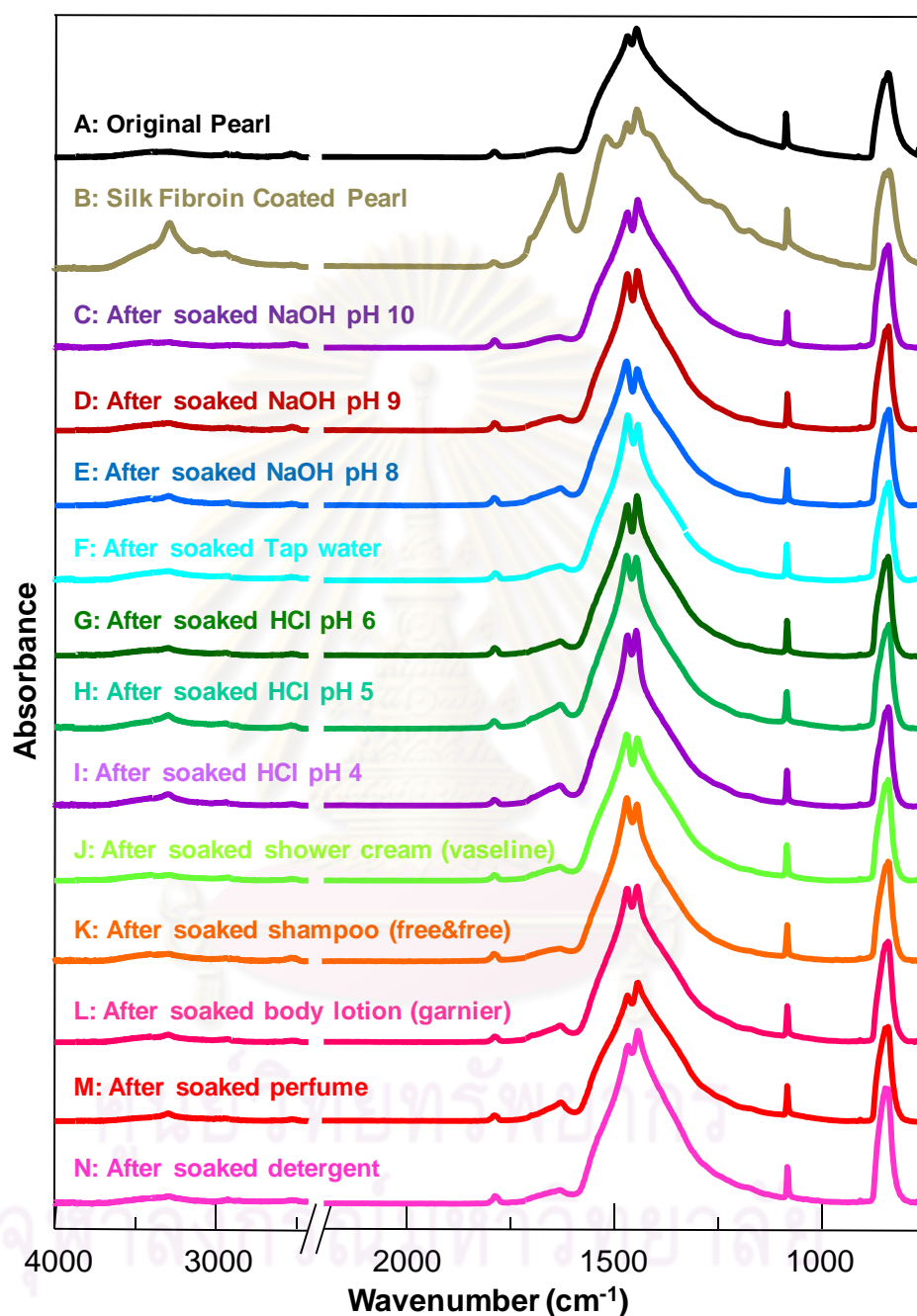


Figure 4.42 ATR FT-IR spectra of freshwater cultured pearl coated silk fibroin solution and soaked with tap water, NaOH solution pH 8, 9 and 10, HCl solution pH 4, 5 and 6, detergent, shower cream, body lotion, shampoo and perfume for 19 hours.

Optical images of freshwater cultured pearl coated silk fibroin solution soaked with tap water, NaOH solution pH 8, 9 and 10, HCl solution pH 4, 5 and 6, detergent, shower cream, body lotion, shampoo and perfume for 19 hours indicated pearl surface did not destroy after that soaked in solvents and detergents (Figure 4.43). It was found that the luster as same as original pearl because the solvent and detergent destroy silk fibroin stuck on pearl surface.

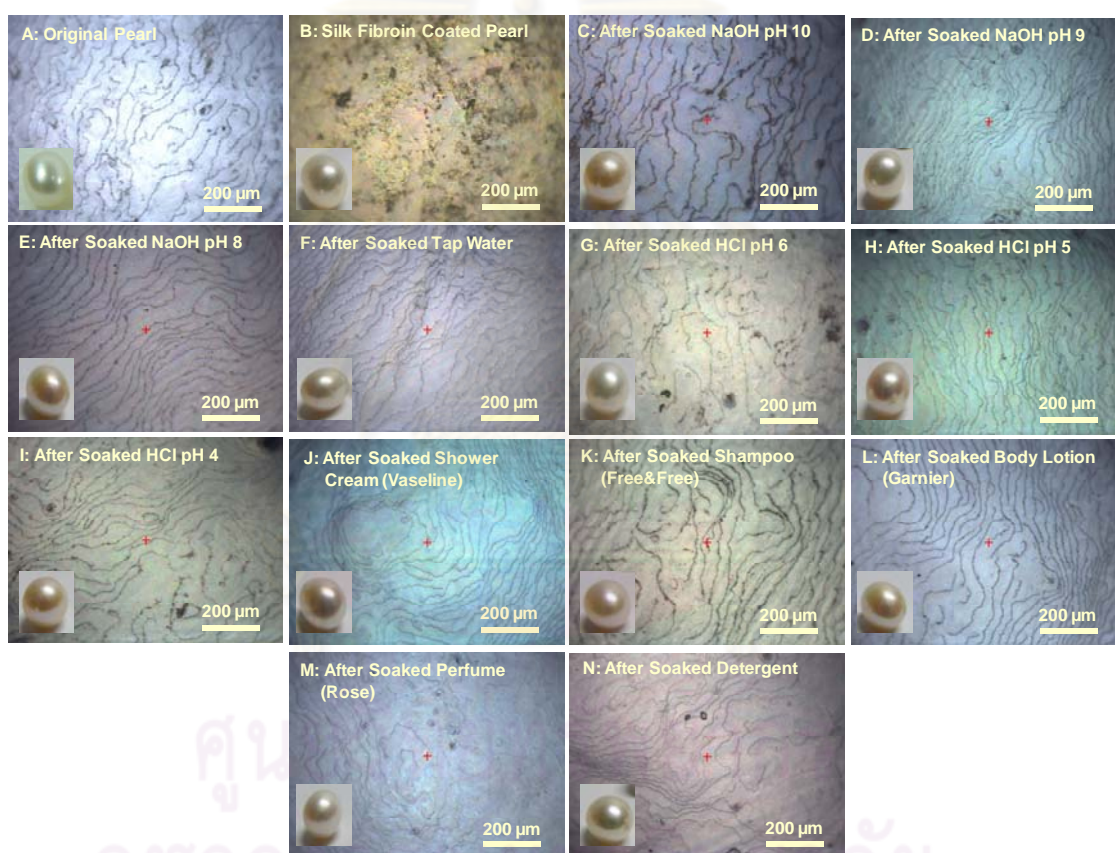


Figure 4.43 Optical images of freshwater cultured pearl coated silk fibroin solution and soaked tap water, NaOH solution pH 8, 9 and 10, HCl solution pH 4, 5 and 6, detergent, shower cream, body lotion, shampoo and perfume for 19 hours.

Furthermore, the spectrum of freshwater cultured pearl coated with silk fibroin solution plus methanol treatment showed character silk fibroin stuck on pearl surface (Figure 4.44). ATR FT-IR spectrum of sample was soaked with tap water, NaOH solution pH 8, 9 and 10, HCl solution pH 4, 5 and 6, detergent, shower cream, body lotion, shampoo and perfume for 19 hours demonstrated that silk fibroin stuck on pearl surface (Figure 4.44). It was found that the solvents and detergents did not destroy silk fibroin stuck on pearl surface but stick performance of silk on pearl surface deceased. Silk fibroin film plus methanol treatment protected pearl surface from damaging by solvents and detergents.



ศูนย์วิทยทรัพยากร
จุฬาลงกรณ์มหาวิทยาลัย

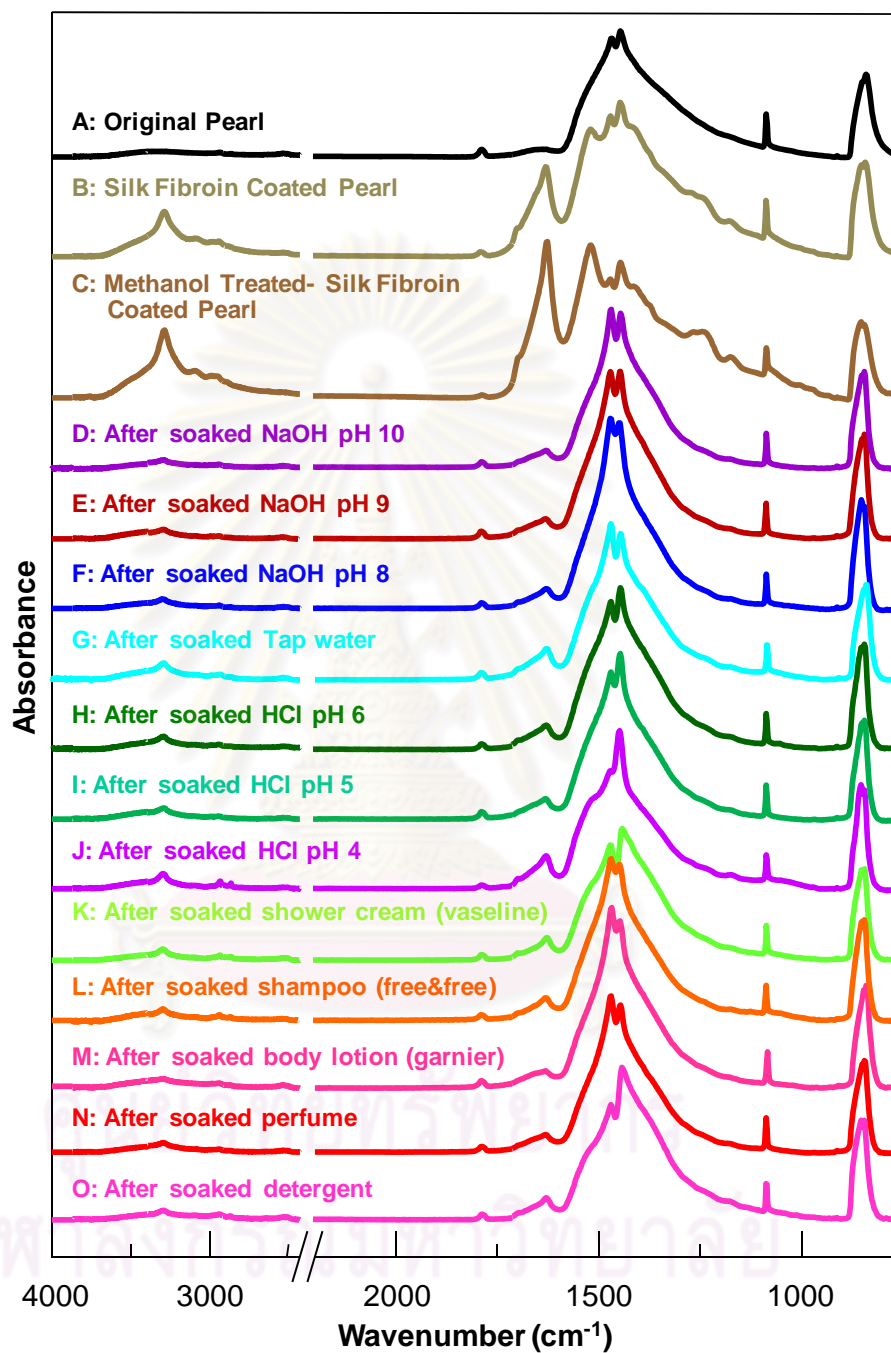


Figure 4.44 ATR FT-IR spectra of freshwater cultured pearl coated silk fibroin solution plus methanol treatment and soaked with tap water, NaOH solution pH 8, 9 and 10, HCl solution pH 4, 5 and 6, detergent, shower cream, body lotion, shampoo and perfume for 19 hours.

Optical images of freshwater cultured pearl coated silk fibroin solution plus methanol treatment and soaked with tap water NaOH solution pH 8, 9 and 10, HCl solution pH 4, 5 and 6, detergent, shower cream, body lotion, shampoo and perfume for 19 hours indicated pearl surface did not destroy after soaking in solvents and detergents (Figure 4.45). It was found that the luster was the same as original pearl because the solvents and detergents did not affect silk fibroin of crystalline structure and film coating protected pearl surface that did not destroy, so the luster of pearl still remains.

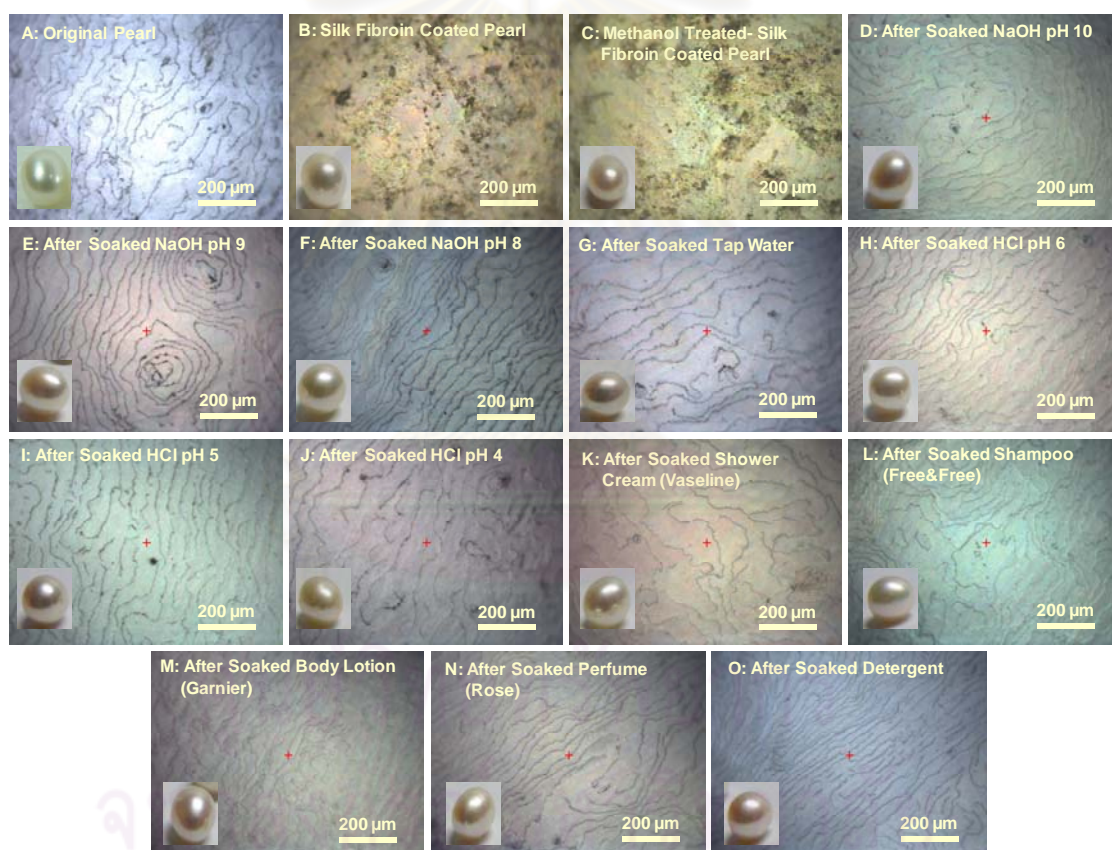


Figure 4.45 Optical images of freshwater cultured pearl coated silk fibroin solution plus methanol treatment and soaked with tap water, NaOH solution pH 8, 9 and 10, HCl solution pH 4, 5 and 6, detergent, shower cream, body lotion, shampoo and perfume for 19 hours.

Table 4.6 Summary of chemical and mechanical resistance test of silk fibroin coated pearls

Chemical / Mechanical Test	Untreated Pearls' Surface	Silk Fibroin Coated Pearls' Surface	Methanol Treated Silk Fibroin Coated Pearls' Surface
NaOH (pH = 10)	✘ (Partially Damaged)	✘ (Partially Damaged)	✓
NaOH (pH = 8)	✘ (Partially Damaged)	✓	✓
Tap Water	✘ (Partially Damaged)	✓	✓
HCl (pH = 6)	✘ (Partially Damaged)	✓	✓
HCl (pH =4)	✘ (Critically Damaged)	✓	✓
Lotion (Garnier)	✘(Critically Damaged)	✓	✓
Perfume	✘ (Partially Damaged)	✓	✓
Shower Cream (Vaseline)	✘ (Partially Damaged)	✓	✓
Detergent (Sunlight)	✘(Critically Damaged)	✓	✓
Shampoo (Free & Free)	✘(Critically Damaged)	✓	✓
Boiling Water	✓	✘ (Fibroin Dissolved)	✓
Polishing with Soft Cloth	✓	✘ (Fibroin Leached)	✓

The results of ATR FT-IR and Raman microspectroscopy suggested that the heat, solvent and detergent did not destroy silk fibroin stuck on pearl surface after methanol treatment. The coating of silk fibroin protected pearl surface from the heat, solvent and detergent.

4.10 The role of the luster of pearl after the coated with silk fibroin solution on surface

From the results of ATR FT-IR and Raman microspectroscopy, it indicated silk fibroin stuck on pearl surface. The increasing stick performance of silk fibroin solution plus methanol treatment due to the methanol extracted water from the molecular structure and changed secondary structure of silk fibroin from random coil and α -helix to β -sheet, showing the amorphous changed to crystalline structure causing water insoluble. Silk fibroin solution stuck on pearl surface due to film protected heat, solvent and detergents. Furthermore, silk fibroin solution increased luster of freshwater cultured pearl. Preliminarily, the observation of luster with the naked eye seeing the intensity of light reflected on surface of pearls as shown in Figure 4.46. Freshwater cultured pearl coated with silk fibroin solution plus methanol treatment increased the luster of original pearl. The results of luster were confirmed by UV-Visible spectroscopy with Integrating Sphere Diffuse Reflectance technology. According to Integrating Sphere instrument for the reflection method had more distance of optical fiber to sample surface affect the intensity of the laser. This method did not suitable for the luster of pearl because of the inappropriate of the instrument.



Figure 4.46 Image of freshwater pearl coated silk fibroin solution plus methanol treatment.

ศูนย์วิทยทรัพยากร
จุฬาลงกรณ์มหาวิทยาลัย

CHAPTER V

CONCLUSIONS

In this research, silk fibroin solution is prepared from the silk fibroin fiber and low grade cocoons from the textile industry. The optimal silk fibroin solution prepared from 2 g (2 % w/v) of silk fibroin fiber dissolved in 0.35 M NaOH which used minimal alkaline concentration and minimal the usage mole of alkali in dissolving 1 g of silk fibroin fiber. The price of NaOH is 7.5 times cheaper than that of LiBr and it is as well cheaper than that of KOH, which helps reduction costs in preparation of silk fibroin solution. We also adjust the pH of the silk fibroin solution to neutral pH that saves time in dialysis up to 3 days for the coating surface of low quality freshwater pearls.

ATR FT-IR and Raman spectroscopy can be characterized the stick of the silk fibroin on pearl surface by elucidating the stick of silk fibrin on pearl surface. The observed characteristic peaks N-H stretching, Amide I, Amide II and Amide III which indicate the molecular information of silk fibroin.

Coating of low quality freshwater pearls surface with silk fibroin solution and methanol treatment protect pearl surface from heating and increase the luster of pearl surface. These can be observed by measuring the intensity of the reflected light on the surface of pearls.

REFERENCES

- [1] Ward, F., and Ward, C. Pearls. 2nd Edition. USA: Gem Book, 1998.
- [2] Read, P.G. Gemmology. 3rd Edition. Burlington: Elsevier Butterworth-Heinemann, 2005.
- [3] PearlParadose.com, Inc. Pearl Education [online]. 1996-2010. Available from: <http://www.pearlparadise.com/pearlqualityguide.html>
- [4] Nina's. Pearl guide [online]. Available from: <http://www.ninasjewellery.com.au/buying-pearls.asp>
- [5] Newman, R. Pearl Buying Guide: How to Identificatify and Evaluate Pearls & Pearl Jewelry. 5th Edition. USA: International Jewelry Publications, 2010.
- [6] Taburiavx, J., and Ehrmanm, J-P. Pearl: their origin, treatment and identification. Philadelphia: Chilton Book Co., 1985.
- [7] Matlins, A. The Pearl Book: The Definitive Buying Guide. 4th Edition. Canada: A Division of LongHill Partners Inc., 2008.
- [8] Chen, R., et al. An Eefficient Biomimetic Process for Fabrication of Artificial Nacre with Ordered-Nanostructure. Mater. Sci. Eng. C 28 (2008): 218–222.
- [9] Tanaka, S., et al. Amino acid composition of conchiolin in pearl and shell. Biochemical Studies on Pearl IX 33, 4 (1960): 543-545.
- [10] Mondal, M., et al. The Silk Proteins, Sericin and Fibroin in Silkworm, *Bombyx mori*. Caspian J. Env. Sci. 5, 2 (2007): 63-76.
- [11] Sonthisombat, A., and Speakman, P. Silk: Queen of fibres - the concise story. Cited in Sandoz colour chronicle (October/December 1990): 1-28.
- [12] Li, Y., et al. Analysis of the Structural Characteristics of Silk Nanoscale Silk Particles. J. Appl. Polymer Sci. 100 (2006): 268-274.
- [13] Sashina, E.S., et al. Structure and Solubility of Natural Silk Fibroin. J. Appl. Chem. 79, 6 (2006): 869-876.
- [14] Zaremba, C.M., et al. Aragonite-Hydroxyapatite Conversion in Gastropod (Abalone) Nacre. Chem. Mater. 10, 12 (1998): 3813-3824.

- [15] Feng, Q.L., et al. Crystal Orientation, Toughening Mechanisms and A Mimic of Nacre. Mater. Sci. Eng. C 11 (2000): 19–25.
- [16] Bruet, B.J.F. Nanoscale Morphology and Indentation of Individual Nacre Tablets from the Gastropod Mollusc *Trochus Niloticus*. J. Mater. Res. 20, 9 (2005): 2400-2419.
- [17] Heinemann, F., et al. Abalone Nacre Insoluble Matrix Induces Growth of Flat and Oriented Aragonite Crystals. Biochem. Bioph. Res. Co. 334 (2006): 45–49.
- [18] Wang, R. Pearl Powder Bio-Coating and Patterning by Electrophoretic Deposition. J. Mater. Sci. 39 (2004): 4961–4964.
- [19] Blank, S., et al. The Nacre Protein Perlucin Nucleates Growth of Calcium Carbonate Crystals. J. Microsc. 212 (2003): 280–291.
- [20] Takahashi, K., et al. Highly Oriented Aragonite Nanocrystal–Biopolymer Composites in an Aragonite Brick of the Nacreous Layer of *Pinctada Fucata*. Chem. Commun. (2004): 996–997.
- [21] Lin, A.Y.M., et al. The Growth of Nacre in the Abalone Shell. Acta Biomater. 4 (2008): 131–138.
- [22] Nudelman, F., et al. Forming Nacreous Layer of the Shells of the Bivalves *Atrina Rigida* and *Pinctada Margaritifera*: An Environmental- and Cryo-Scanning Electron Microscopy Study. J. Struct. Biol. 162 (2008): 290-300.
- [23] Stempfle, P., and Brendle, M. Tribological Behaviour of Nacre—Influence of the Environment on the Elementary wear Processes. Tribol. Int. 39 (2006): 1485–1496.
- [24] Okumura, K., and de Gennes, P.G. Why is Nacre Strong? Elastic Theory and Fracture Mechanics for Biocomposites with Stratified Structures. Eur. Phys. J. E 4 (2001): 121–127.
- [25] Katti, K.S., and Katti, D.R. Why is Nacre so Tough and Strong?. Mater. Sci. Eng. C 26 (2006): 1317–1324.
- [26] Katti, D.R., et al. 3D Finite Element Modeling of Mechanical Response in Nacre-Based Hybrid Nanocomposites. Comput. Theor. Polym. S. 11 (2001): 397-404.

- [27] Zhou, G.T., et al. Sonochemical Synthesis of Aragonite-Type Calcium Carbonate with Different Morphologies. New. J. Chem. 28 (2004): 1027–1031.
- [28] Cifrulak, S.D. High Pressure Mid-Infrared Studies of Calcium Carbonate. Am. Mineral. 55 (1970): 815-824.
- [29] Wang, Y., et al. Synthesis and Characterization of Lamellar Aragonite with Hydrophobic Property. Mater. Sci. Eng. C 29 (2008): 843-846.
- [30] Dauphin, Y., and Denis, A. Structure and Composition of the Aragonitic Crossed Lamellar Layers in Six Species of Bivalvia and Gastropoda. Comp. Biochem. Physiol. Part A 126 (2000): 367–377.
- [31] Tavender, S.M., et al. The Carbonate in Solution Studied by Resonance Raman Spectroscopy. Laser Chem. 19 (1999): 311 316.
- [32] Chakrabarty, D., and Mahapatra, S. Aragonite Crystals with Unconventional Morphologies. J. Mater. Chem. 9 (1999): 2953-2957.
- [33] Verma, D., et al. Photoacoustic FTIR Spectroscopic Study of Undisturbed Nacre from Red Abalone. Spectrochim. Acta A 64 (2006): 1051–1057.
- [34] Ma, H.Y., and Lee, I.-S. Characterization of Vaterite in Low Quality Freshwater-Cultured Pearls. J. Mater. Sci. Eng. C 26 (2006): 721–723.
- [35] Qiao, L., et al. A Novel Bio-Vaterite in Freshwater Pearls with High Thermal Stability and Low Dissolubility. Mater. Lett. 62 (2008): 1793–1796.
- [36] Tan, T.L., et al. Iridescence of a Shell of Mollusk *Haliotis Glabra*. Optics Express 12, 20 (2004): 4847-4854.
- [37] Verma, D., et al. Nature of Water in Nacre: A 2D Fourier Transform Infrared Spectroscopic Study. Spectrochim. Acta A 64 (2007): 784–788.
- [38] Tan, T.L., et al. Identification of An Imitation of Pearl by FTIR, EDXRF and SEM. J. Gemm. 29 (2005): 316-324.
- [39] Zhang, C., et al. A Novel Matrix Protein p10 from the Nacre of Pearl Oyster (*Pinctada fucata*) and Its Effects on Both CaCO₃ Crystal Formation and Mineralogenic Cells. Marine Biotechnology 8 (2006): 624–633.
- [40] Kontoyannis, C.G., and Vagenas, N.V. Calcium Carbonate Phase Analysis Using XRD and FT-Raman Spectroscopy. Analyst. 125 (2000): 251–255.

- [41] Soldati, A.L., et al. Micro-Raman Spectroscopy of Pigments Contained in Different Calcium Carbonate Polymorphs from Freshwater Cultured Pearls. J. Raman Spectrosc. 39 (2008): 525–536.
- [42] Qiao, L., et al. In Vitro Growth of Nacre-like Tablet Forming: From Amorphous Calcium Carbonate, Nanostacks to Hexagonal Tablets. J. Cryst. Growth & Design 8, 5 (2008): 1155-1514.
- [43] Park, S.C., et al. Wide area illumination Raman scheme for simple and nondestructive discrimination of seawater cultured pearls. J. Raman Spectrosc. 40 (2009): 2187–2192.
- [44] Yan, Z., et al. N40, A Novel Nonacidic Matrix Protein from Pearl Oyster Nacre, Facilitates Nucleation of Aragonite in Vitro. Biomacromolecules 8 (2007): 3597-3601.
- [45] Samata, T., et al. A New Matrix Protein Family Related to the Nacreous Layer Formation of *Pinctada Fucata*. FEBS Letters 462 (1999): 225-229.
- [46] Zhang, Y., et al. A Novel Matrix Protein Participating in the Nacre Framework Formation of Pearl Oyster, *Pinctada Fucata*. Comp. Biochem. Physiol. Part B 135 (2003): 565–573.
- [47] Bowen, C.E., and Tang, H. Conchiolin-Protein in Aragonite Shells of Mollusks. Comp. Biochem. Physiol. 115 A, 4 (1996): 269-275.
- [48] Caiping, M., et al. Extraction and Purification of Matrix Protein from the Nacre of Pearl Oyster *Pinctada fucata*. Tsinghua Science and Technology 10, 4 (2005): 499-503.
- [49] Pereira-Mouriès, L., et al. Soluble Silk-Like Organic Matrix in the Nacreous Layer of the Bivalve *Pinctada Maxima*. Eur. J. Biochem. 269 (2002): 4994–5003.
- [50] Matsushiro, A., et al. Presence of Protein Complex is Prerequisite for Aragonite Crystallization in the Nacreous Layer. Mar. Biotechnol. 5 (2003): 37–44.
- [51] Krampitz, G., et al. Simultaneous Binding of Calcium and Bicarbonate by Conchiolin of Oyster Shells. Experientia 39 (1983): 1104-1105.
- [52] Levi-Kalisman, Y., et al. Structure of the Nacreous Organic Matrix of a Bivalve Mollusk Shell Examined in the Hydrated State Using Cryo-TEM. J. Struct. Biol. 135 (2001): 8–17.

- [53] Moutahir-Belqasmi, F., et al. Effect of Water Soluble Extract of Nacre (*Pinctada Maxima*) on Alkaline Phosphatase Activity and Bcl-2 Expression in Primary Cultured Osteoblasts from Neonatal Rat Calvaria. J. Mater. Sci. 12 (2001): 1-6.
- [54] Petsko G.A., and Ringe, D. Protein Structure and Function. USA: New Science Press, 2004.
- [55] Robson, R.M. In Silk; Composition, Structure and Properties. Handbook of Fibre Science and Technology, Volume 4. New York, 1985.
- [56] Entry Posting. Levels of protein Organization [online]. 2008. Available from: http://thehills48.blogspot.com/2008_02_12_archive.html [2008, February, 12]
- [57] Wikipedia. Content [online]. 2007. Available from: http://wiki.verkata.com/en/wiki/Beta_sheet [2007, January, 21]
- [58] Raghava, G.P.S., and Kaur, H. A server for β -turn types prediction [online]. 2004. Available from: www.imtech.res.in/raghava/beteturns/turn.html
- [59] Seidman, L. Chapter 2: Protein structure [online]. 2007. Available from: <http://matcmadison.edu/biotech/resources/proteins/labManual/chapter2.html> [2007, February, 7]
- [60] Jin, H.J., et al. Biomaterial Films of *Bombyx Mori* Silk Fibroin with Poly (ethylene oxide). Biomacromolecules 5 (2004): 711-717.
- [61] Kim, U.J., et al. Structure and Properties of Silk Hydrogels. Biomacromolecules 5 (2004): 786-792.
- [62] Tamada, Y. New Process to Form a Silk Fibroin Porous 3-D Structure. Biomacromolecules 6 (2005): 3100-3106.
- [63] Xie, F., et al. Effect of shearing on formation of silk fibers from regenerated *Bombyx mori* silk fibroin aqueous solution. Int. J. Biol. Macromol. 38 (2006): 284–288.
- [64] Srisuwan, Y., and Srihanam, P. Dissolution of *philosoma ricini* Silk Film: Properties and Functions in Different Solutions. J. Applied Sci. (2009): 1-5.
- [65] Du, C., et al. Novel silk fibroin/hydroxyapatite composite films: Structure and properties. Mater. Sci. Eng. C 29 (2009): 62–68.

- [66] Lee, K.G., et al. Silk Fibroin Microsphere and Its Characterization. Int. J. Indust. Entomol. 6, 2 (2003): 151-155.
- [67] Urban, M.W. Attenuated Total Reflectance Spectroscopy of Polymer: Theory and Practice. Washington: American Chemical Society, 1996.
- [68] Smith, B.C. Fundamental of Fourier transform infrared spectroscopy. USA: CRC places, 1996.
- [69] Stuart, B. Infrared Spectroscopy: Fundamentals and Application. New York: Harrick Scientific Corporation, 1979.
- [70] Chalmers, J.M. Handbook of Vibrational Spectroscopy Vol 2. UK: John Wiley & Sons, 2002.
- [71] Ishida, H., and Ekgasit, S. New Quantitative Optical Depth Profiling Methods by Attenuated Total Reflectance Fourier Transform Infrared Spectroscopy: Multiple Angle/ Single Frequency and Single Angle/ Multiple Frequency Approaches Fourier Transform Spectroscopy: 11th International conference (1998): 40-59.
- [72] Ekgasit, S., and Padermshoke, A. Optical Contact in ATR/FT-IR Spectroscopy. Appl. Spectrosc. 55 (2001): 1352-1359.
- [73] Ekgasit, S., and Ishida, H. New Optical Depth-profiling Technique by Use of the Multiple-Frequency Approach with Single ATR FT-IR Spectrum; Theoretical Development. Appl. Spectrosc. 51 (2007): 1488-1495.
- [74] Ekgasit, S., et al. A Novel ATR FT-IR Microspectroscopy Technique for Surface Contamination Analysis without Interference of the Substrate. Anal. Sci. 23 (2007): 1-8.
- [75] Aruldas, G. Molecular structure and spectroscopy. New Delhi: Prentice-Hall of India Private Limited, 2006.
- [76] Pelletier, M.J. Analytical applications of Raman spectroscopy. US: Wiley-Blackwell, 1999.
- [77] Colthup, N.B., et al. Introduction to Infrared and Raman Spectroscopy. New York: Academic Press, 1990.
- [78] Ferraro, J.R., et al. Introductory Raman Spectroscopy. 2nd Edition. UK: Academic Pr., 2002.

- [79] Nakamoto, K. Infrared and Raman spectra of Inorganic and Coordination Compounds Part A. 6th Edition. Canada: John Wiley & Sons, Inc., 2009.
- [80] Ayutsede, J., et al. Regeneration of *Bombyx mori* silk by eletrospinning. Part 3: characterization of electrospun nonwoven mat. Polymer 46 (2005): 1625-1634.
- [81] Chen, Y.Y., et al. Study on Bombyx mori silk treated by oxygen plasma. J. Zhejiang Univ. Sci. 5 (2004): 918-922.
- [82] Taketani, I., et al. The secondary structure control of silk fibroin thin film by post treatment. Appl. Surf. Sci. 244 (2005): 623-626.
- [83] Suanpoot, P., et al. Surfacer analysis of hydrophobicity of thai silk treated by SF₆ plasma. Surf. Coat. Tech. 202 (2008): 5543-5549.
- [84] Iridag, Y., et al. Preparation and characteriation of Bombyx mori silk fibroin and wool keratin. Biopolymers 25 (1986): 469-487.
- [85] Dong, Q., et al. In situ depositing silver nanoclusters on silk fibroin fibers supports by a novel biotemplate redox technique at room temperature. J. Phys. Chem. 109 (2005): 17429-17434.
- [86] Grandhi, M., et al. Post spinning modification of electrospun nanofiber nanocomposite from Bombyx mori silk and carbon nanotubes. Polymer 50 (2009): 1918-1924.
- [87] Wang, X., et al. Biomaterial coatings by stepwise deposition of silk fibroin. Langmuir 21 (2005): 11335-11341.
- [88] Zong, X.-H., et al. Effect of pH and Copper (II) on the Conformation Transitions of Silk Fibroin Based on EPR, NMR, and Raman Spectroscopy. Biochemistry 43 (2004): 11932-11941.
- [89] Rousseau, M.-E., et al. Study of Protein Conformation and Orientation in Silkworm and Spider Silk Fibers Using Raman Microspectroscopy. Biomacromolecules 5 (2004): 2247-2257.
- [90] Monti, P., et al. Vibrational spectroscopic study of sulphated silk proteins. J. Mol. Struc. 834-836 (2007): 202-206.

VITAE

Name: Miss Kanokwan Kumkhai

Date of Birth: May 10, 1982 **Birth place:** Nakhonpathom,
Thailand

Address: 320 Moo1, Tambon Donyaihom, Mueang, Nakhonpathom,
Thailand,
E-mail address: kanokwan.chula@hotmail.com

Education:

2005 Bachelor of Science (Chemistry), Nakhonpathom Rajabhat
University, Nakhonpathom, Thailand

2010 Master of Science (Petrochemistry and Polymer Science),
Chulalongkorn University, Bangkok, Thailand

Conferences:

October 2008 The 34th Congress on Science and Technology of Thailand

November 2008 The CGI Award for Young Scientists 2008

January 2009 Pure and Applied Chemistry International Conference 2009,
Thailand

March, 2009 The Science Forum 2009 (The 17th Annual Academic Meeting
of the Faculty of Science, Chulalongkorn University)

May 2009 The 2nd Polymer Graduate Conference of Thailand

January 2010 Pure and Applied Chemistry International Conference 2010,
Thailand

July 2010 Graduate Conference The 25th Anniversary

August 2010 ASEAN Sericulture Conference 2010